Supplementary Information

Regulation of MALAT1 triple helix stability and in vitro degradation by diphenylfurans

Anita Donlic,[1] Martina Zafferani,[1] Giacomo Padroni,[1] Malavika Puri,[1] Amanda E. Hargrove[1,2*]

[1]Department of Chemistry, Duke University, 124 Science Drive, Durham, NC 27708, USA

[2]Department of Biochemistry, Duke University School of Medicine, Durham, NC, 27710, USA

* To whom correspondence should be addressed. Tel: 919-660-1522; Fax: 919-660-1522; e-mail: amanda.hargrove@duke.edu

Present Address: Amanda E. Hargrove, Department of Chemistry, Duke University, Durham, NC 27708, USA

Contents

A. Supplementary Figures S1-S36

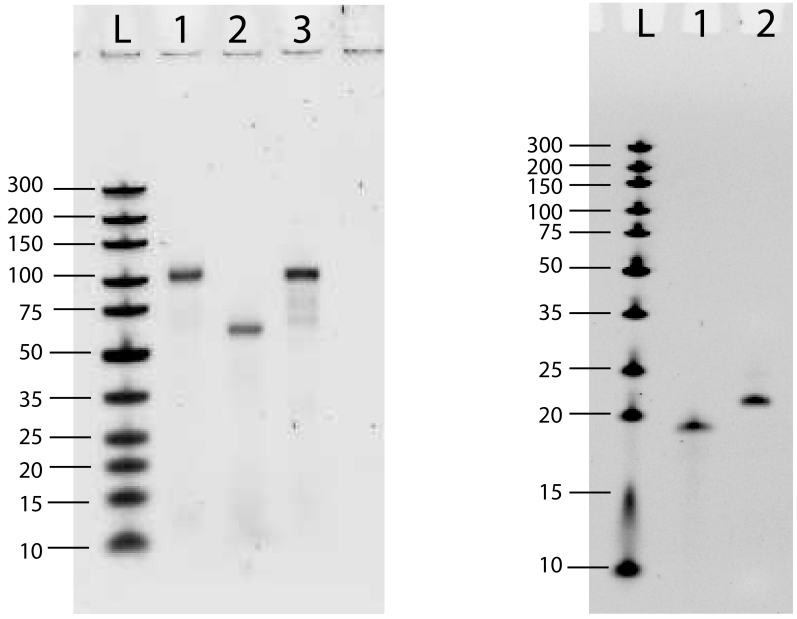

Figure S1. Left: 8% PAGE-Urea gel run at 180V for 20 min in 1X TBE buffer (100 mM Tris base, 100 mM Borate, 2 mM EDTA) buffer. L = O'GeneRuler Ultra Low Range DNA Ladder (Thermo Scientific), 1 - MALAT1 triple helix RNA, 2 – MALAT1 stem loop RNA, 3 – NEAT1 triple helix RNA. Right: 15% PAGE-Urea gel run at 180V for 1 h in 1X TBE buffer (100 mM Tris base, 100 mM Borate, 2 mM EDTA) buffer. L = O'GeneRuler Ultra Low Range DNA Ladder (Thermo Scientific), 1 = AT-rich DNA duplex, 2 – RRE Stem Loop IIB RNA.

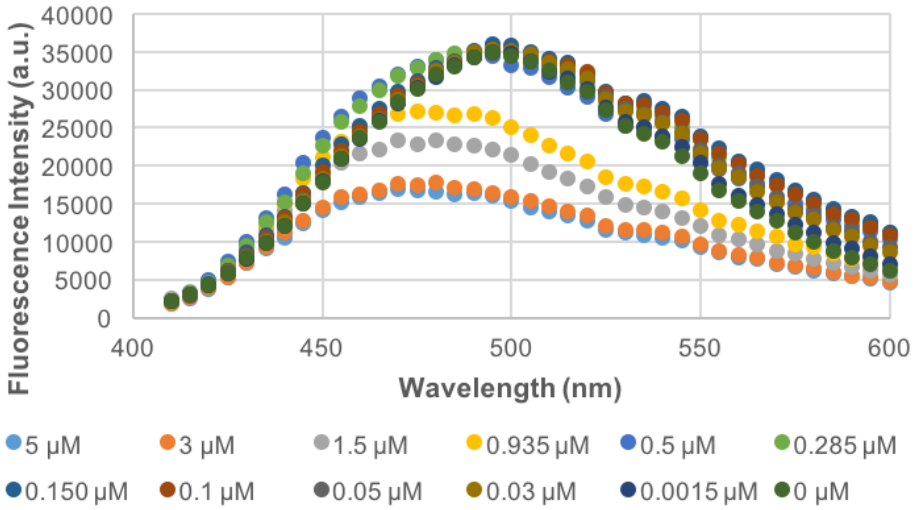

Figure S2. Example fluorescence profile of **DPFp20** with increasing amounts of the MALAT1 triple helix RNA as described in "Fluorescence Binding Experiments" section of Materials and Methods. Excitation: 380 nm.

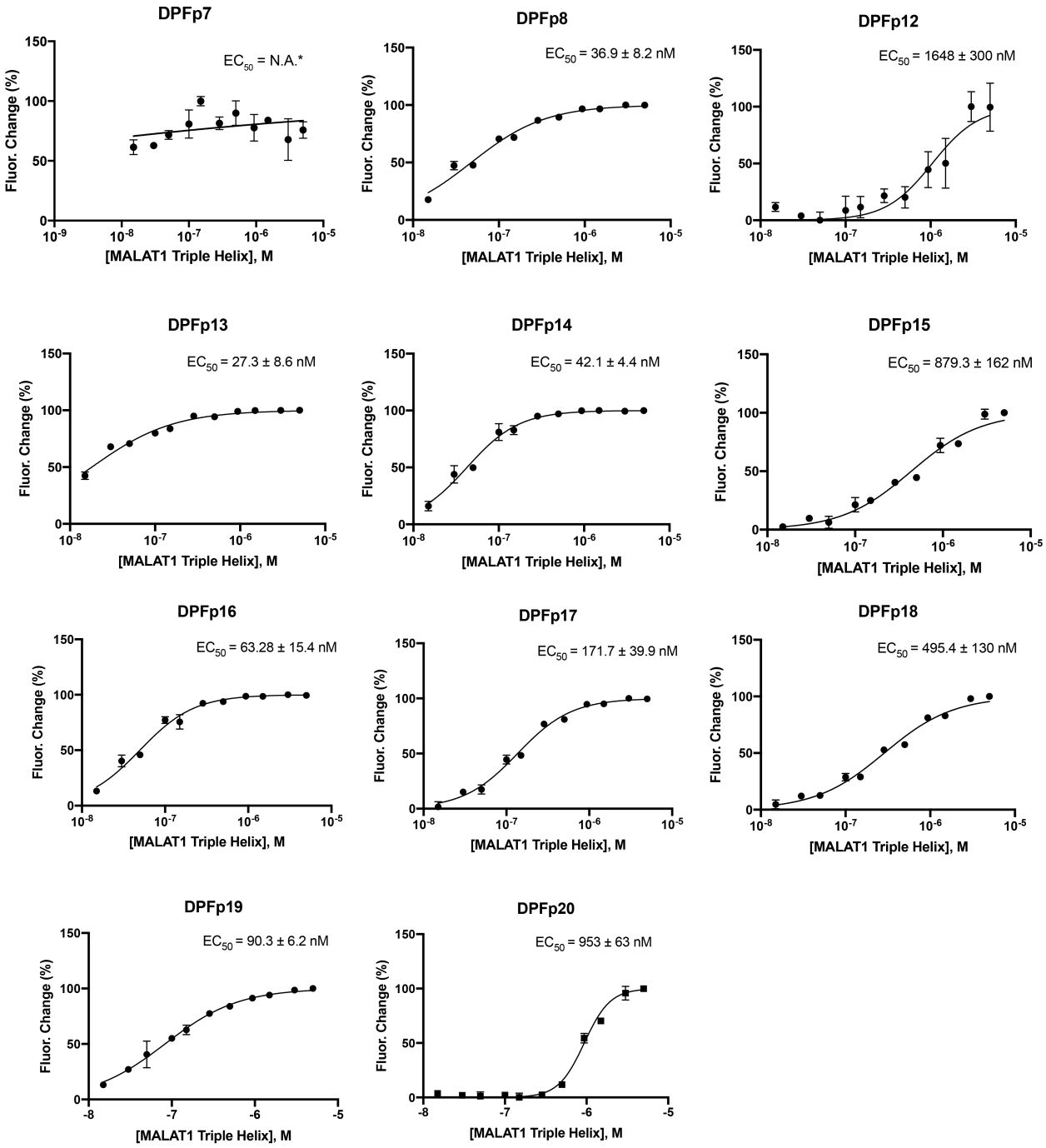

Figure S3. EC_{50} binding curves from fluorescence binding experiments with the MALAT1 triple helix in phosphate screening buffer (10 mM NaH_2PO_4, 25 mM NaCl, 4 mM $MgCl_2$, 0.5 mM EDTA, pH 7.3). N.A.* - not available; indicates curves for which no EC_{50} value was obtained due to little to no change in DPF fluorescence.

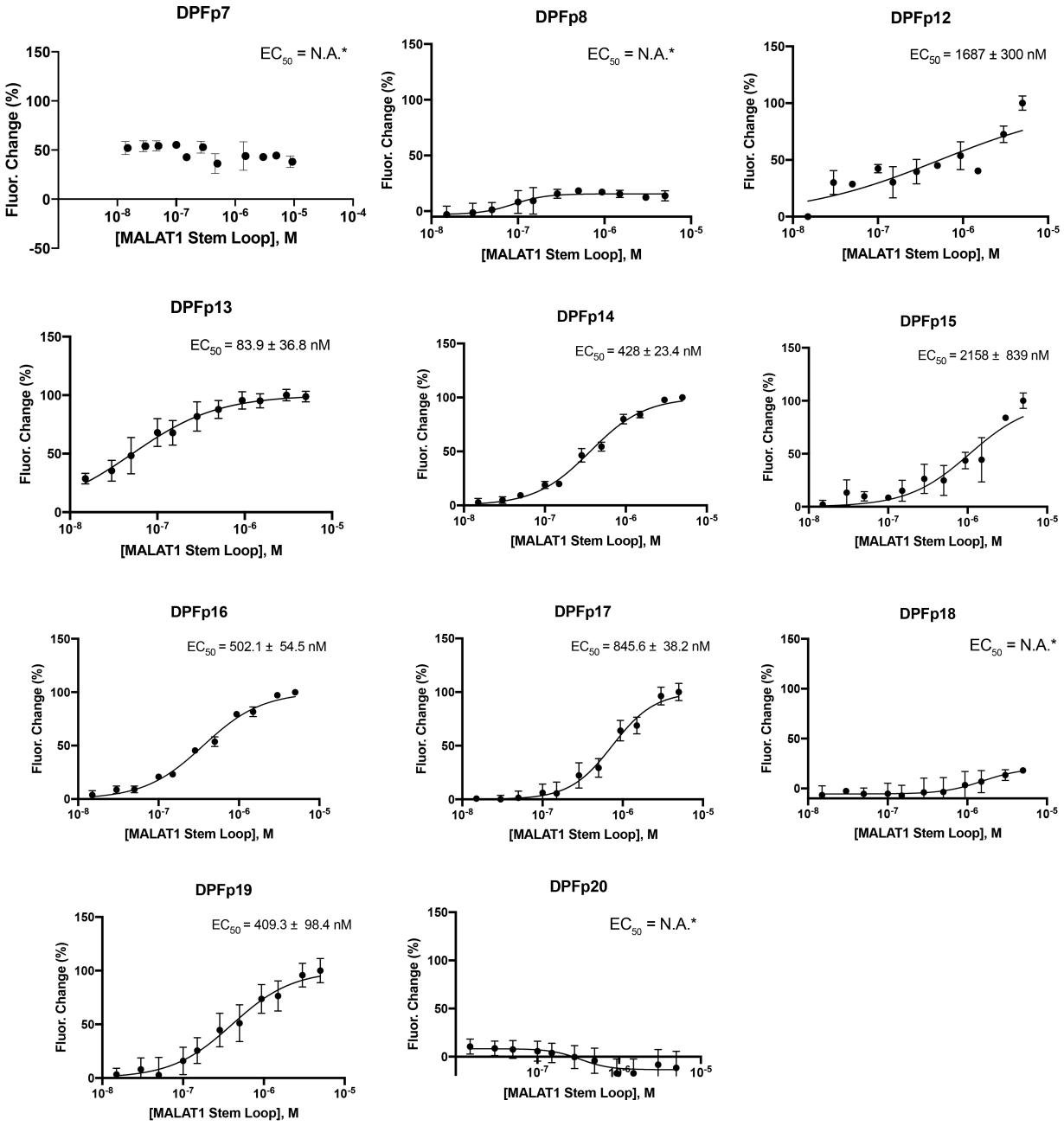

Figure S4. EC_{50} binding curves from fluorescence binding experiments with the MALAT1 stem loop in phosphate screening buffer (10 mM NaH_2PO_4, 25 mM NaCl, 4 mM $MgCl_2$, 0.5 mM EDTA, pH 7.3). N.A.* - not available; indicates curves for which no EC_{50} value was obtained due to little to no change in DPF fluorescence.

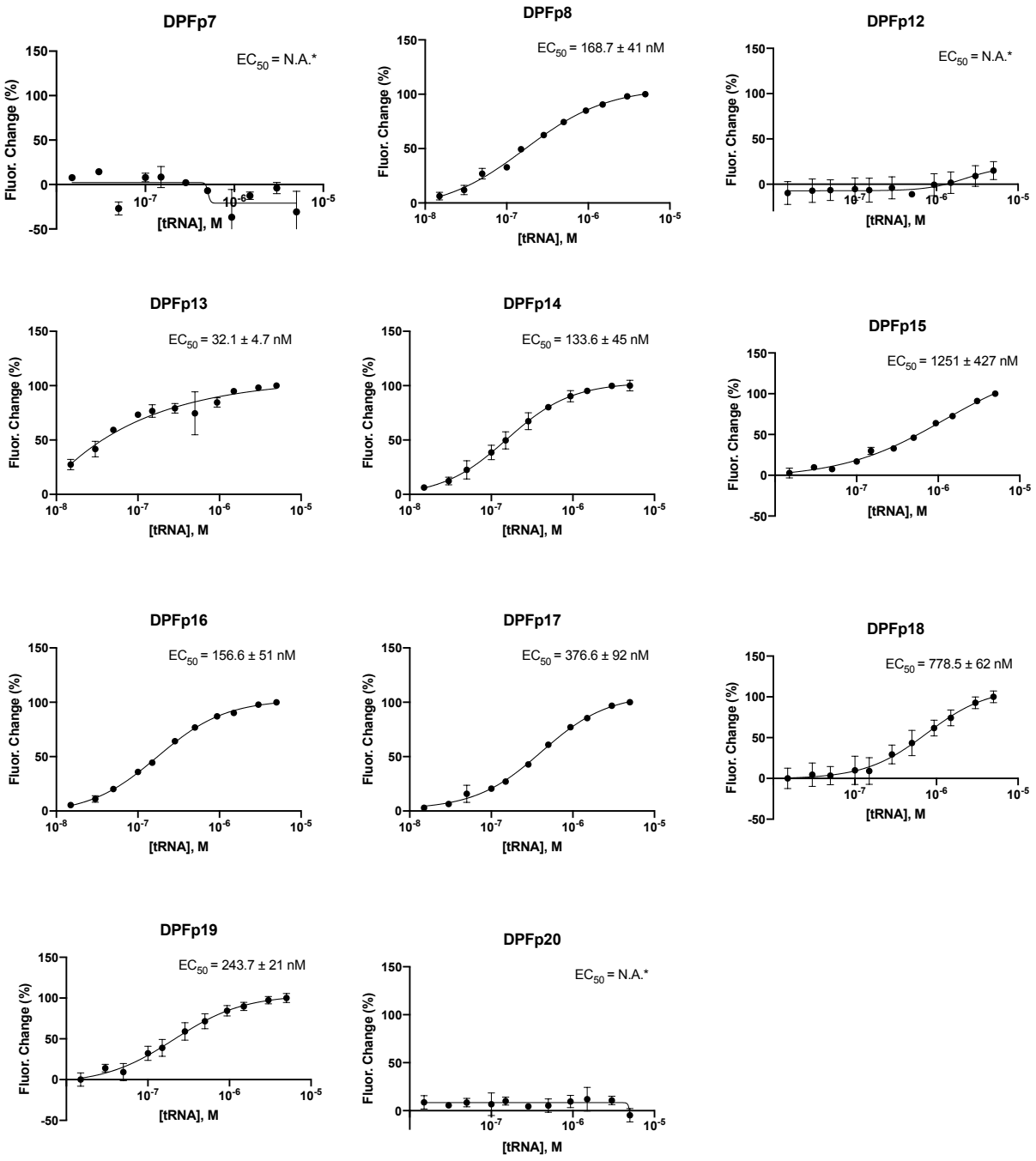

Figure S5. EC_{50} binding curves from fluorescence binding experiments with yeast tRNA in phosphate screening buffer (10 mM NaH_2PO_4, 25 mM NaCl, 4 mM $MgCl_2$, 0.5 mM EDTA, pH 7.3). N.A.* - not available; indicates curves for which no EC_{50} value was obtained due to little to no change in DPF fluorescence.

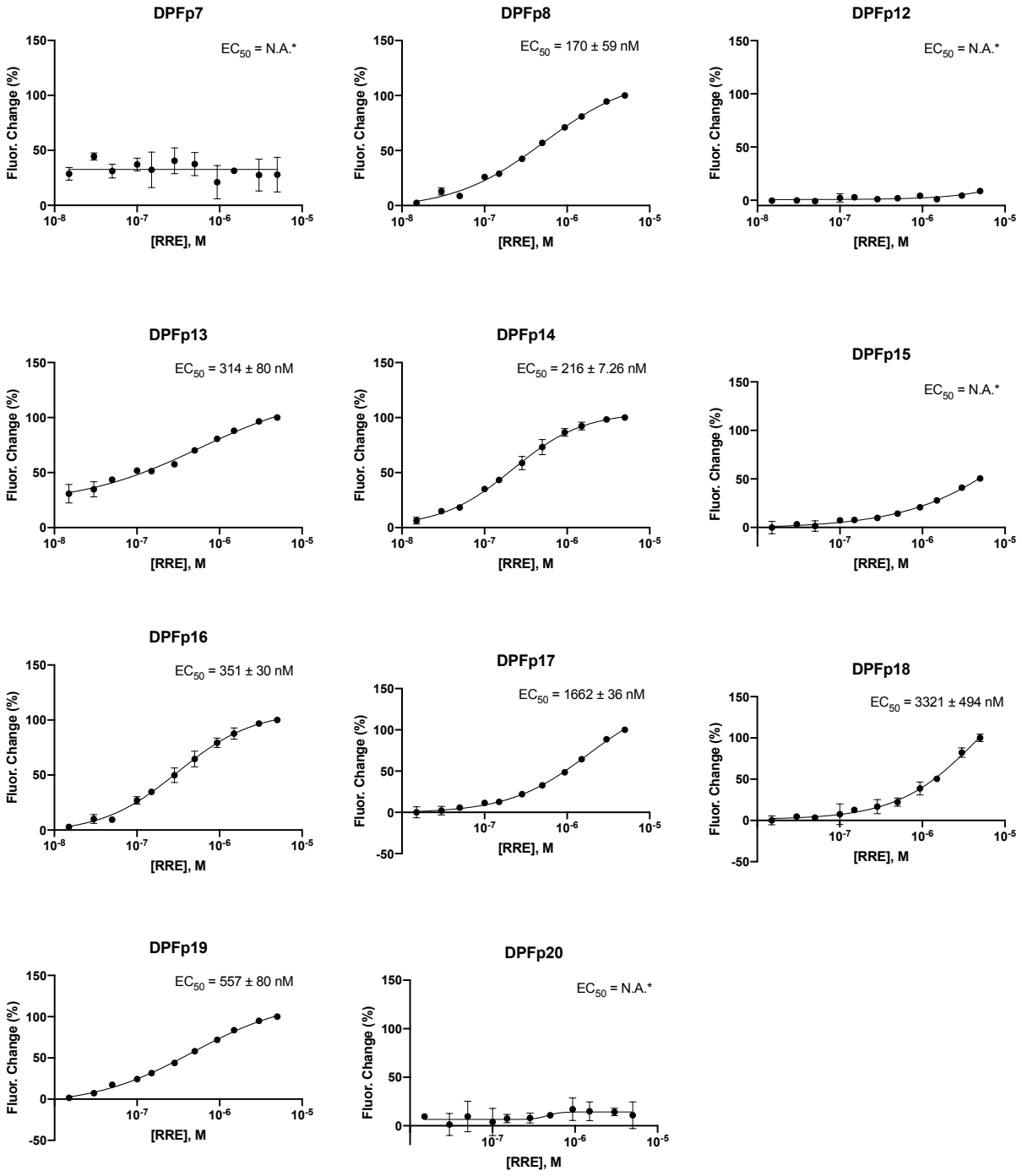

Figure S6. EC_{50} binding curves from fluorescence binding experiments with the RRE Stem loop IIB RNA in phosphate screening buffer (10 mM NaH_2PO_4, 25 mM NaCl, 4 mM $MgCl_2$, 0.5 mM EDTA, pH 7.3). N.A.* - not available; indicates curves for which no EC_{50} value was obtained due to little to no change in DPF fluorescence.

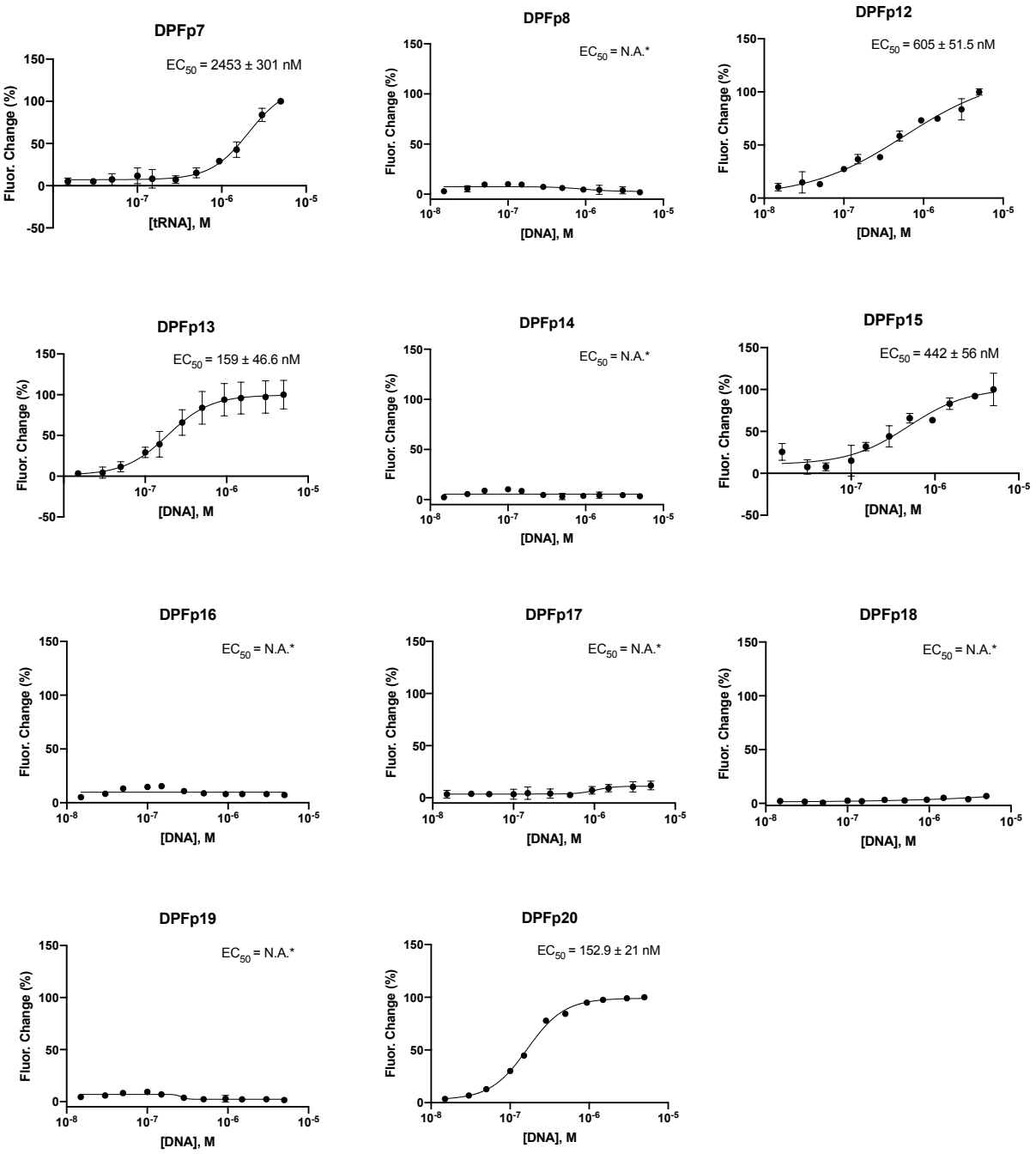

Figure S7. EC_{50} binding curves from fluorescence binding experiments with the AT-rich DNA duplex in phosphate screening buffer (10 mM NaH_2PO_4, 25 mM NaCl, 4 mM $MgCl_2$, 0.5 mM EDTA, pH 7.3). N.A.* - not available; indicates curves for which no EC_{50} value was obtained due to little to no change in DPF fluorescence.

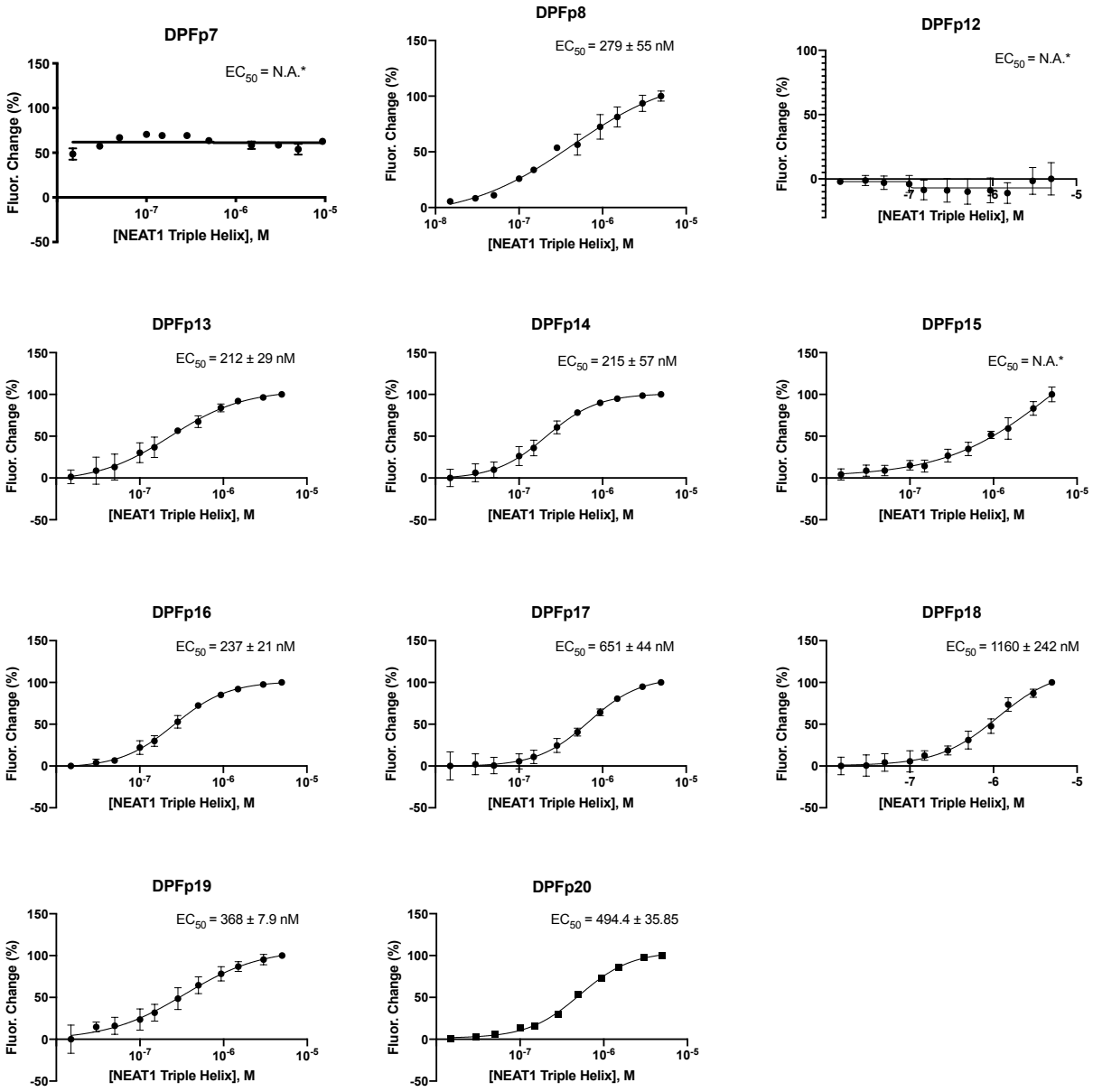

Figure S8. EC_{50} binding curves from fluorescence binding experiments with the NEAT1 triple helix in phosphate screening buffer (10 mM NaH_2PO_4, 25 mM NaCl, 4 mM $MgCl_2$, 0.5 mM EDTA, pH 7.3). N.A.* - not available; indicates curves for which no EC_{50} value was obtained due to little to no change in DPF fluorescence.

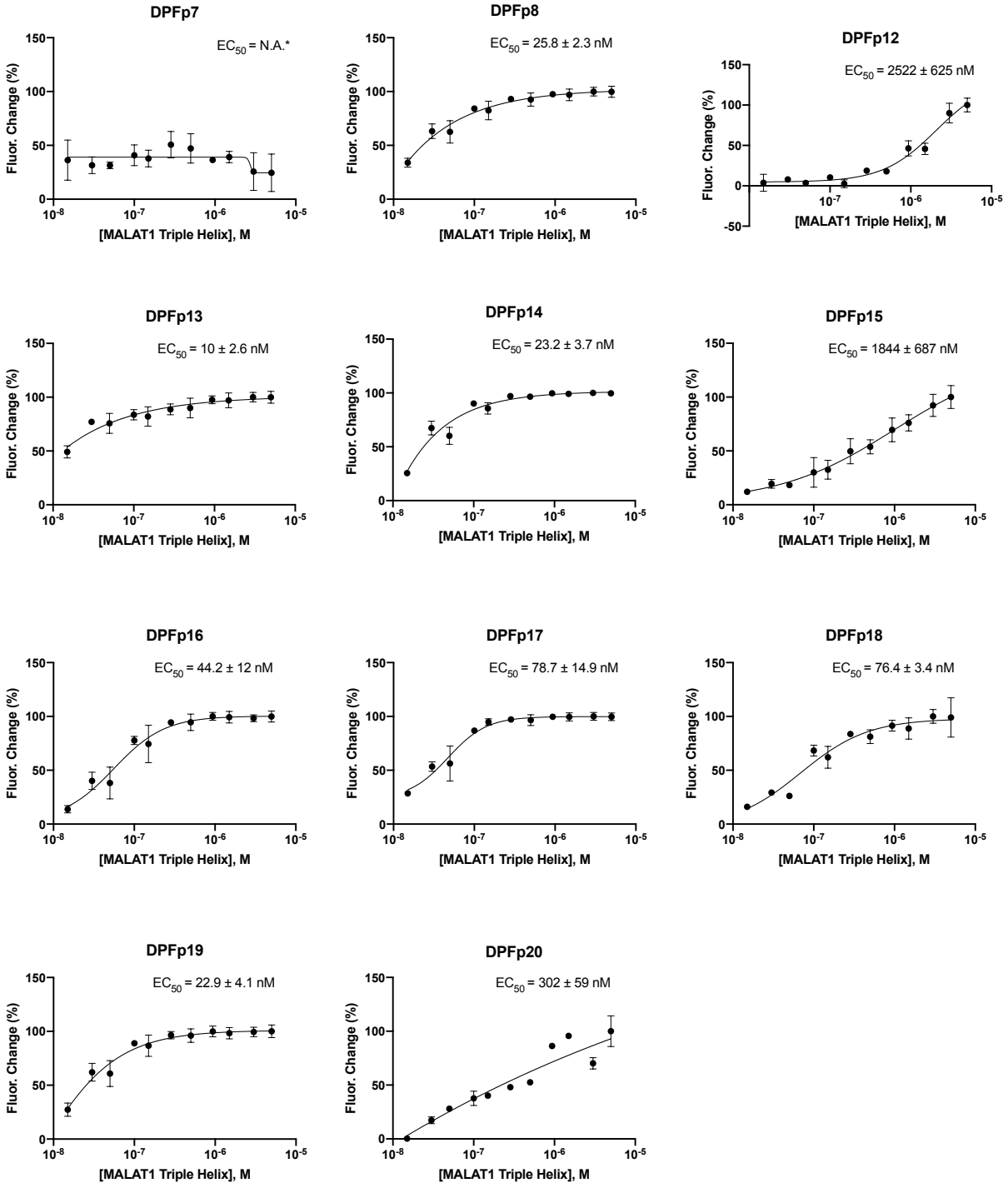

Figure S9. EC_{50} binding curves from fluorescence binding experiments with the MALAT11 triple helix in low ionic buffer, Buffer 2 (20 mM HEPES-KOH pH 7.4 at 25ºC, 52 mM KCl, 0.1 mM $MgCl_2$). N.A.* - not available; indicates curves for which no EC_{50} value was obtained due to little to no change in DPF fluorescence.

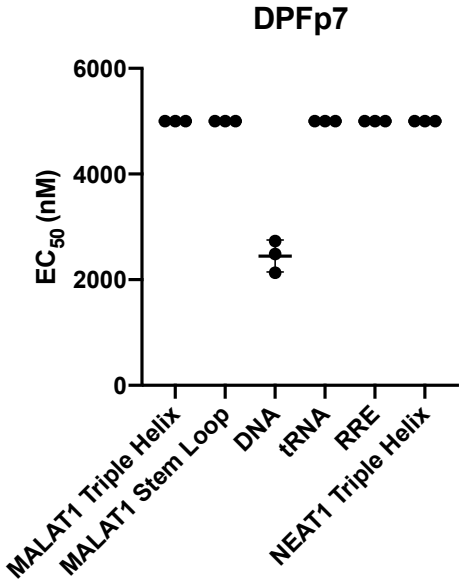

Tukey's multiple comparisons test	Mean Diff.	95.00% CI of diff.	Significant?	Summary	Adjusted P Value
MALAT1 Triple Helix vs. MALAT1 Stem Loop	0.000	-337.8 to 337.8	No	ns	>0.9999
MALAT1 Triple Helix vs. DNA	2546	2208 to 2884	Yes	****	<0.0001
MALAT1 Triple Helix vs. tRNA	0.000	-337.8 to 337.8	No	ns	>0.9999
MALAT1 Triple Helix vs. RRE	0.000	-337.8 to 337.8	No	ns	>0.9999
MALAT1 Triple Helix vs. NEAT1 Triple Helix	0.000	-337.8 to 337.8	No	ns	>0.9999
MALAT1 Stem Loop vs. DNA	2546	2208 to 2884	Yes	****	<0.0001
MALAT1 Stem Loop vs. tRNA	0.000	-337.8 to 337.8	No	ns	>0.9999
MALAT1 Stem Loop vs. RRE	0.000	-337.8 to 337.8	No	ns	>0.9999
MALAT1 Stem Loop vs. NEAT1 Triple Helix	0.000	-337.8 to 337.8	No	ns	>0.9999
DNA vs. tRNA	-2546	-2884 to -2208	Yes	****	<0.0001
DNA vs. RRE	-2546	-2884 to -2208	Yes	****	<0.0001
DNA vs. NEAT1 Triple Helix	-2546	-2884 to -2208	Yes	****	<0.0001
tRNA vs. RRE	0.000	-337.8 to 337.8	No	ns	>0.9999
tRNA vs. NEAT1 Triple Helix	0.000	-337.8 to 337.8	No	ns	>0.9999
RRE vs. NEAT1 Triple Helix	0.000	-337.8 to 337.8	No	ns	>0.9999

Figure S10. Statistical analysis for the selectivity screen of DPFp7. Its binding to the MALAT1 targets were previously reported.(1) One-way ANOVA followed by Tukey's multiple comparisons test was performed using GraphPad Prism version 8.0.2 for Macintosh, GraphPad Software, La Jolla California USA, www.graphpad.com. Summary of P-values: ns = 0.1234, * = 0.0332, ** = 0.0021, *** = 0.0002, **** = <0.0001.

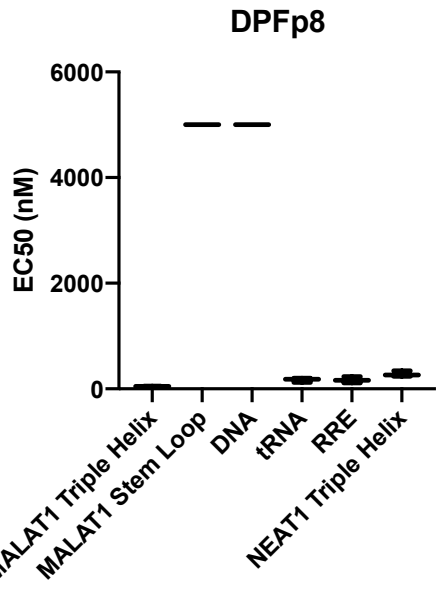

Tukey's multiple comparisons test	Mean Diff.	95.00% CI of diff.	Significant?	Summary	Adjusted P Value
MALAT1 Triple Helix vs. MALAT1 Stem Loop	-4953	-5055 to -4851	Yes	****	<0.0001
MALAT1 Triple Helix vs. DNA	-4953	-5055 to -4851	Yes	****	<0.0001
MALAT1 Triple Helix vs. tRNA	-121.8	-224.0 to -19.65	Yes	*	0.0168
MALAT1 Triple Helix vs. RRE	-123.1	-225.3 to -20.95	Yes	*	0.0156
MALAT1 Triple Helix vs. NEAT1 Triple Helix	-232.9	-335.0 to -130.7	Yes	****	<0.0001
MALAT1 Stem Loop vs. DNA	0.000	-102.2 to 102.2	No	ns	>0.9999
MALAT1 Stem Loop vs. tRNA	4831	4729 to 4933	Yes	****	<0.0001
MALAT1 Stem Loop vs. RRE	4830	4728 to 4932	Yes	****	<0.0001
MALAT1 Stem Loop vs. NEAT1 Triple Helix	4720	4618 to 4822	Yes	****	<0.0001
DNA vs. tRNA	4831	4729 to 4933	Yes	****	<0.0001
DNA vs. RRE	4830	4728 to 4932	Yes	****	<0.0001
DNA vs. NEAT1 Triple Helix	4720	4618 to 4822	Yes	****	<0.0001
tRNA vs. RRE	-1.300	-103.5 to 100.9	No	ns	>0.9999
tRNA vs. NEAT1 Triple Helix	-111.1	-213.2 to -8.910	Yes	*	0.0305
RRE vs. NEAT1 Triple Helix	-109.8	-211.9 to -7.610	Yes	*	0.0328

Figure S11. Statistical analysis for the selectivity screen of DPFp8. Its binding to the MALAT1 targets, tRNA, RRE and DNA were previously reported.(1) One-way ANOVA followed by Tukey's multiple comparisons test was performed using GraphPad Prism version 8.0.2 for Macintosh, GraphPad Software, La Jolla California USA, www.graphpad.com. Summary of P-values: ns = 0.1234, * = 0.0332, ** = 0.0021, *** = 0.0002, **** = <0.0001.

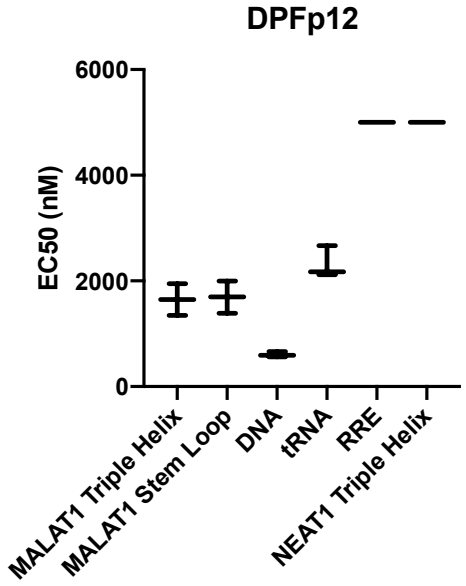

Tukey's multiple comparisons test	Mean Diff.	95.00% CI of diff.	Significant?	Summary	Adjusted P Value
MALAT1 Triple Helix vs. MALAT1 Stem Loop	-45.67	-635.7 to 544.4	No	ns	0.9998
MALAT1 Triple Helix vs. DNA	1042	452.1 to 1632	Yes	***	0.0008
MALAT1 Triple Helix vs. tRNA	-671.0	-1261 to -80.94	Yes	*	0.0230
MALAT1 Triple Helix vs. RRE	-3352	-3942 to -2762	Yes	****	<0.0001
MALAT1 Triple Helix vs. NEAT1 Triple Helix	-3352	-3942 to -2762	Yes	****	<0.0001
MALAT1 Stem Loop vs. DNA	1088	497.7 to 1678	Yes	***	0.0005
MALAT1 Stem Loop vs. tRNA	-625.3	-1215 to -35.27	Yes	*	0.0357
MALAT1 Stem Loop vs. RRE	-3306	-3896 to -2716	Yes	****	<0.0001
MALAT1 Stem Loop vs. NEAT1 Triple Helix	-3306	-3896 to -2716	Yes	****	<0.0001
DNA vs. tRNA	-1713	-2303 to -1123	Yes	****	<0.0001
DNA vs. RRE	-4394	-4984 to -3804	Yes	****	<0.0001
DNA vs. NEAT1 Triple Helix	-4394	-4984 to -3804	Yes	****	<0.0001
tRNA vs. RRE	-2681	-3271 to -2091	Yes	****	<0.0001
tRNA vs. NEAT1 Triple Helix	-2681	-3271 to -2091	Yes	****	<0.0001
RRE vs. NEAT1 Triple Helix	0.000	-590.1 to 590.1	No	ns	>0.9999

Figure S12. Statistical analysis for the selectivity screen of DPFp12. One-way ANOVA followed by Tukey's multiple comparisons test was performed using GraphPad Prism version 8.0.2 for Macintosh, GraphPad Software, La Jolla California USA, www.graphpad.com. Summary of P-values: ns = 0.1234, * = 0.0332, ** = 0.0021, *** = 0.0002, **** = <0.0001.

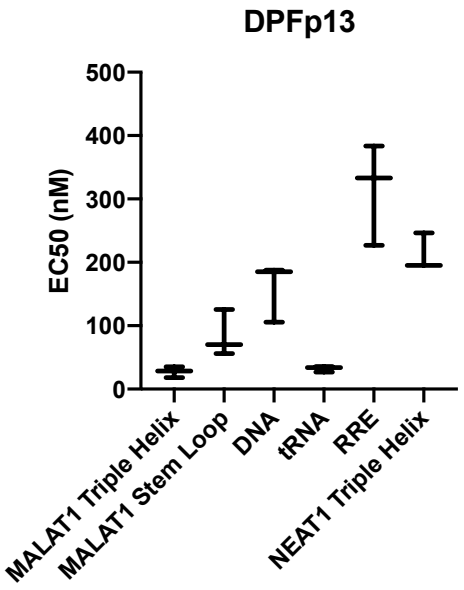

Tukey's multiple comparisons test	Mean Diff.	95.00% CI of diff.	Significant?	Summary	Adjusted P Value
MALAT1 Triple Helix vs. MALAT1 Stem Loop	-56.58	-173.5 to 60.31	No	ns	0.5986
MALAT1 Triple Helix vs. DNA	-132.3	-249.2 to -15.40	Yes	*	0.0237
MALAT1 Triple Helix vs. tRNA	-4.797	-121.7 to 112.1	No	ns	>0.9999
MALAT1 Triple Helix vs. RRE	-287.3	-404.2 to -170.4	Yes	****	<0.0001
MALAT1 Triple Helix vs. NEAT1 Triple Helix	-184.8	-301.7 to -67.93	Yes	**	0.0020
MALAT1 Stem Loop vs. DNA	-75.70	-192.6 to 41.18	No	ns	0.3151
MALAT1 Stem Loop vs. tRNA	51.78	-65.10 to 168.7	No	ns	0.6776
MALAT1 Stem Loop vs. RRE	-230.7	-347.6 to -113.8	Yes	***	0.0003
MALAT1 Stem Loop vs. NEAT1 Triple Helix	-128.2	-245.1 to -11.35	Yes	*	0.0289
DNA vs. tRNA	127.5	10.60 to 244.4	Yes	*	0.0299
DNA vs. RRE	-155.0	-271.9 to -38.12	Yes	**	0.0079
DNA vs. NEAT1 Triple Helix	-52.53	-169.4 to 64.35	No	ns	0.6652
tRNA vs. RRE	-282.5	-399.4 to -165.6	Yes	****	<0.0001
tRNA vs. NEAT1 Triple Helix	-180.0	-296.9 to -63.13	Yes	**	0.0025
RRE vs. NEAT1 Triple Helix	102.5	-14.42 to 219.3	No	ns	0.0991

Figure S13. Statistical analysis for the selectivity screen of DPFp13. One-way ANOVA followed by Tukey's multiple comparisons test was performed using GraphPad Prism version 8.0.2 for Macintosh, GraphPad Software, La Jolla California USA, www.graphpad.com. Summary of P-values: ns = 0.1234, * = 0.0332, ** = 0.0021, *** = 0.0002, **** = <0.0001.

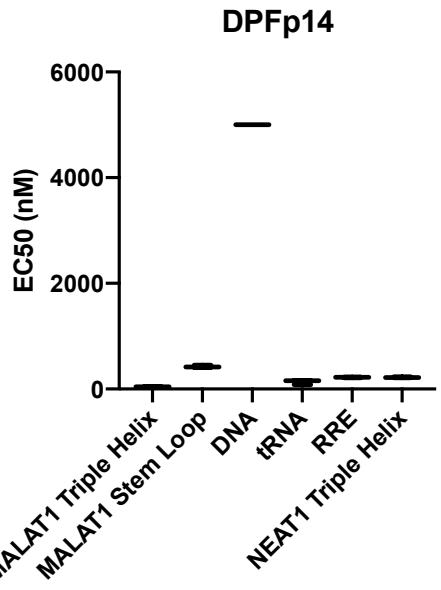

Tukey's multiple comparisons test	Mean Diff.	95.00% CI of diff.	Significant?	Summary	Adjusted P Value
MALAT1 Triple Helix vs. MALAT1 Stem Loop	-385.9	-444.3 to -327.6	Yes	****	<0.0001
MALAT1 Triple Helix vs. DNA	-4958	-5016 to -4900	Yes	****	<0.0001
MALAT1 Triple Helix vs. tRNA	-91.53	-149.9 to -33.17	Yes	**	0.0021
MALAT1 Triple Helix vs. RRE	-173.9	-232.3 to -115.6	Yes	****	<0.0001
MALAT1 Triple Helix vs. NEAT1 Triple Helix	-180.9	-239.3 to -122.5	Yes	****	<0.0001
MALAT1 Stem Loop vs. DNA	-4572	-4630 to -4514	Yes	****	<0.0001
MALAT1 Stem Loop vs. tRNA	294.4	236.0 to 352.8	Yes	****	<0.0001
MALAT1 Stem Loop vs. RRE	212.0	153.6 to 270.4	Yes	****	<0.0001
MALAT1 Stem Loop vs. NEAT1 Triple Helix	205.0	146.7 to 263.4	Yes	****	<0.0001
DNA vs. tRNA	4866	4808 to 4925	Yes	****	<0.0001
DNA vs. RRE	4784	4726 to 4842	Yes	****	<0.0001
DNA vs. NEAT1 Triple Helix	4777	4719 to 4835	Yes	****	<0.0001
tRNA vs. RRE	-82.40	-140.8 to -24.04	Yes	**	0.0049
tRNA vs. NEAT1 Triple Helix	-89.36	-147.7 to -31.00	Yes	**	0.0026
RRE vs. NEAT1 Triple Helix	-6.967	-65.33 to 51.39	No	ns	0.9983

Figure S14. Statistical analysis for the selectivity screen of DPFp14. One-way ANOVA followed by Tukey's multiple comparisons test was performed using GraphPad Prism version 8.0.2 for Macintosh, GraphPad Software, La Jolla California USA, www.graphpad.com. Summary of P-values: ns = 0.1234, * = 0.0332, ** = 0.0021, *** = 0.0002, **** = <0.0001.

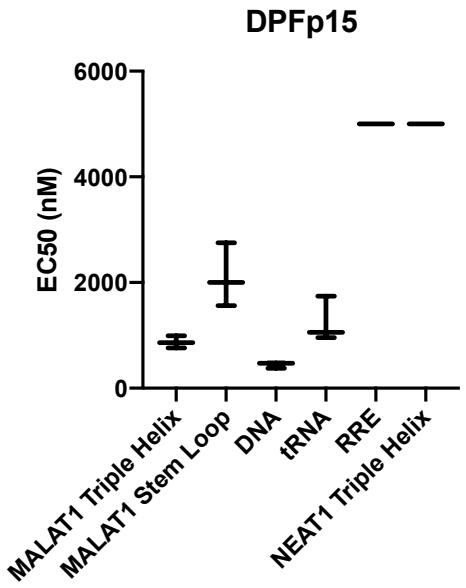

Tukey's multiple comparisons test	Mean Diff.	95.00% CI of diff.	Significant?	Summary	Adjusted P Value
MALAT1 Triple Helix vs. MALAT1 Stem Loop	-1231	-2068 to -393.2	Yes	**	0.0036
MALAT1 Triple Helix vs. DNA	431.9	-405.7 to 1269	No	ns	0.5381
MALAT1 Triple Helix vs. tRNA	-377.3	-1215 to 460.3	No	ns	0.6633
MALAT1 Triple Helix vs. RRE	-4126	-4963 to -3288	Yes	****	<0.0001
MALAT1 Triple Helix vs. NEAT1 Triple Helix	-4126	-4963 to -3288	Yes	****	<0.0001
MALAT1 Stem Loop vs. DNA	1663	825.0 to 2500	Yes	***	0.0003
MALAT1 Stem Loop vs. tRNA	853.4	15.82 to 1691	Yes	*	0.0450
MALAT1 Stem Loop vs. RRE	-2895	-3733 to -2057	Yes	****	<0.0001
MALAT1 Stem Loop vs. NEAT1 Triple Helix	-2895	-3733 to -2057	Yes	****	<0.0001
DNA vs. tRNA	-809.2	-1647 to 28.41	No	ns	0.0605
DNA vs. RRE	-4558	-5395 to -3720	Yes	****	<0.0001
DNA vs. NEAT1 Triple Helix	-4558	-5395 to -3720	Yes	****	<0.0001
tRNA vs. RRE	-3748	-4586 to -2911	Yes	****	<0.0001
tRNA vs. NEAT1 Triple Helix	-3748	-4586 to -2911	Yes	****	<0.0001
RRE vs. NEAT1 Triple Helix	0.000	-837.6 to 837.6	No	ns	>0.9999

Figure S15. Statistical analysis for the selectivity screen of DPFp15. One-way ANOVA followed by Tukey's multiple comparisons test was performed using GraphPad Prism version 8.0.2 for Macintosh, GraphPad Software, La Jolla California USA, www.graphpad.com. Summary of P-values: ns = 0.1234, * = 0.0332, ** = 0.0021, *** = 0.0002, **** = <0.0001.

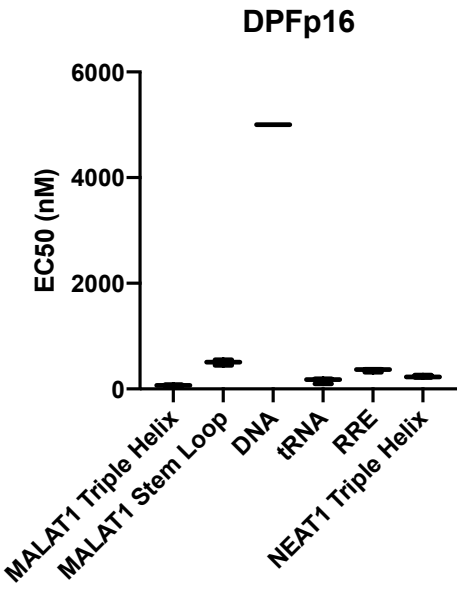

Tukey's multiple comparisons test	Mean Diff.	95.00% CI of diff.	Significant?	Summary	Adjusted P Value
MALAT1 Triple Helix vs. MALAT1 Stem Loop	-438.8	-533.3 to -344.2	Yes	****	<0.0001
MALAT1 Triple Helix vs. DNA	-4937	-5031 to -4842	Yes	****	<0.0001
MALAT1 Triple Helix vs. tRNA	-93.38	-187.9 to 1.156	No	ns	0.0536
MALAT1 Triple Helix vs. RRE	-288.2	-382.7 to -193.6	Yes	****	<0.0001
MALAT1 Triple Helix vs. NEAT1 Triple Helix	-174.2	-268.8 to -79.68	Yes	***	0.0005
MALAT1 Stem Loop vs. DNA	-4498	-4593 to -4403	Yes	****	<0.0001
MALAT1 Stem Loop vs. tRNA	345.4	250.8 to 439.9	Yes	****	<0.0001
MALAT1 Stem Loop vs. RRE	150.6	56.03 to 245.1	Yes	**	0.0019
MALAT1 Stem Loop vs. NEAT1 Triple Helix	264.5	170.0 to 359.1	Yes	****	<0.0001
DNA vs. tRNA	4843	4749 to 4938	Yes	****	<0.0001
DNA vs. RRE	4649	4554 to 4743	Yes	****	<0.0001
DNA vs. NEAT1 Triple Helix	4763	4668 to 4857	Yes	****	<0.0001
tRNA vs. RRE	-194.8	-289.3 to -100.3	Yes	***	0.0002
tRNA vs. NEAT1 Triple Helix	-80.84	-175.4 to 13.70	No	ns	0.1114
RRE vs. NEAT1 Triple Helix	114.0	19.43 to 208.5	Yes	*	0.0156

Figure S16. Statistical analysis for the selectivity screen of DPFp16. One-way ANOVA followed by Tukey's multiple comparisons test was performed using GraphPad Prism version 8.0.2 for Macintosh, GraphPad Software, La Jolla California USA, www.graphpad.com. Summary of P-values: ns = 0.1234, * = 0.0332, ** = 0.0021, *** = 0.0002, **** = <0.0001.

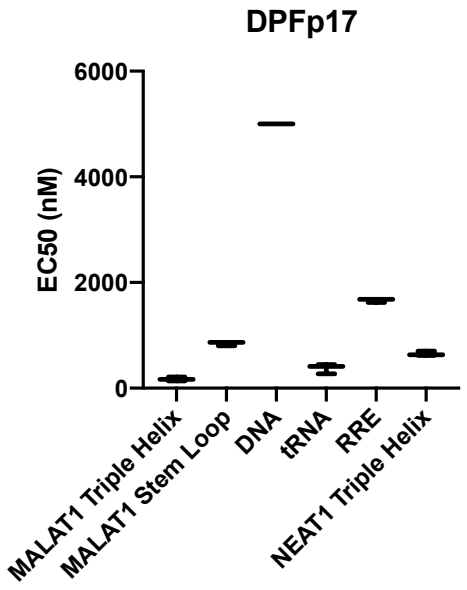

Tukey's multiple comparisons test	Mean Diff.	95.00% CI of diff.	Significant?	Summary	Adjusted P Value
MALAT1 Triple Helix vs. MALAT1 Stem Loop	-673.9	-810.2 to -537.7	Yes	****	<0.0001
MALAT1 Triple Helix vs. DNA	-4828	-4965 to -4692	Yes	****	<0.0001
MALAT1 Triple Helix vs. tRNA	-204.9	-341.2 to -68.66	Yes	**	0.0030
MALAT1 Triple Helix vs. RRE	-1491	-1627 to -1354	Yes	****	<0.0001
MALAT1 Triple Helix vs. NEAT1 Triple Helix	-479.2	-615.5 to -343.0	Yes	****	<0.0001
MALAT1 Stem Loop vs. DNA	-4154	-4291 to -4018	Yes	****	<0.0001
MALAT1 Stem Loop vs. tRNA	469.0	332.7 to 605.3	Yes	****	<0.0001
MALAT1 Stem Loop vs. RRE	-816.7	-952.9 to -680.4	Yes	****	<0.0001
MALAT1 Stem Loop vs. NEAT1 Triple Helix	194.7	58.43 to 331.0	Yes	**	0.0045
DNA vs. tRNA	4623	4487 to 4760	Yes	****	<0.0001
DNA vs. RRE	3338	3201 to 3474	Yes	****	<0.0001
DNA vs. NEAT1 Triple Helix	4349	4213 to 4485	Yes	****	<0.0001
tRNA vs. RRE	-1286	-1422 to -1149	Yes	****	<0.0001
tRNA vs. NEAT1 Triple Helix	-274.3	-410.6 to -138.0	Yes	***	0.0002
RRE vs. NEAT1 Triple Helix	1011	875.1 to 1148	Yes	****	<0.0001

Figure S17. Statistical analysis for the selectivity screen of DPFp17. One-way ANOVA followed by Tukey's multiple comparisons test was performed using GraphPad Prism version 8.0.2 for Macintosh, GraphPad Software, La Jolla California USA, www.graphpad.com. Summary of P-values: ns = 0.1234, * = 0.0332, ** = 0.0021, *** = 0.0002, **** = <0.0001.

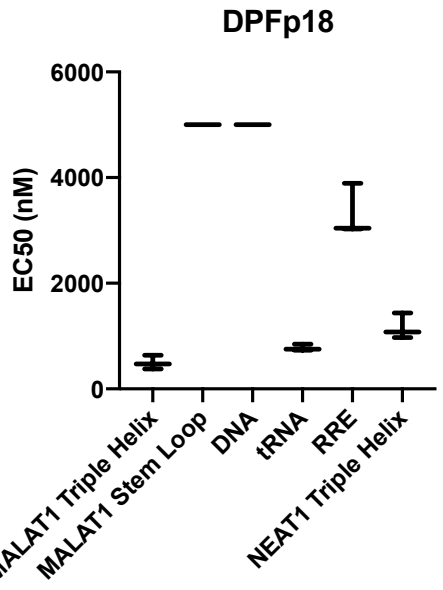

Tukey's multiple comparisons test	Mean Diff.	95.00% CI of diff.	Significant?	Summary	Adjusted P Value
MALAT1 Triple Helix vs. MALAT1 Stem Loop	-4505	-5143 to -3867	Yes	****	<0.0001
MALAT1 Triple Helix vs. DNA	-4505	-5143 to -3867	Yes	****	<0.0001
MALAT1 Triple Helix vs. tRNA	-283.1	-921.1 to 354.9	No	ns	0.6762
MALAT1 Triple Helix vs. RRE	-2826	-3464 to -2188	Yes	****	<0.0001
MALAT1 Triple Helix vs. NEAT1 Triple Helix	-665.6	-1304 to -27.57	Yes	*	0.0392
MALAT1 Stem Loop vs. DNA	0.000	-638.0 to 638.0	No	ns	>0.9999
MALAT1 Stem Loop vs. tRNA	4222	3584 to 4859	Yes	****	<0.0001
MALAT1 Stem Loop vs. RRE	1679	1041 to 2317	Yes	****	<0.0001
MALAT1 Stem Loop vs. NEAT1 Triple Helix	3839	3201 to 4477	Yes	****	<0.0001
DNA vs. tRNA	4222	3584 to 4859	Yes	****	<0.0001
DNA vs. RRE	1679	1041 to 2317	Yes	****	<0.0001
DNA vs. NEAT1 Triple Helix	3839	3201 to 4477	Yes	****	<0.0001
tRNA vs. RRE	-2543	-3180 to -1905	Yes	****	<0.0001
tRNA vs. NEAT1 Triple Helix	-382.5	-1020 to 255.5	No	ns	0.3888
RRE vs. NEAT1 Triple Helix	2160	1522 to 2798	Yes	****	<0.0001

Figure S18. Statistical analysis for the selectivity screen of DPFp18. One-way ANOVA followed by Tukey's multiple comparisons test was performed using GraphPad Prism version 8.0.2 for Macintosh, GraphPad Software, La Jolla California USA, www.graphpad.com. Summary of P-values: ns = 0.1234, * = 0.0332, ** = 0.0021, *** = 0.0002, **** = <0.0001.

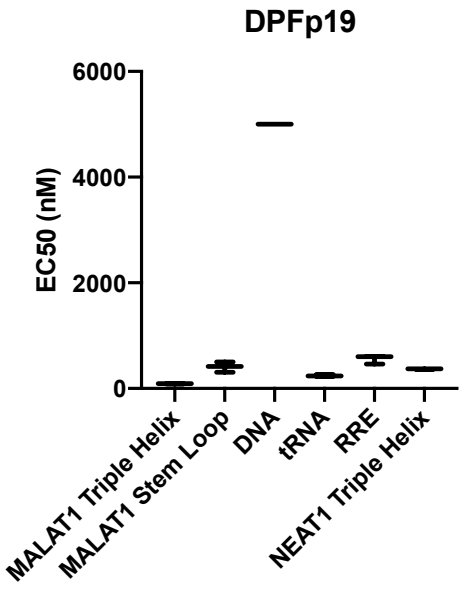

Tukey's multiple comparisons test	Mean Diff.	95.00% CI of diff.	Significant?	Summary	Adjusted P Value
MALAT1 Triple Helix vs. MALAT1 Stem Loop	-319.0	-463.9 to -174.0	Yes	****	<0.0001
MALAT1 Triple Helix vs. DNA	-4910	-5055 to -4765	Yes	****	<0.0001
MALAT1 Triple Helix vs. tRNA	-153.4	-298.3 to -8.410	Yes	*	0.0360
MALAT1 Triple Helix vs. RRE	-466.9	-611.8 to -321.9	Yes	****	<0.0001
MALAT1 Triple Helix vs. NEAT1 Triple Helix	-277.5	-422.4 to -132.5	Yes	***	0.0004
MALAT1 Stem Loop vs. DNA	-4591	-4736 to -4446	Yes	****	<0.0001
MALAT1 Stem Loop vs. tRNA	165.6	20.68 to 310.6	Yes	*	0.0223
MALAT1 Stem Loop vs. RRE	-147.9	-292.9 to -2.947	Yes	*	0.0446
MALAT1 Stem Loop vs. NEAT1 Triple Helix	41.53	-103.4 to 186.5	No	ns	0.9214
DNA vs. tRNA	4756	4611 to 4901	Yes	****	<0.0001
DNA vs. RRE	4443	4298 to 4588	Yes	****	<0.0001
DNA vs. NEAT1 Triple Helix	4632	4487 to 4777	Yes	****	<0.0001
tRNA vs. RRE	-313.5	-458.5 to -168.6	Yes	***	0.0001
tRNA vs. NEAT1 Triple Helix	-124.1	-269.1 to 20.85	No	ns	0.1107
RRE vs. NEAT1 Triple Helix	189.4	44.48 to 334.4	Yes	**	0.0088

Figure S19. Statistical analysis for the selectivity screen of DPFp19. One-way ANOVA followed by Tukey's multiple comparisons test was performed using GraphPad Prism version 8.0.2 for Macintosh, GraphPad Software, La Jolla California USA, www.graphpad.com. Summary of P-values: ns = 0.1234, * = 0.0332, ** = 0.0021, *** = 0.0002, **** = <0.0001.

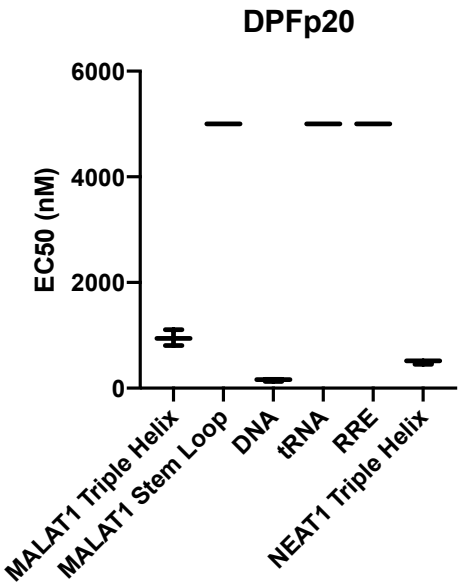

Tukey's multiple comparisons test	Mean Diff.	95.00% CI of diff.	Significant?	Summary	Adjusted P Value
MALAT1 Triple Helix vs. MALAT1 Stem Loop	-4047	-4222 to -3872	Yes	****	<0.0001
MALAT1 Triple Helix vs. DNA	799.9	625.1 to 974.7	Yes	****	<0.0001
MALAT1 Triple Helix vs. tRNA	-4047	-4222 to -3872	Yes	****	<0.0001
MALAT1 Triple Helix vs. RRE	-4047	-4222 to -3872	Yes	****	<0.0001
MALAT1 Triple Helix vs. NEAT1 Triple Helix	458.4	283.6 to 633.2	Yes	****	<0.0001
MALAT1 Stem Loop vs. DNA	4847	4672 to 5022	Yes	****	<0.0001
MALAT1 Stem Loop vs. tRNA	0.000	-174.8 to 174.8	No	ns	>0.9999
MALAT1 Stem Loop vs. RRE	0.000	-174.8 to 174.8	No	ns	>0.9999
MALAT1 Stem Loop vs. NEAT1 Triple Helix	4506	4331 to 4680	Yes	****	<0.0001
DNA vs. tRNA	-4847	-5022 to -4672	Yes	****	<0.0001
DNA vs. RRE	-4847	-5022 to -4672	Yes	****	<0.0001
DNA vs. NEAT1 Triple Helix	-341.5	-516.3 to -166.7	Yes	***	0.0003
tRNA vs. RRE	0.000	-174.8 to 174.8	No	ns	>0.9999
tRNA vs. NEAT1 Triple Helix	4506	4331 to 4680	Yes	****	<0.0001
RRE vs. NEAT1 Triple Helix	4506	4331 to 4680	Yes	****	<0.0001

Figure S20. Statistical analysis for the selectivity screen of DPFp20. One-way ANOVA followed by Tukey's multiple comparisons test was performed using GraphPad Prism version 8.0.2 for Macintosh, GraphPad Software, La Jolla California USA, www.graphpad.com. Summary of P-values: ns = 0.1234, * = 0.0332, ** = 0.0021, *** = 0.0002, **** = <0.0001.

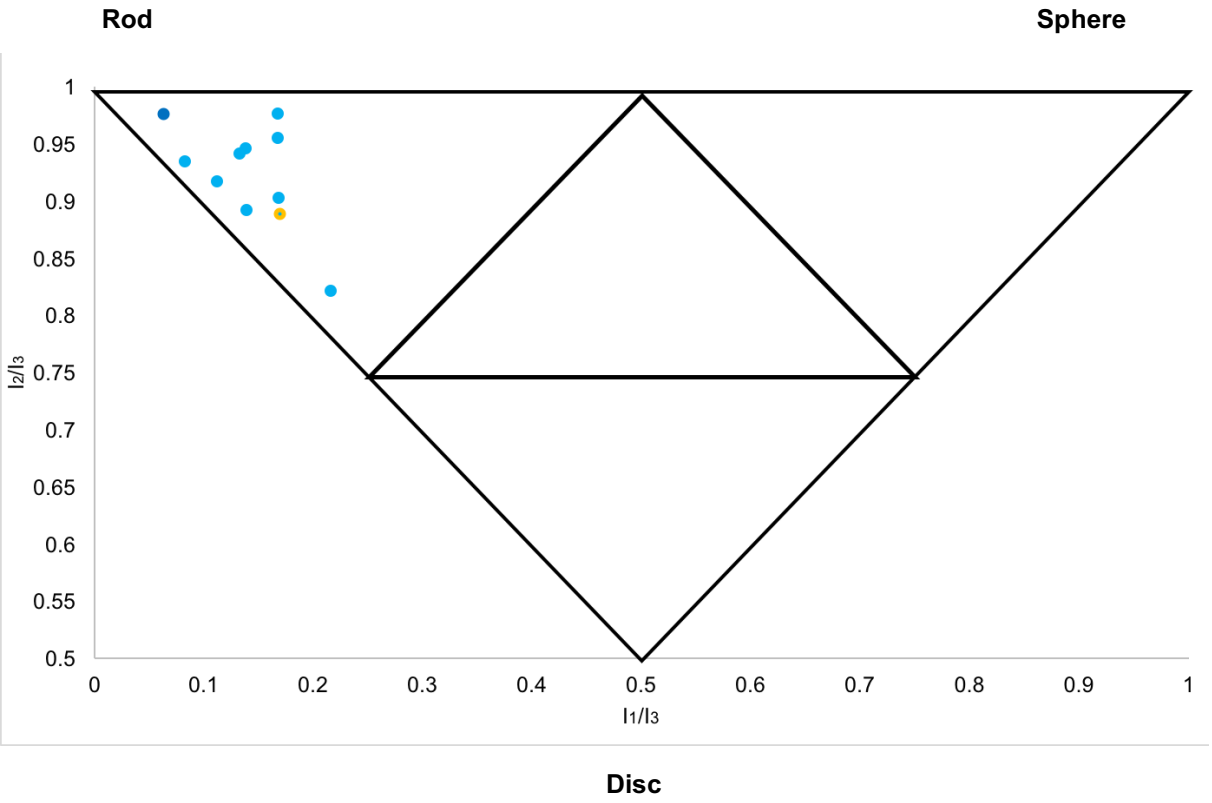

Figure S21. Principal moments of inertia (PMI) plot of the next-generation DPF ligands (light blue), DPFp8 (dark blue), and DPFp7 (orange). Details for calculations and plot generation are described in the Materials and Methods Section.

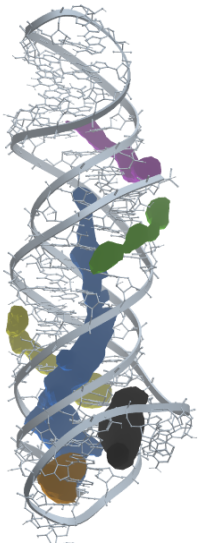

Figure S22. Depiction of the six binding pockets predicted by ICM for the MALAT1 triple helix structure (PDB ID: 4PLX, pocket 1 = blue; pocket 2 = yellow; pocket 3 =black; pocket 4 = green; pocket 5 = orange; pocket 6 =purple). Pocket numbering was assigned arbitrarily.

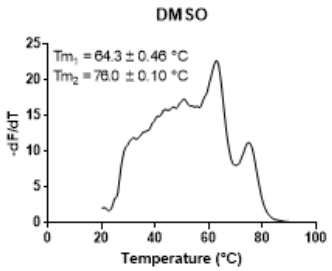
DMSO
Tm1 = 64.3 ± 0.46 °C
Tm2 = 76.0 ± 0.10 °C
-dF/dT
Temperature (°C)

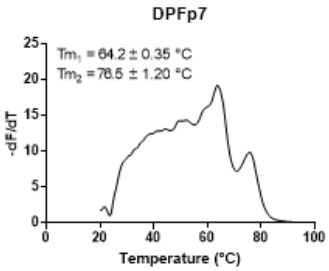
DPFp7
Tm1 = 64.2 ± 0.35 °C
Tm2 = 76.5 ± 1.20 °C
-dF/dT
Temperature (°C)

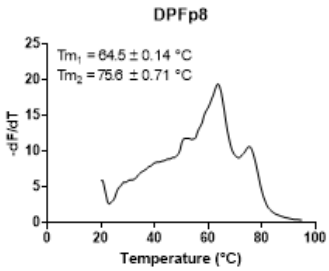
DPFp8
Tm1 = 64.5 ± 0.14 °C
Tm2 = 75.6 ± 0.71 °C
-dF/dT
Temperature (°C)

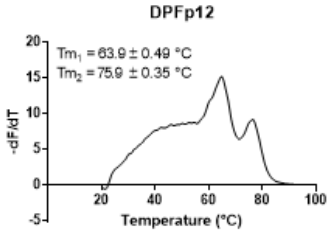
DPFp12
Tm1 = 63.9 ± 0.49 °C
Tm2 = 75.9 ± 0.35 °C
-dF/dT
Temperature (°C)

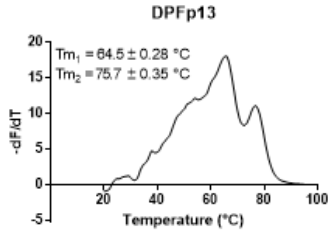
DPFp13
Tm1 = 64.5 ± 0.28 °C
Tm2 = 75.7 ± 0.35 °C
-dF/dT
Temperature (°C)

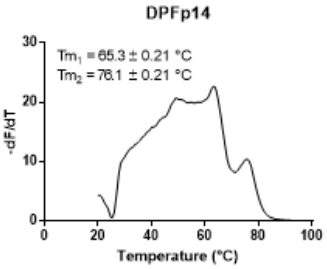
DPFp14
Tm1 = 65.3 ± 0.21 °C
Tm2 = 76.1 ± 0.21 °C
-dF/dT
Temperature (°C)

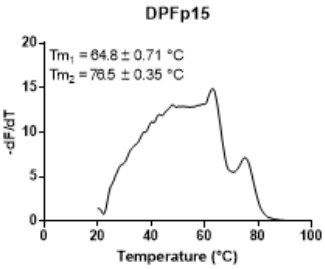
DPFp15
Tm1 = 64.8 ± 0.71 °C
Tm2 = 76.5 ± 0.35 °C
-dF/dT
Temperature (°C)

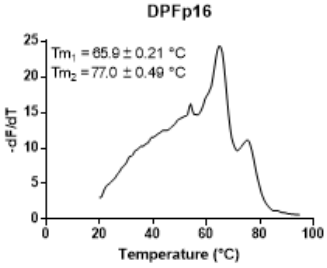
DPFp16
Tm1 = 65.9 ± 0.21 °C
Tm2 = 77.0 ± 0.49 °C
-dF/dT
Temperature (°C)

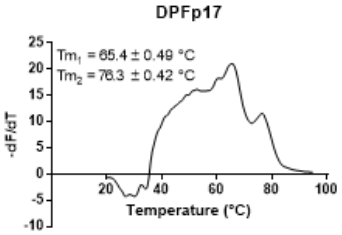
DPFp17
Tm1 = 65.4 ± 0.49 °C
Tm2 = 76.3 ± 0.42 °C
-dF/dT
Temperature (°C)

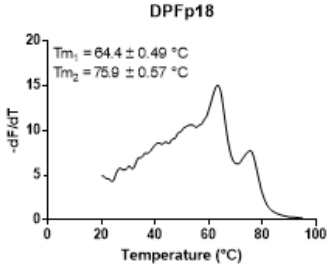
DPFp18
Tm1 = 64.4 ± 0.49 °C
Tm2 = 75.9 ± 0.57 °C
-dF/dT
Temperature (°C)

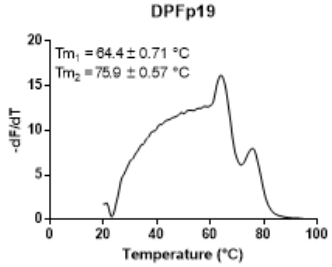
DPFp19
Tm1 = 64.4 ± 0.71 °C
Tm2 = 75.9 ± 0.57 °C
-dF/dT
Temperature (°C)

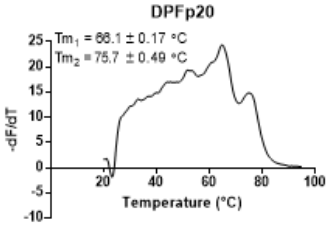
DPFp20
Tm1 = 66.1 ± 0.17 °C
Tm2 = 75.7 ± 0.49 °C
-dF/dT
Temperature (°C)

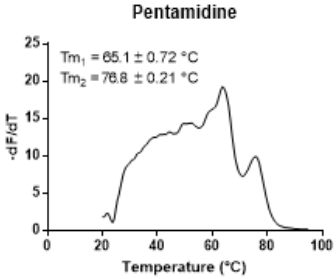
Pentamidine
Tm1 = 65.1 ± 0.72 °C
Tm2 = 76.8 ± 0.21 °C
-dF/dT
Temperature (°C)

Figure S23. First derivative melting profiles of MALAT1 obtained via differential scanning fluorimetry (DSF) for the MALAT1 triple helix RNA upon addition of DMSO or DPFs in high-ionic buffer, Buffer 1 (20 mM HEPES-KOH pH 7.4 at 25 ºC, 152.6 mM KCl, 1 mM $MgCl_2$). T_m1 is proposed to be the melting temperature of the Hoogsteen base-paired, triplex-forming strand; and T_m2 is proposed to be the melting temperature of the remaining structure(2). Errors represent the standard deviation of three independent experiments. ΔT_m errors were calculated through standard error propagation.

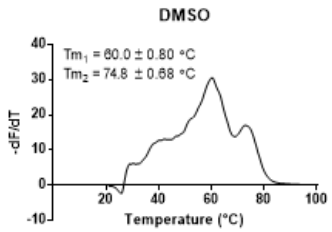
DMSO
Tm1 = 60.0 ± 0.80 °C
Tm2 = 74.8 ± 0.68 °C
-dF/dT
Temperature (°C)

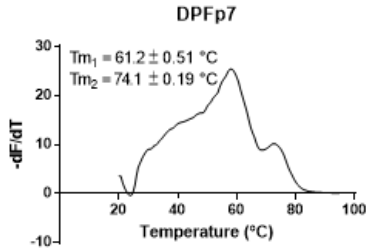
DPFp7
Tm1 = 61.2 ± 0.51 °C
Tm2 = 74.1 ± 0.19 °C
-dF/dT
Temperature (°C)

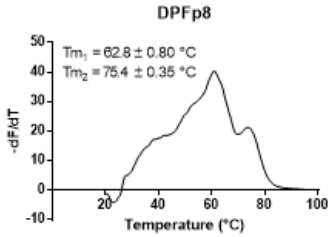
DPFp8
Tm1 = 62.8 ± 0.80 °C
Tm2 = 75.4 ± 0.35 °C
-dF/dT
Temperature (°C)

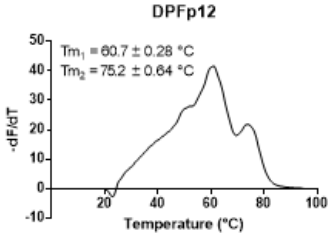
DPFp12
Tm1 = 60.7 ± 0.28 °C
Tm2 = 75.2 ± 0.64 °C
-dF/dT
Temperature (°C)

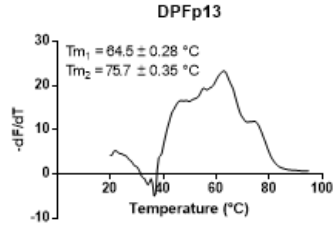
DPFp13
Tm1 = 64.5 ± 0.28 °C
Tm2 = 75.7 ± 0.35 °C
-dF/dT
Temperature (°C)

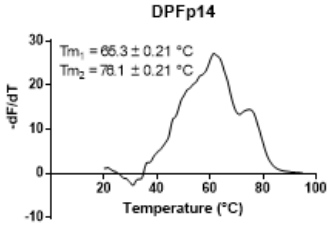
DPFp14
Tm1 = 65.3 ± 0.21 °C
Tm2 = 78.1 ± 0.21 °C
-dF/dT
Temperature (°C)

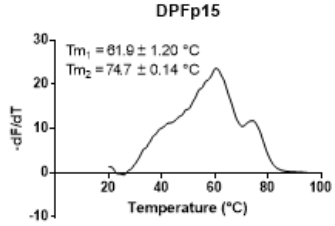
DPFp15
Tm1 = 61.9 ± 1.20 °C
Tm2 = 74.7 ± 0.14 °C
-dF/dT
Temperature (°C)

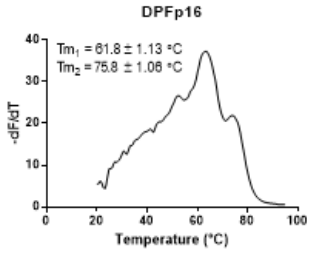
DPFp16
Tm1 = 61.8 ± 1.13 °C
Tm2 = 75.8 ± 1.06 °C
-dF/dT
Temperature (°C)

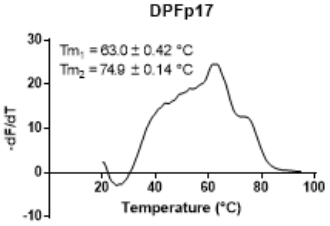
DPFp17
Tm1 = 63.0 ± 0.42 °C
Tm2 = 74.9 ± 0.14 °C
-dF/dT
Temperature (°C)

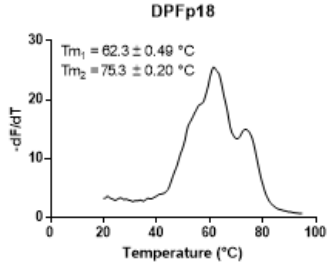
DPFp18
Tm1 = 62.3 ± 0.49 °C
Tm2 = 75.3 ± 0.20 °C
-dF/dT
Temperature (°C)

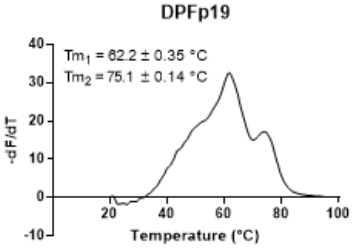
DPFp19
Tm1 = 62.2 ± 0.35 °C
Tm2 = 75.1 ± 0.14 °C
-dF/dT
Temperature (°C)

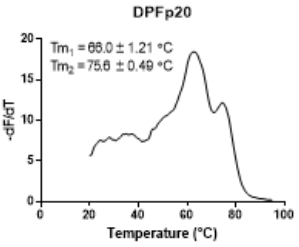
DPFp20
Tm1 = 66.0 ± 1.21 °C
Tm2 = 75.6 ± 0.49 °C
-dF/dT
Temperature (°C)

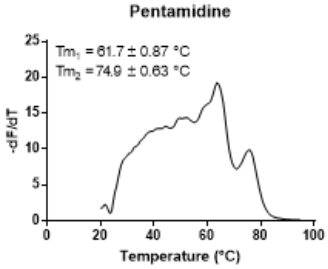
Pentamidine
Tm1 = 61.7 ± 0.87 °C
Tm2 = 74.9 ± 0.63 °C
-dF/dT
Temperature (°C)

Figure S24. First derivative melting profiles obtained via differential scanning fluorimetry (DSF) for the MALAT1 triple helix RNA upon addition of DMSO or DPFs in low ionic buffer, Buffer 2 (20 mM HEPES-KOH pH 7.4 at 25 ºC, 52 mM KCl, 0.1 mM $MgCl_2$). T_m1 is proposed to be the melting temperature of the Hoogsteen base-paired, triplex-forming strand; and T_m2 is proposed to be the melting temperature of the remaining structure(2). Errors represent the standard deviation of three independent experiments. ΔT_m errors were calculated through standard error propagation.

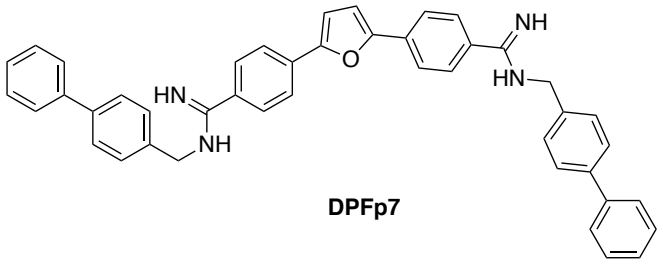

DPFp7

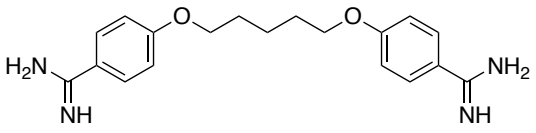

Pentamidine

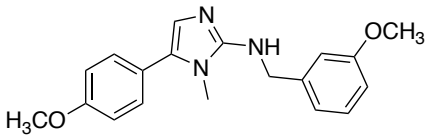

SM5

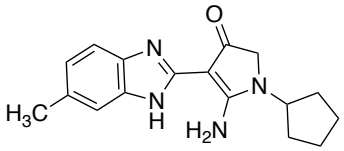

SM16

Figure S25. Structures of additional small molecules utilized in this study that were not synthesized in this work. **DPFp7** (4,4'-(furan-2,5-diyl)bis(*N*-([1,1'-biphenyl]-4-ylmethyl)benzimidamide)) was a previously reported non-binder of the MALAT1 triple helix and stem loop by Hargrove and co-workers(1). Pentamidine (4,4'-(pentane-1,5-diylbis(oxy))dibenzimidamide) is a known and promiscuous RNA-binding diamidine(3-6). **SM5** (*N*-(3-methoxybenzyl)-5-(4-methoxyphenyl)-1-methyl-1*H*-imidazol-2-amine) and **SM16** (5-amino-1-cyclopentyl-4-(6-methyl-1*H*-benzo[*d*]imidazol-2-yl)-1,2-dihydro-3*H*-pyrrol-3-one) are MALAT1 triple helix-destabilizing molecules as reported by Le Grice and co-workers(7).

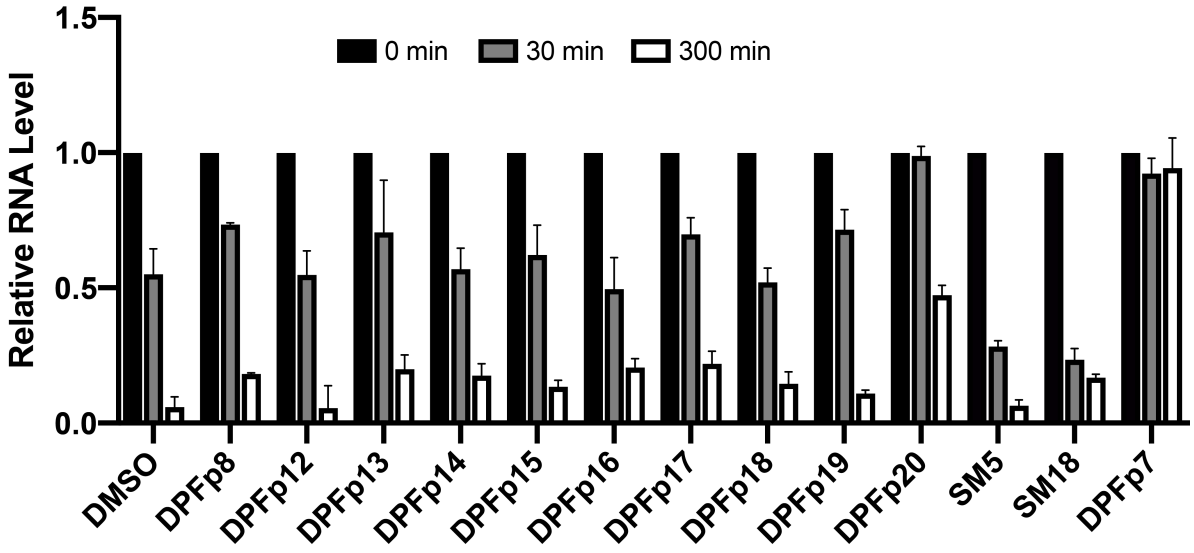

Figure S26. Results of RNase R exonucleolytic degradation experiments as observed by denaturing gel electrophoresis and quantified by ImageJ software(8) as described in Materials and Methods Section. 0.2 μM RNA and 0.2 μM DPF or 1 μM SM5 or SM16 were incubated with 5U of RNase R in low ionic buffer conditions. No degradation was observed without RNase R over the time course monitored.

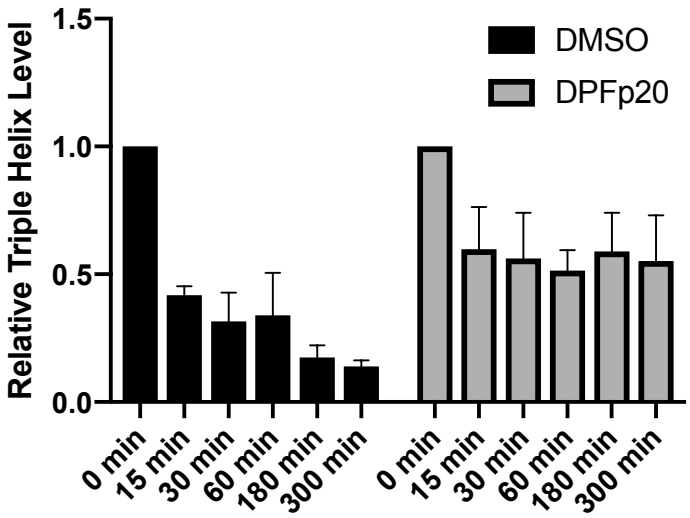

Figure S27. Semi-quantitative denaturing PAGE gel analysis of RNase R exonucleolytic degradation control experiment with 5 time points using Image J software (1.52k) (8) to ensure linear phase decay. Measurements beyond the 5 h timepoint were not taken as very low levels of RNA remain at that point, not allowing for accurate quantification and assessment of linear decay afterwards. While the 30 min timepoint appears to be at the border of linear decay, it is the earliest time point that enabled us to see clear differences between the different DPF ligands and thus rank their relative protective effects. 0.2 μM RNA and 0.2 μM DPF or DMSO were incubated with 5U of RNase R in low ionic buffer conditions (20 mM HEPES-KOH pH 7.4 at 25 ºC, 52 mM KCl, 0.1 mM $MgCl_2$). Values are normalized to Timepoint 0 and the loading control as described in "RNase R Exonucleolytic Degradation Experiments" of Materials and Methods. Error bars represent standard deviation from three independent experiments.

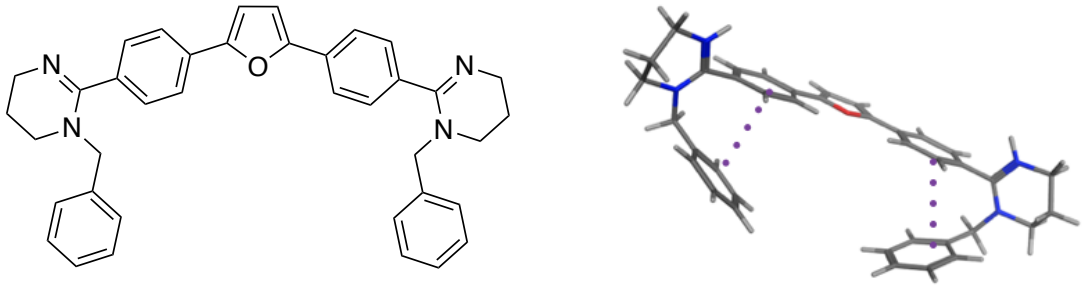

Figure S28. Structure of **DPFp12** and its low energy conformer (ΔE = 0) from computational calculations in the Molecular Operating Environment (MOE) conformational search. Purple dots indicate face-to-face intramolecular π-π interactions.

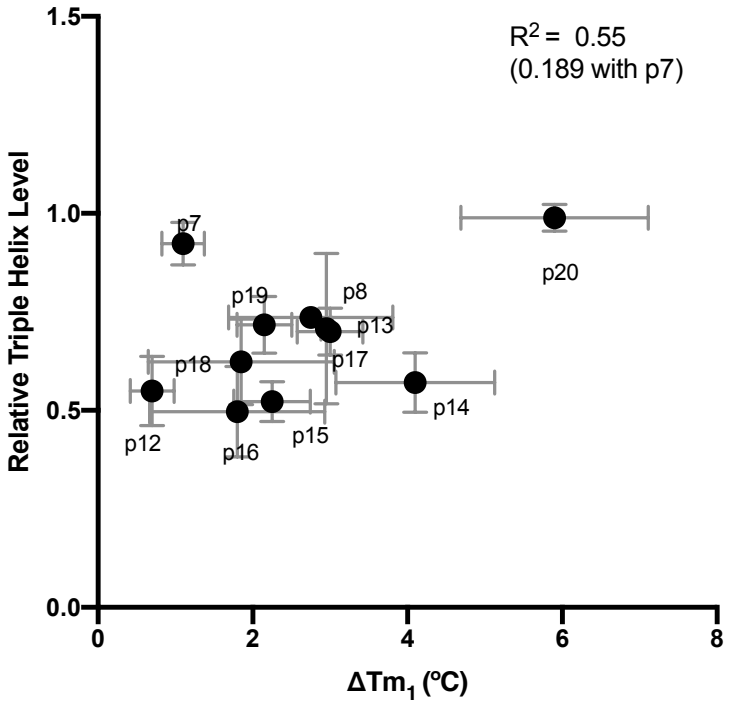

Figure S29. Correlation between melting temperature shifts as measured by DSF experiments in low ionic buffer conditions and level of MALAT1 Triple Helix at the 30 min timepoint during an RNase R incubation in low ionic buffer conditions as measured by denaturing gel electrophoresis and quantified in ImageJ software. The value was measured relative to the loading control and the 0 min timepoint sample. Melting temperature denotes the first peak in the first derivative graph of the melting profile, proposed to be the triple helix-melting peak(2). ΔT_m = T_m (DPF) – T_m (DMSO). Errors represent standard deviation from three independent experiments.

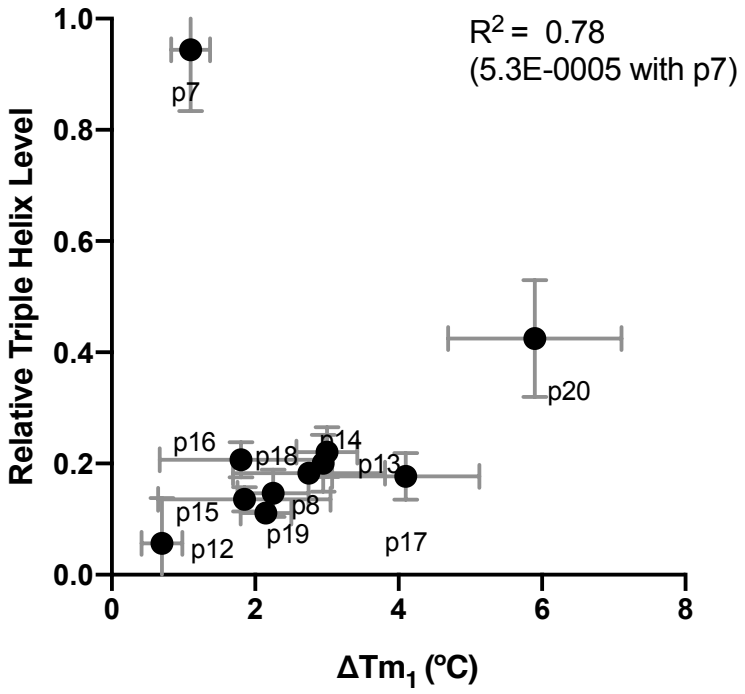

Figure S30. Correlation between melting temperature shifts as measured by DSF experiments in low ionic buffer conditions and level of MALAT1 Triple Helix at the 300 min timepoint during an RNase R incubation in low ionic buffer conditions as measured by denaturing gel electrophoresis and quantified in ImageJ software. The value was measured relative to the loading control and the 0 min timepoint sample. Melting temperature denotes the first peak in the first derivative graph of the melting profile, proposed to be the triple helix-melting peak(2). ΔT_m = T_m (DPF) – T_m (DMSO). Errors represent standard deviation from three independent experiments.

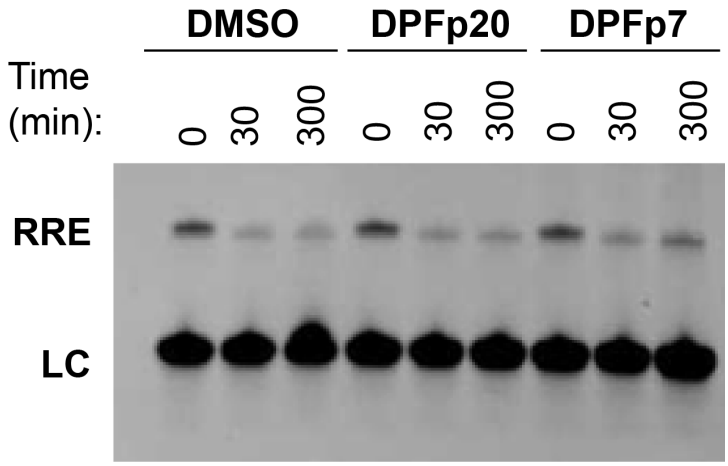

Supplementary Figure S31. Results of RNase R exonucleolytic degradation experiments as observed by denaturing gel electrophoresis and described in Materials and Methods section. 0.2 μM RNA and 0.2 μM DPF were incubated with 5U of RNase R in low ionic buffer conditions.

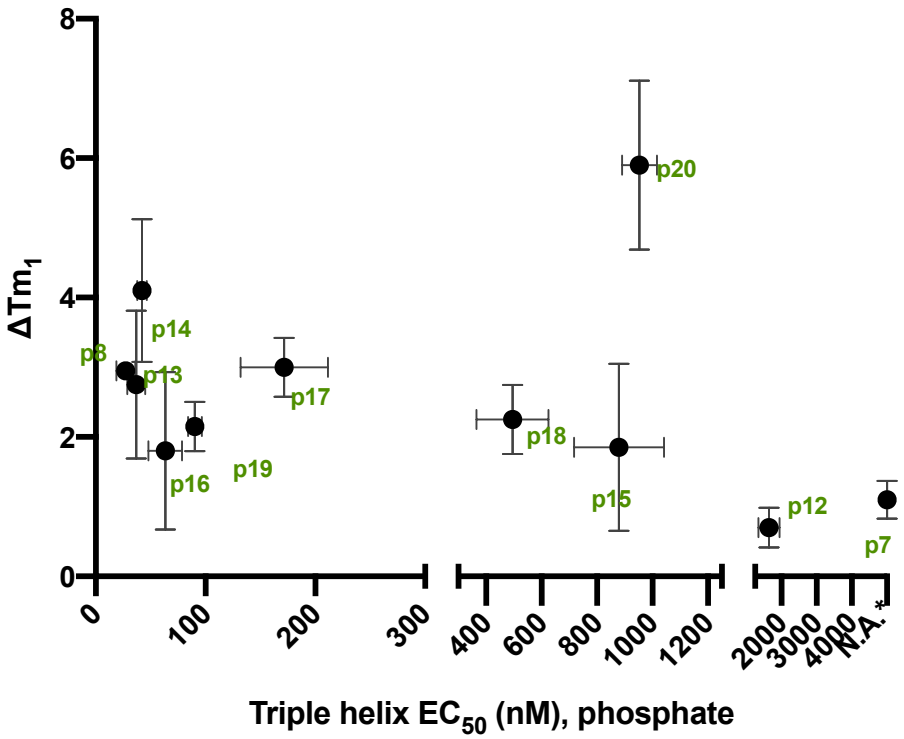

Figure S32. Correlation between EC_{50} values as measured by fluorescence-based titration experiments in phosphate screening buffer and thermal stabilization of the MALAT1 triple helix Tm_1 in low-ionic buffer conditions as measured by Differential Scanning Fluorimetry. Melting temperature denotes the first peak in the first derivative graph of the melting profile, proposed to be the triple helix-melting peak(2). $\Delta T_m = T_m$ (DPF) – T_m (DMSO). N.A.* - not available; indicates curves for which no EC_{50} value was obtained due to little to no change in DPF fluorescence. Errors represent standard deviation between three independent measurements.

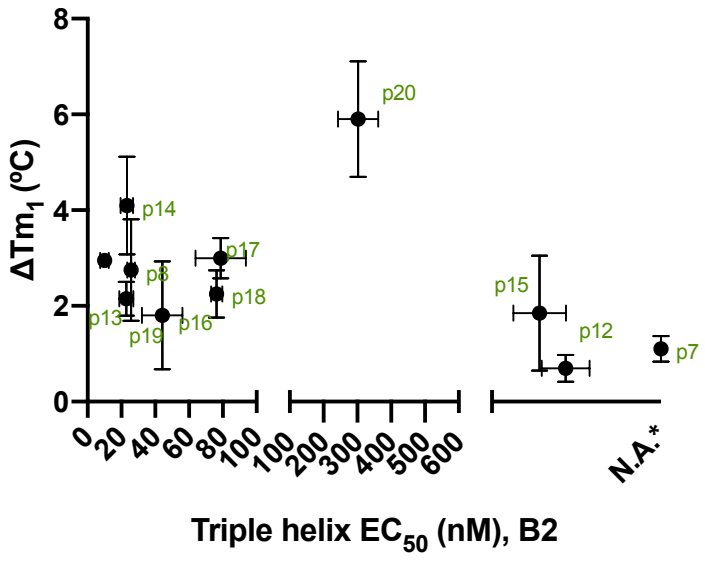

Figure S33. Correlation between EC_{50} values as measured by fluorescence-based titration experiments in low-ionic buffer, B2, and thermal stabilization of the MALAT1 triple helix Tm_1 in low-ionic buffer conditions as measured by Differential Scanning Fluorimetry. Melting temperature denotes the first peak in the first derivative graph of the melting profile, proposed to be the triple helix-melting peak(2). $\Delta T_m = T_m$ (DPF) – T_m (DMSO). N.A.* - not available; indicates curves for which no EC_{50} value was obtained due to little to no change in DPF fluorescence. Errors represent standard deviation between three independent measurements.

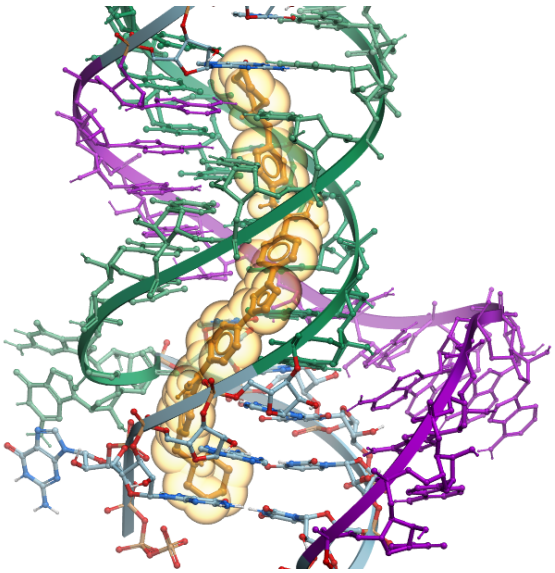

Figure S34. Docking result of DPFp20 in pocket 1 predicted by ICM. Note that intercalative binding modes are difficult to model and predict in docking programs(9). See Materials and Methods section for details.

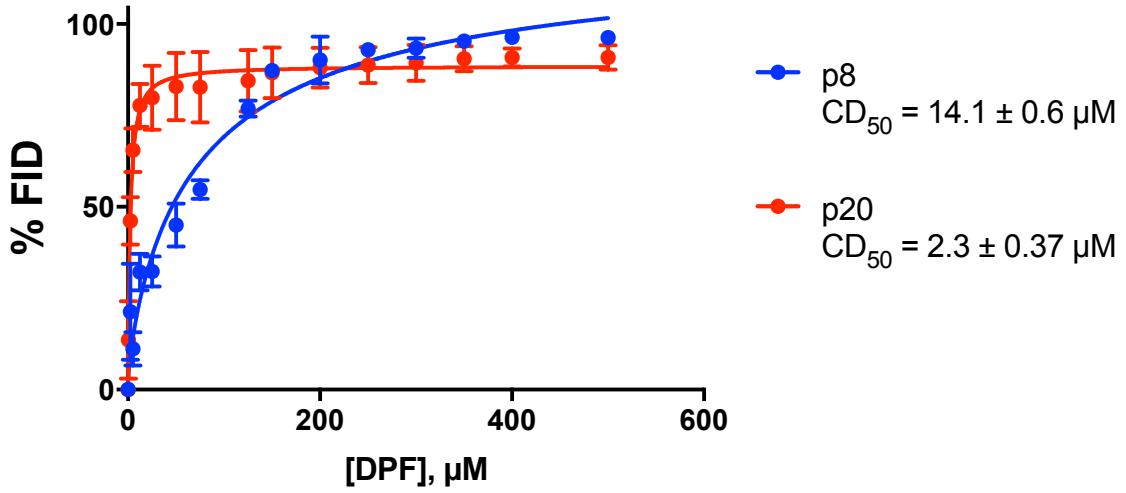

Figure S35. Fluorescence indicator displacement (FID) assay of intercalative ligand SYBR Green II and increasing concentrations of DPFp8 and p20 in low-ionic buffer conditions ((20 mM HEPES-KOH pH 7.4 at 25 ºC, 52 mM KCl, 0.1 mM $MgCl_2$). Error bars represent the standard deviation of three technical replicates. See Materials and Methods for CD_{50} value calculation. CD_{50} values represent averages of three independent experiments ± standard deviation.

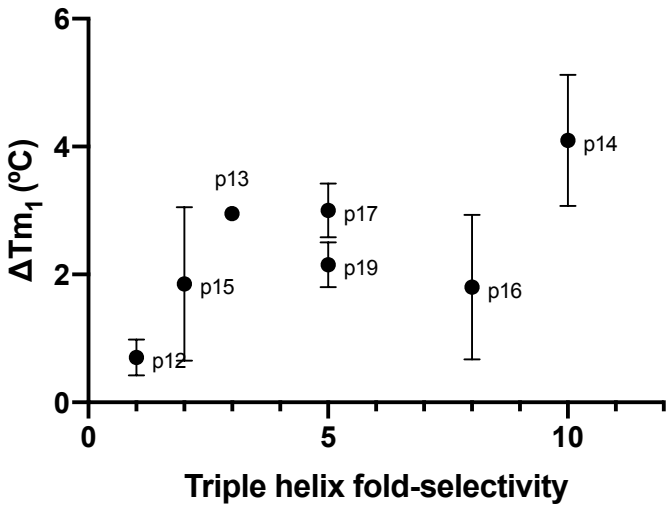

Figure S36. Correlation between triple helix fold-selectivity as measured by EC_{50} values from fluorescence binding experiments and increase in triple helix thermal stability as measured by DSF experiments in low-ionic buffer conditions. Fold-selectivity = EC_{50} (TH) / EC_{50} (SL). Fold-selectivity values for DPFp7, DPFp8, DPFp18 and DPFp20 were not assigned or plotted due to EC_{50} value(s) not being available. The resulting low number of data points precluded quantitative correlation insights, and linear regression analysis was therefore not performed.

B.Supplementary Tables S1-S15

Table S1. Sequences of final RNA/DNA sequences utilized for experiments.

RNA	**SEQUENCE (5' – 3')**
MALAT1 STEM LOOP	GGAAGGUUUUUCUUUUCCUGAGAAAACAACACGUAUUGUUUUCUCAGGUUUUGCUUUUUGGCCUUUU
MALAT1 TRIPLE HELIX	GGAAGGUUUUUCUUUUCCUGAGAAAACAACACUAUUGUUUUCUCAGGUUUUGCUUUUUGGCCUUUUUCUAGCUUAAAAAAAAAAAAAAGCAAAA
NEAT1 TRIPLE HELIX	GGAGGUGUUUCUUUUACUGAGUGCAGCCCAUGGCCGCACUCAGGUUUUGCUUUUCACCUUCCCAUCUGUGAAAGAGUGAGCAGGAAAAAGCAAAA
RRE STEM LOOP IIB	GGUCUGGGCGCAGCGCAAGCUGACGGUACAGGCC
AT-RICH DNA DUPLEX	ATATATATATATGAAAATATATATATAT
DNA DUPLEX (LOADING CONTROL)	GGCCGGCCGAAAGGCCGGCC

Table S2. EC_{50} values ± standard deviation of three independent fluorescence binding experiments with next-generation DPFs and the MALAT1 triple helix (TH) or stem loop (SL) RNAs. Up to 5 μM RNA was titrated into 1 μM DPF in phosphate screening buffer (10 mM NaH_2PO_4, 25 mM NaCl, 4 mM $MgCl_2$, 0.5 mM EDTA, pH 7.3). N.A.* - not available; indicates curves for which no EC_{50} value was obtained due to little to no change in DPF fluorescence. Fold-selectivity = EC_{50} (TH) / EC_{50} (SL). **Value was not assigned due to EC_{50} value(s) not being available.

DPF	***EC_{50} (TH), nM***	***EC_{50} (SL), nM***	***Triple helix fold-selectivity***
p7	N.A.*	N.A.*	N.A.**
p8	36.89 ± 8.23	N.A.*	N.A.**
p12	1648 ± 300	1687 ± 300	1
p13	27.30 ± 8.60	83.9 ± 36.8	3
p14	42.07 ± 4.40	428 ± 23.4	10
p15	879.3 ± 162	2158 ± 839	2
p16	63.28 ± 15.4	502.1 ± 54.5	8
p17	171.7 ± 39.9	845.6 ± 38.2	5
p18	495.4 ± 130	N.A.*	N.A.**
p19	90.33 ± 6.22	409.3 ± 98.4	5
p20	953 ± 63	N.A.*	N.A.**

Table S3. EC_{50} values from the fluorescence-based selectivity screen of DPF ligands and various nucleic acid constructs. Up to 5 μM nucleic acid was titrated into 1 μM DPF. TH – MALAT1 triple helix; SL – MALAT1 stem loop; tRNA – Baker's yeast transfer RNA mix; RRE – Rev Response Element Stem Loop IIB; DNA – AT-rich DNA Duplex; NEAT1 – NEAT1 triple helix. Errors represent the standard deviation of three independent experiments. N.A.* - not available; indicates curves for which no EC_{50} value was obtained due to little to no change in DPF fluorescence.

	EC_{50} (TH), nM	EC_{50} (SL), nM	EC_{50} (tRNA), nM	EC_{50} (RRE), nM	EC_{50} (DNA), nM	EC_{50} (NEAT1), nM
DPF	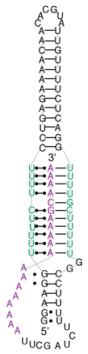	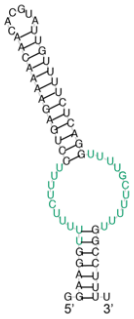	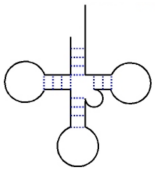	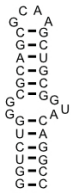	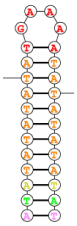	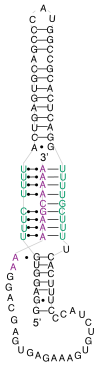
p7	N.A.*	N.A.*	N.A.*	N.A.*	2453 ± 301	N.A.*
p8	36.89 ± 8.23	N.A.*	168.7 ± 41.3	170 ± 59.1	N.A.*	581.4 ± 84.3
p12	1648 ± 300	1687 ± 300	2319 ± 303	N.A.*	605.9 ± 51.5	N.A.*
p13	27.30 ± 8.60	83.9 ± 36.8	32.1 ± 4.74	314.6 ± 80	159.6 ± 46.6	212.1 ± 29.7
p14	42.07 ± 4.40	428 ± 23.4	133.6 ± 44.7	216 ± 7.26	N.A.*	223 ± 10
p15	879.3 ± 162	2158 ± 839	1251 ± 427	N.A.*	442.4 ± 56	N.A.*
p16	63.28 ± 15.4	502.1 ± 54.5	156.7 ± 50.7	351.5 ± 30	N.A.*	237.5 ± 21.3
p17	171.7 ± 39.9	845.6 ± 38.2	376.7 ± 92.2	1662 ± 36.7	N.A.*	651 ± 43.8
p18	495.4 ± 130	N.A.*	778.5 ± 61.9	3321 ± 494	N.A.*	1161 ± 242.7
p19	90.33 ± 6.22	409.3 ± 98.4	243.7 ± 21.7	557.2 ± 80.6	N.A.*	367.8 ± 8
p20	953 ± 63	N.A.*	N.A.*	N.A.*	152.9 ± 21.1	494.4 ± 35.9

Table S4. SMILES strings of DPF molecules utilized for conformational search and PMI calculations. Strings for DPFp7 and p8 were reported previously.(1)

DPF	SMILES STRING
p7	N=C(NCC1=CC=C(C2=CC=CC=C2)C=C1)C(C=C3)=CC=C3C4=CC=C(C5=CC=C(C(NCC6=CC=C(C7=CC=CC=C7)C=C6)=N)C=C5)O4
p8	N=C(NC1CCN(CC2=CC=CC=C2)CC1)C(C=C3)=CC=C3C4=CC=C(C5=CC=C(C(NC6CCN(CC7=CC=CC=C7)CC6)=N)C=C5)O4
p12	C(N1CCC[NH+]=C1C1=CC=C(C=C1)C1=CC=C(O1)C1=CC=C(C=C1)C1=[NH+]CCCN1CC1=CC=CC=C1)C1=CC=CC=C1
p13	[NH2+]=C(NCCC1CC[NH+](CC2=CC=CC=C2)CC1)C1=CC=C(C=C1)C1=CC=C(O1)C1=CC=C(C=C1)C(=[NH2+])NCCC1CC[NH+](CC2=CC=CC=C2)CC1
p14	C[NH+]1CCC(CC1)NC(=[NH2+])C1=CC=C(C=C1)C1=CC=C(O1)C1=CC=C(C=C1)C(=[NH2+])NC1CC[NH+](C)CC1
p15	[NH2+]=C(N[C@H]1CCC[NH+](CC2=CC=CC=C2)C1)C1=CC=C(C=C1)C1=CC=C(O1)C1=CC=C(C=C1)C(=[NH2+])N[C@H]1CCC[NH+](CC2=CC=CC=C2)C1
p16	C[NH+]1CCC(CNC(=[NH2+])C2=CC=C(C=C2)C2=CC=C(O2)C2=CC=C(C=C2)C(=[NH2+])NCC2CC[NH+](C)CC2)CC1
p17	[NH2+]=C(NCCN1CC[NH+](CC2=CC=CC=C2)CC1)C1=CC=C(C=C1)C1=CC=C(O1)C1=CC=C(C=C1)C(=[NH2+])NCCN1CC[NH+](CC2=CC=CC=C2)CC1
p18	[NH2+]=C(N[C@@H]1CCC[NH+](CC2=CC=CC=C2)C1)C1=CC=C(C=C1)C1=CC=C(O1)C1=CC=C(C=C1)C(=[NH2+])N[C@@H]1CCC[NH+](CC2=CC=CC=C2)C1
p19	CC[NH+](CCCNC(=[NH2+])C1=CC=C(C=C1)C1=CC=C(O1)C1=CC=C(C=C1)C(=[NH2+])NCCC[NH+](CC)CC1=CC=CC=C1)CC1=CC=CC=C1
p20	[NH2+]=C(NC1=CC=C(C[NH+]2CCCCC2)C=C1)C1=CC=C(C=C1)C1=CC=C(O1)C1=CC=C(C=C1)C(=[NH2+])NC1=CC=C(C[NH+]2CCCCC2)C=C1

Table S5. Principal moments of inertia (PMI) coordinates and corresponding location in rod-, disc-, sphere- and hybrid-subtriangles. The coordinates for DPFp7 and DPFp8 were reported previously.(1) See Materials and Methods section for details.

DPF	I_1/I_3	I_2/I_3	*Sub-triangle*
p7	0.169	0.889	Rod
p8	0.063	0.976	Rod
p12	0.167	0.955	Rod
p13	0.216	0.821	Rod
p14	0.139	0.891	Rod
p15	0.129	0.957	Rod
p16	0.112	0.917	Rod
p17	0.341	0.913	Rod
p18	0.118	0.976	Rod
p19	0.169	0.902	Rod
p20	0.086	0.934	Rod

Table S6. Predicted intramolecular interactions for the low-energy conformers (ΔE = 0) of next-generation DPF ligands from the MOE conformational search. P = phenyl ring on scaffold, S = subunit. The interactions for DPFp7 and p8 were reported previously.(1) See Materials and Methods for details.

DPF	*Intramolecular interactions*
p7	--
p8	--
p12	π - π: P-S; π - π: P-S
p13	--
p14	--
p15	--
p16	--
p17	--
p18	--
p19	CH - π: P-S
p20	--

Table S7. Molecular docking energetic values obtained from three independent docking runs considering the preferred binding pocket 1. Edock = grid docking energy, Egb = hydrogen bonding grid energy, Ege = electrostatic grid potential, Egs = hydrophobic potential, Egv = grid-based van der Waals. Errors represent standard deviations from three independent docking runs.

DPF	*Edock*	*Egb*	*Ege*	*Egs*	*Egv*
p7	-4.38 ± 1.67	-4.14 ± 0.88	-19.95 ± 0.73	2.65 ± 1.55	-105.04 ± 2.08
p8	-53.08 + 0.96	-5.89 ± 0.31	-33.04 ± 1.46	3.69 ± 1.46	-109.85 ± 0.46
p12	-38.64 ± 0.52	-2.81 ± 0.93	-17.70 ± 1.18	2.59 ± 0.17	-96.50 ± 1.61
p13	-53.37 ± 1.30	-5.77 ± 0.68	-31.38 ± 2.95	2.91 ± 0.87	-120.50 ± 4.99
p15	-28.95 ± 3.88	-4.87 ± 2.56	-33.05 ± 1.99	3.96 ± 0.53	-107.31 ± 3.82
p18	-30.10 ± 0.84	-3.75 ± 0.69	-30.92 ± 3.02	3.13 ± 0.96	-109.43 ± 1.01
p20	-32.31 ± 1.18	-6.26 ± 1.72	-28.86 ± 2.15	2.69 ± 0.72	-111.09 ± 2.42

Table S8. Intermolecular hydrogen bonding interactions between DPFs and MALAT1 triple helix assigned by ICM for each docking run. G – guanine, U – uracil, C – cytosine, A – adenine, O-oxygen, O1p/O2p-phosphate oxygens. Numbers indicate individual docking runs.

Docked DPF conformer	*MALAT1-1 residue*	*Acceptor atom ID*	*DPF atom donor*	*Distance (Å)*
p7_1	G2	O1p	NH-amidine	2.23
	U7	O4	NH-amidine	2.68
	U8	O4	NH-amidine	2.61
	U8	O4	NH-amidine	1.95
	U47	O1p	NH-amidine	2.56
	G48	O2p	NH-amidine	2.69
p7_2	C12	O2p	NH-amidine	2.3
	C12	O2p	NH-amidine	2.48
	U13	O4	NH-amidine	2.66
	C42	O2p	NH-amidine	2.21
	U43	O1p	NH-amidine	2.63
p7_3	A4	N7	NH-Amidine	2.25
	G5	N7	NH-Amidine	2.13
	U43	O1p	NH-Amidine	2.76
	U43	O1p	NH-Amidine	2.21
	U43	O5'	NH-Amidine	2.44
	U44	O1p	NH-Amidine	1.94
p8_1	G2	O2p	NH-piperidine	2.43
	A4	O2p	NH-amidine	2.51
	U8	O4	NH-amidine	1.93
	U9	O4	NH-amidine	2.34
	U43	O4	NH-piperidine	2.17
	U44	O4	NH-amidine	2.26
p8_2	G2	O1p	NH-piperidine	2.42
	A3	O2p	NH-amidine	2.67
	A4	O2p	NH-amidine	2.01
	U7	O1p	NH-amidine	2.45
	U43	O4	NH-piperidine	2.37
p8_3	G2	O1p	NH-Amidine	2.35
	G2	O1p	NH-Amidine	2.21
	U7	O1p	NH-Amidine	2.71

	U7	O1p	NH-Amidine	2.22
	U44	O4	NH-piperidine	2.02
p12_1	U7	O1p	NH-amidine	2.15
p12_2	U8	O1p	NH-amidine	2.28
	U46	O1p	NH-amidine	2.54
p12_3	A4	n7	NH-Amidine	2.58
	U7	o1p	NH-Amidine	2.13
p13_1	G6	O6	NH-amidine	2.39
	G41	N7	NH-piperidine	2.44
	U43	O4	NH-amidine	2.57
	U46	O1p	NH-amidine	2.65
p13_2	U7	O4	NH-amidine	2.29
	U8	O4	NH-amidine	1.9
	U13	O4	NH-piperidine	2.39
p13_3	G6	O6	NH-Amidine	2.33
	C42	O2p	NH-Amidine	2.75
	U43	O1p	NH-Amidine	2.51
	U43	O4	NH-Amidine	2.7
	U46	O1p	NH-Amidine	2.67
p15_1	A4	O2p	NH-amidine	2.09
	U7	O1p	NH-amidine	2.08
	U10	O4	NH-piperidine	2.51
p15_2	A4	N7	NH-amidine	2.5
	G5	O6	NH-amidine	2.37
	U8	O1p	NH-amidine	2.59
	U8	O1p	NH-amidine	2.19
	U9	O4	NH-amidine	2.48
p15_3	A4	O2p	NH-Amidine	2.1
	U7	O1p	NH-Amidine	2.7
	U43	O1p	NH-Amidine	2.25
	U44	O1p	NH-Amidine	2.51
p18_1	A3	O2p	NH-piperidine	2.72
	U8	O1p	NH-amidine	2.34
	U9	O4	NH-amidine	2.35
	U46	O1p	NH-amidine	2.41
p18_2	U9	O1p	NH-amidine	2.3
	U9	O5'	NH-amidine	2.35
	U10	O1p	NH-amidine	2.17
	U46	O4	NH-amidine	2.16
p18_3	U9	O1p	NH-Amidine	2.21
	U9	O5'	NH-Amidine	2.31
	U10	O1p	NH-Amidine	2.23

	U46	O4	NH-Amidine	2.18
	U47	O4	NH-Amidine	2.77
p20_1	A3	O2p	NH-amidine	2.65
	U7	O1p	NH-amidine	2.07
	U10	O4	NH-piperidine	2.32
p20_2	G2	O1p	NH-amidine	2.73
	A3	O2p	NH-amidine	2.14
	U7	O1p	NH-amidine	2.24
	U10	O4	NH-piperidine	2.14
p20_3	G2	O1p	NH-piperidine	2.29
	U7	O1p	NH-Amidine	2.13
	U10	O4	NH-piperidine	2.32
	U46	O2p	NH-Amidine	2.23
	U46	O1p	NH-Amidine	2.67
	U47	O1p	NH-Amidine	2.25

Table S9. Root-mean-square deviations of the starting low-energy DPF conformer from the MOE conformational search (ΔE=0) and the final docked DPF conformation in the binding pocket 1. Errors represent standard deviations from three independent docking runs.

DPF	**RMSD (Å)**
p7	4.19 ± 0.28
p8	2.41 ± 0.29
p12	2.62 ± 0.76
p13	1.08 ± 0.05
p15	2.44 ± 1.13
p18	2.85 ± 0.19
p20	2.41 ± 0.31

Table S10. Melting temperature values obtained via differential scanning fluorimetry (DSF) for the MALAT1 triple helix RNA upon addition of DMSO or DPFs in high-ionic buffer, Buffer 1 (20 mM HEPES-KOH pH 7.4 at 25 ºC, 152.6 mM KCl, 1 mM $MgCl_2$). T_m1 is proposed to be the melting temperature of the Hoogsteen base-paired, triplex-forming strand; and T_m2 is proposed to be the melting temperature of the remaining structure(2). Errors represent the standard deviation of three independent experiments. ΔT_m errors were calculated through standard error propagation.

DPF	***T_m1 / ºC***	***Δ T_m1 / ºC***	***T_m2 / ºC***	***Δ T_m2/ ºC***
DMSO	64.3 ± 0.46	n/a	76.0 ± 0.10	n/a
Pentamidine	65.1 ± 0.72	0.54 ± 0.31	76.8 ± 0.21	0.7 ± 0.12
p7	64.2 ± 0.35	0.11 ± 0.58	76.5 ± 1.20	0.50 ± 0.81
p8	64.5 ± 0.14	0.20 ± 0.48	75.6 ± 0.71	-0.25 ± 0.79
p12	63.9 ± 0.49	-0.45 ± 0.67	75.9 ± 0.35	0.00 ± 0.50
p13	64.5 ± 0.28	0.20 ± 0.54	75.7 ± 0.35	-0.20 ± 0.50
p14	65.3 ± 0.21	0.95 ± 0.50	76.1 ± 0.21	0.20 ± 0.41
p15	64.8 ± 0.71	0.50 ± 0.84	76.5 ± 0.35	0.60 ± 0.50
p16	65.9 ± 0.21	1.55 ± 0.50	77.0 ± 0.49	1.10 ± 0.61
p17	65.4 ± 0.49	1.05 ± 0.67	76.3 ± 0.42	0.45 ± 0.55
p18	64.4 ± 0.49	0.05 ± 0.67	75.9 ± 0.28	0.05 ± 0.45
p19	64.4 ± 0.71	0.10 ± 0.84	75.9 ± 0.57	0.05 ± 0.67
p20	66.1 ±0.17	1.80 ± 0.49	75.7 ±0.49	-0.12 ± 0.61

Table S11. Melting temperature values obtained via differential scanning fluorimetry (DSF) for the MALAT1 triple helix RNA upon addition of DMSO or DPFs in low ionic buffer, Buffer 2 (20 mM HEPES-KOH pH 7.4 at 25 ºC, 52 mM KCl, 0.1 mM $MgCl_2$). T_m1 is proposed to be the melting temperature of the Hoogsteen base-paired, triplex-forming strand; and T_m2 is proposed to be the melting temperature of the remaining structure(2). Errors represent the standard deviation of three independent experiments. ΔT_m errors were calculated through standard error propagation.

DPF	***T_m1 / ºC***	***ΔT_m1 / ºC***	***T_m2 / ºC***	***ΔT_m2 / ºC***
DMSO	60.0 ± 0.80	n/a	74.8 ± 0.68	n/a
Pentamidine	61.7 ± 0.87	1.40 ± 0.92	74.9 ± 0.63	0.04 ± 0.14
p7	61.18 ± 0.51	1.10 ± 0.83	74.2 ± 0.19	0.17 ± 0.52
p8	62.8 ± 1.06	2.75 ± 1.33	75.4 ± 0.35	0.20 ± 0.73
p12	60.7 ± 0.28	0.70 ± 0.85	75.2 ± 0.64	0.00 ± 0.90
p13	63.0 ± 0.07	2.95 ± 0.80	75.0 ± 0.07	-0.20 ± 0.64
p14	64.1 ± 1.03	4.13 ± 1.30	75.8 ± 0.68	0.62 ± 0.93
p15	61.9 ± 1.20	1.85 ± 1.44	74.7 ± 0.14	-0.45 ± 0.65
p16	61.8 ± 1.13	1.80 ± 1.39	75.2 ± 1.06	0.00 ± 1.24
p17	63.0 ± 0.42	3.00 ± 0.91	74.9 ± 0.14	-0.25 ± 0.65
p18	62.3 ± 0.49	2.25 ± 0.94	75.3 ± 0.20	0.15 ± 0.64
p19	62.2 ± 0.35	2.15 ± 0.87	75.1 ± 0.14	-0.05 ± 0.65
p20	66.0 ± 1.21	5.97 ± 1.45	75.6 ± 0.49	0.42 ± 0.81

Table S12. Semi-quantitative denaturing PAGE gel analysis of RNase R exonucleolytic degradation experiments using Image J software (1.52k).(8) 0.2 μM RNA and 0.2 μM DPF or 1 μM SM5 or SM16 were incubated with 5U of RNase R in low ionic buffer conditions (20 mM HEPES-KOH pH 7.4 at 25 ºC, 52 mM KCl, 0.1 mM $MgCl_2$). T1 and T2 refer to 30 minute and 300 minute timepoints, respectively. Values are normalized to Timepoint 0 and the loading control as described in Materials and Methods, giving the starting value of 1. Errors represent standard deviation from three independent experiments. TH = triple helix.

DPF	*Rel. TH level, T1*	*Rel TH level, T2*
DMSO	0.552 ± 0.092	0.061 ± 0.036
p7	0.923 ± 0.054	0.944 ± 0.110
p8	0.736 ± 0.004	0.183 ± 0.003
p12	0.549 ± 0.088	0.056 ± 0.082
p13	0.707 ± 0.191	0.200 ± 0.051
p14	0.571 ± 0.076	0.177 ± 0.042
p15	0.623 ± 0.109	0.136 ± 0.022
p16	0.497 ± 0.115	0.207 ± 0.032
p17	0.700 ± 0.059	0.221 ± 0.045
p18	0.522 ± 0.051	0.147 ± 0.043
p19	0.717 ± 0.072	0.111 ± 0.010
p20	0.889 ± 0.034	0.425 ± 0.105
SM5	0.285 ± 0.020	0.066 ± 0.021
SM16	0.235 ± 0.041	0.169 ± 0.011

Table S13. Semi-quantitative denaturing PAGE gel analysis of RNase R exonucleolytic degradation control experiments with 5 time points using Image J software (1.52k)(8) to ensure linear phase decay. 0.2 μM RNA and 0.2 μM DPF or DMSO were incubated with 5U of RNase R in low ionic buffer conditions (20 mM HEPES-KOH pH 7.4 at 25 ºC, 52 mM KCl, 0.1 mM $MgCl_2$). Values are normalized to Timepoint 0 and the loading control as described in Materials and Methods, giving the starting value of 1. Errors represent standard deviation from three independent experiments.

Sample	***Relative triple helix level***				
	15 min	**30 min**	**60 min**	**180 min**	**300 min**
DMSO	0.418 ± 0.035	0.316 ± 0.112	0.340 ± 0.165	0.174 ± 0.048	0.139 ± 0.024
DPFp20	0.599 ± 0.165	0.562 ± 0.178	0.514 ± 0.081	0.589 ± 0.151	0.551 ± 0.178

Table S14. EC_{50} values ± standard deviation of three independent fluorescence binding experiments with next-generation DPFs and the MALAT1 triple helix (TH). Up to 5 μM RNA was titrated into 1 μM DPF in low-ionic buffer conditions, Buffer 2 (20 mM HEPES-KOH pH 7.4 at 25 ºC, 52 mM KCl, 0.1 mM $MgCl_2$). N.A.* - not available; indicates curves for which no EC_{50} value was obtained due to little to no change in DPF fluorescence.

DPF	EC_{50} (TH), nM
p7	N.A.*
p8	25.8 ± 2.3
p12	2522 ± 624.9
p13	10.0 ± 2.6
p14	23.2 ± 3.7
p15	1844 ± 688
p16	44.1 ± 12.1
p17	78.7 ± 14.9
p18	76.4 ± 3.4
p19	22.9 ± 4.1
p20	302.3 ± 59.2

Table S15. DNA sequences utilized for the synthesis of NEAT1 and RRE constructs.

DNA	DNA SEQUENCE (5' – 3')
NEAT1 TEMPLATE	GGAGGUGUUUCUUUUACUGAGUGCAGCCCAUGGCCGCACUCAGGUUUUGCUUUUCACCUUCCCAUCUGUGAAAGAGUGAGCAGGAAAAAGCAAAA
NEAT1 FORWARD PRIMER	GAAATTAATACGACTCACTATAGGAGGTG
NEAT1 REVERSE PRIMER	mUmUTTGCTTTTTCCTGCTCACTC
RRE SENSE STRAND	GCAGCTAATACGACTCACTATAGGTCTGGGCGCAGCGCAAGCTGACGGTACAGGCC
RRE ANTISENSE STRAND	GGCCTGTACCGTCAGCTTGCGCTGCGCCCAGACCTATAGTGAGTCGTATTAGCTGC

C. Preparation of NEAT1 and RRE Stem loop RNA

The NEAT1 DNA template for *in-vitro* transcription was prepared through polymerase chain reaction (PCR) (see **SI Table S15** for sequences). Specifically, 65 µL of 5X Q5 Polymerase buffer (New England Biolabs), 6.5 µL of 10 mM each dNTP (New England Biolabs), 16.25 µL of 10µM forward and reverse primers (Integrated DNA Technologies), 6.5 µL of 50 ng/µL template DNA (Integrated DNA Technologies), 211.25 µL nuclease-free water and 3.25 µL of 2000 U/µL Q5 Hot Start Polymerase (New England Biolabs) were mixed and aliquoted into 12 individual wells in a 96 well PCR well plate (Thermo Fisher). The plate was then put in a thermocycler programmed as follows: 98 ºC for 30s, 30x (98 ºC for 15s, 55 ºC for 15 s, 72 ºC for 30 s), 72 ºC for 2 min and then placed on ice prior to clean-up using the DNA CleanUp & Concentrate kit (Zymo Research). The concentration, quality and length of PCR products were determined using the 2100 Bioanalyzer instrument (Agilent). PCR products were then utilized as templates for *in vitro* transcription. In a typical reaction, a mixture of 60 µL of 25 mM each rNTP (New England Biolabs), 15 µL of 1M $MgCl_2$, 24 µL of 1M Tris (pH=8.0), 15 µL of 100 mM spermidine (Sigma), 6 µL of 1% Triton X-100 (Sigma), 6 µL of 1 M dithiothreitol (Sigma), 381 µL of nuclease-free water, 3 µL of 100 U/mL Inorganic yeast Pyrophosphatase (New England Biolabs), and 30 µL T7 RNA polymerase (Custom) were aliquoted into 12 individual wells in a 96 PCR well plate containing 5 µL of 50 ng/µL DNA template. Reactions were incubated in a thermocycler for 8 h at 37 ºC and then placed on ice. Each reaction was treated with 1 µL of 2U/µL TURBO DNase (Ambion) twice for 30 min at 37 ºC. 10% volume of 0.5 M EDTA was added to the mixture, and an extraction was conducted utilizing 25:24:1 phenol:chloroform:isoamyl alcohol (Sigma). Buffer-exchange into 0.2X Tris-

EDTA buffer (Amibon) was then conducted using 3kDa Amicon Ultra Centrifugal Filters (EMD Milipore) by centrifuging the supernatant three times at 4,000 rpm for 20 min.

For IVT of the RRE Stem loop IIB, the sense and antisense DNA templates carrying the T7 promoter (**SI Table S15**) were purchased from Integrated DNA Technologies as 100 μM solutions. Strand annealing was performed by combining 45 uL of the sense strand, 45 uL of the antisense strand, 54 uL of 0.01 M MgCl2 and 36 uL of nuclease-free water in a 1.5-mL microcentrifuge tube. The tube was incubated at 95°C for 10 min in an Eppendorf ThermoMixer, then snap-cooled on ice for at least one hour. DNA annealing was confirmed by running the annealed sample on a Novex® DNA retardation gel. In a typical IVT reaction, 0.091 M Tris (pH = 7.4), 0.023 M MgCl2, 0.027 M dithiothreitol, 0.002 M Spermidine, 2.7 mM rATP, 2.7 mM rCTP, 2.7 mM rGTP, 2.7 mM rUTP, 0.4 uM annealed double-stranded DNA template and 2.7 U/uL T7 RNA polymerase were combined in a 15-mL falcon tube and incubated at 37°C in an Eppendorf ThermoMixer for 14 to 20 hours. The crude IVT mixture was treated with DNase I to remove the DNA template as outlined above. The RNA was then purified using the ZymoResearch Clean & ConcentratorTM kit following the manufacturer's protocol, except that three wash steps were performed instead of two.

D. General chemistry methods and procedures

Reagents were purchased from commercial suppliers and were used without further purification. Except for anhydrous THF, all solvents were ACS grade or better and used without further purification. Anhydrous THF was dispensed from a Pure Solv (Innovative Technology) solvent purification system. All microwave reactions were run on a Biotage Initiator^{+} reactor from Biotage Inc. All chromatographic purifications were conducted via flash chromatography using ultra-pure silica gel (230-400 mesh, 60 Å) purchased from Silicycle as the stationary phase. Thin Layer Chromatography was performed with alumina-backed silica gel plates ($^{60}F_{254}$) purchased from Sigma and visualized with 254 nm UV light. All deuterated solvents for NMR spectra acquisition were purchased from Cambridge Isotope Laboratories. Deuterated chloroform was deacidifed using potassium carbonate before use. All ^{1}H and ^{13}C NMR spectra were recorded using 400 MHz Varian INOVA or 500 MHz Bruker Advance Neo spectrometers. The corresponding ^{13}C resonance frequencies were 100 MHz and 125 MHz, respectively. Chemical shifts are expressed as parts per million from tetramethylsilane. ^{1}H chemical shifts were referenced with that of the solvent (7.26 for $CDCl_3$, 2.50 for $(CD_3)_2SO$, 3.31 for CD_3OD) and coupling constants (*J* values) are reported in units of Hertz (Hz). Splitting patterns have been designated as follows: s (singlet), d (doublet), dd (doublet of doublets), qd (quartet of doublets), ddd (doublet of doublets of doublets), t (triplet), dt (doublet of triplets), q (quartet), dq (doublet of quartets), p (pentet), m (multiplet), br (broad). Low and high-resolution electrospray ionization (ESI) and gas chromatography (GC) mass spectra were recorded on an Agilent MSD-trap Spectrometer at Duke University and are available upon request. HPLC spectra were recorded using a Shimadzu SIL-20AHT Prominence

instrument. All HPLC experiments were run at room temperature on a Phenomenex Luna 5 µ C18(2) 100 Å column (140 x 4.6 mm) using 90-10% gradients of 0.1% TFA in water and acetonitrile as solvents A and B, respectively. Yields refer to ≥ 95% spectroscopically and chromatographically pure compounds (determined at 360 nm for all compounds except for **DPFp20**, which was determined at 380 nm).

E. Synthesis of next-generation DPF ligands

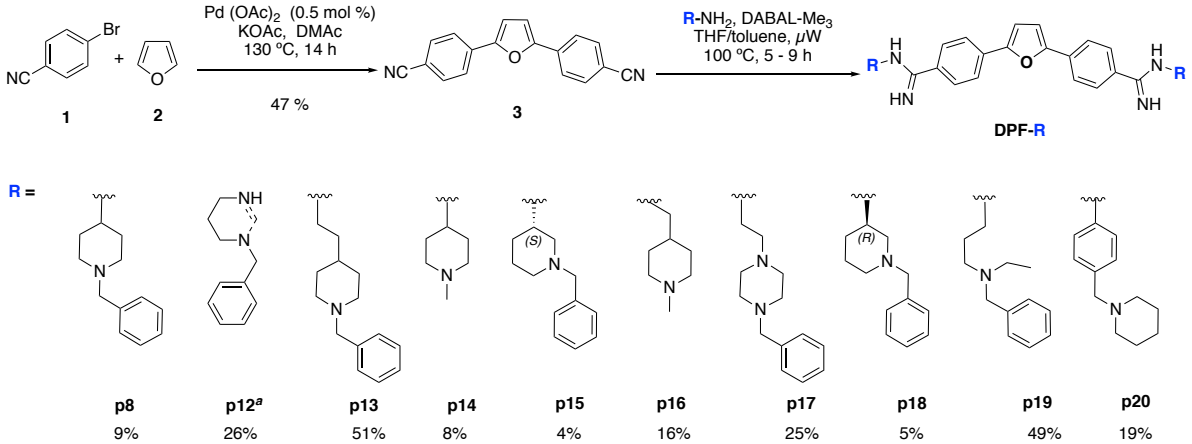

SI Scheme S1. Synthetic scheme for the synthesis of next-generation DPF ligands. [a]The primary amine reagent utilized for the synthesis of this ligand is *N*-benzyl-1,3-propanediamine.

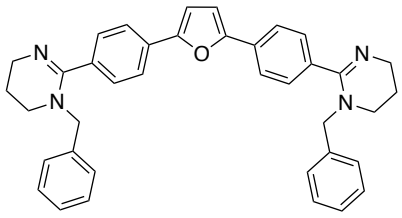

DPFp12

2,5-bis(4-(1-benzyl-1,4,5,6-tetrahydropyrimidin-2-yl)phenyl)furan.

Reaction time: 8 h. ^{1}H NMR (400 MHz, DMSO-d_6) δ 7.88 (d, J = 7.6 Hz, 4H), 7.55 (d, J = 7.6 Hz, 4H), 7.38 – 7.34 (m, 4H), 7.30 – 7.18 (m, 8H), 4.35 (s, 4H), 3.50 – 3.40 (m, 4H), 3.35 – 3.26 (m, 4H), 1.94 – 1.85 (m, 4H).^{13}C NMR (126 MHz, DMSO-d_6) δ 159.8, 152.8, 137.1, 133.4, 131.6, 129.2, 129.0, 127.9, 127.4, 123.9, 110.2, 55.6, 46.0, 42.6, 23.4. MS-ESI (m/z) Calcd for $C_{38}H_{36}N_4O$ ($[M+2H]^{2+}$) = 283.1517. Found: 283.1520. Error = -1.0 ppm. Calcd for ($[M+H]^{+}$): 565.2962. Found: 565.2968. Error = -1.2 ppm.

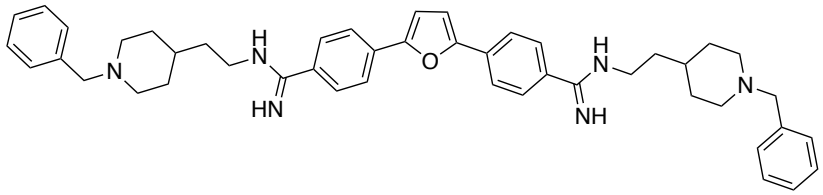

DPFp13

4,4'-(furan-2,5-diyl)bis(*N*-(2-(1-benzylpiperidin-4-yl)ethyl)benzimidamide)

Reaction time: 9 h. ^{1}H NMR (400 MHz, Methanol-*d4*) δ 7.77 (d, *J* = 8.5 Hz, 4H), 7.65 (d, *J* = 8.5 Hz, 4H), 7.17 – 7.21 (m, 4H), 7.14 – 7.03 (m, 6H), 6.92 (s, 2H), 3.34 (t, *J* = 6.8 Hz, 4H), 2.92 (d, *J* = 11.6 Hz, 4H), 2.59 (t, *J* = 6.8 Hz, 4H), 2.47 (d, *J* = 6.9 Hz, 4H), 2.04 – 1.91 (m, 4H), 1.58 (d, *J* = 13.2 Hz, 4H), 1.47 – 1.53 (m, 2H), 1.24 – 1.19 (m, 4H). ^{13}C NMR (101 MHz, Methanol-d_4) δ 164.0, 154.4, 141.6, 136.3, 133.7, 130.1, 129.2, 128.5, 126.9, 124.7, 110.1, 58.7, 55.0, 44.0, 42.3, 39.0, 32.9. MS-ESI (m/z) Calcd for $C_{46}H_{54}N_6O$ ([M+2H] $^{2+}$) = 354.2252. Found: 354.2249 ([M+2H]$^{2+}$). Error = 0.9 ppm.

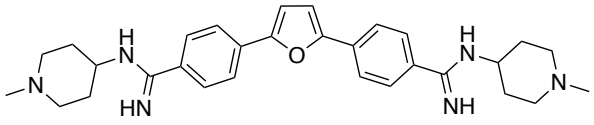

DPFp14

4,4'-(furan-2,5-diyl)bis(*N*-(1-methylpiperidin-4-yl)benzimidamide)

Reaction time: 6 h. ^{1}H NMR (400 MHz, Methanol-d_4) δ 7.91 (d, *J* = 8.4 Hz, 4H), 7.73 (d, *J* = 8.3 Hz, 4H), 7.08 (s, 2H), 3.69 – 3.57 (m, 2H), 2.94 (d, *J* = 11.8 Hz, 4H), 2.32 (s, 6H), 2.22 (t, *J* = 11.6 Hz, 4H), 2.05 (d, *J* = 11.5 Hz, 4H), 1.76 – 1.65 (m, 4H). ^{13}C NMR

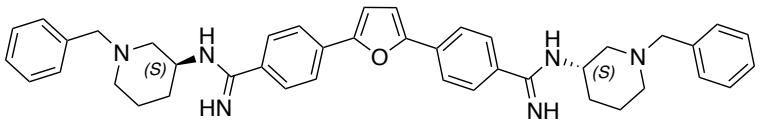

DPFp15

(101 MHz, Methanol-d_4) δ 164.6, 154.6, 134.7, 133.6, 129.3, 125.1, 110.9, 55.6, 46.4, 46.1, 32.2. MS-ESI (m/z) Calcd for $C_{30}H_{38}N_6O$ ($[M+2H]^{2+}$) = 250.1626. Found: 250.1626. Error = 0.1 ppm. Calcd for ($[M+H]^+$): 499.3180. Found: 499.3183. Error = -0.6 ppm.

4,4'-(furan-2,5-diyl)bis(*N*-((*S*)-1-benzylpiperidin-3-yl)benzimidamide)

Reaction time: 6 h. ^{1}H NMR (400 MHz, Methanol-d_4) δ 7.82 (d, *J* = 8.4 Hz, 4H), 7.66 (d, *J* = 8.3 Hz, 4H), 7.35 – 7.32 (m, 8H), 7.24 – 7.27 (m, 2H), 6.98 (s, 2H), 3.75 (m, 2H), 3.60 – 3.51 (m, 4H), 2.90 (d, *J* = 10.0 Hz, 2H), 2.71 (d, *J* = 10.0 Hz, 2H), 2.22 – 2.10 (m, 4H), 1.95 – 1.89 (m, 2H), 1.76 – 1.66 (m, 4H), 1.42 (q, *J* = 9.0, 8.9 Hz, 2H). ^{13}C NMR (101 MHz, Methanol-d_4) δ 163.3, 154.4, 133.7, 130.6, 129.3, 128.6, 128.4, 124.7, 110.1, 64.1, 59.4, 54.4, 50.8, 30.9, 24.5. MS-ESI (m/z) Calcd for $C_{42}H_{46}N_6O$ ($[M+H]^+$): 651.3806. Found: 651.3812. Error = -0.9 ppm.

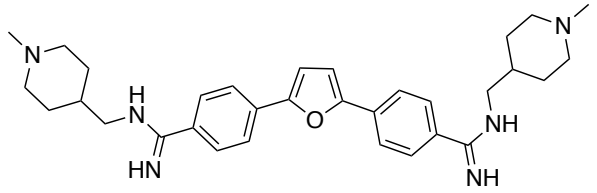

DPFp16

4,4'-(furan-2,5-diyl)bis(*N*-((1-methylpiperidin-4-yl)methyl)benzimidamide)

Reaction time: 8 h. ^{1}H NMR (400 MHz, DMSO-d_6) δ 7.93 (d, *J* = 8.1 Hz, 4H), 7.85 (d, *J* = 8.2 Hz, 4H), 7.29 (s, 2H), 3.13 (d, *J* = 6.6 Hz, 4H), 2.77 (d, *J* = 10.6 Hz, 4H), 2.14 (s, 6H), 1.83 (t, *J* = 12.3 Hz, 4H), 1.74 (d, *J* = 13.2 Hz, 4H), 1.60 (s, 2H), 1.24 - 1.16 (m, 4H). ^{13}C NMR (101 MHz, Methanol-d_4) δ 165.2, 154.6, 135.4, 132.3, 129.6, 125.3,

111.5, 56.4, 46.6, 38.3, 35.9, 30.9. MS-ESI (m/z) Calcd for $C_{32}H_{42}N_6O$ ($[M+H]^+$): 527.3493. Found: 527.3488. Error = 1.0 ppm.

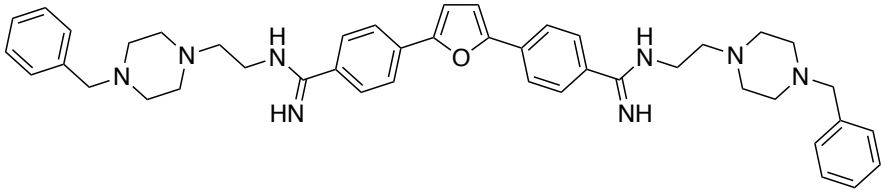

DPFp17

4,4'-(furan-2,5-diyl)bis(*N*-(2-(4-benzylpiperazin-1-yl)ethyl)benzimidamide)

Reaction time: 8 h. ^{1}H NMR (400 MHz, Methanol-d_4) δ 7.87 (d, J = 8.4 Hz, 4H), 7.72 (d, J = 8.4 Hz, 4H), 7.28 (d, J = 4.3 Hz, 8H), 7.22 (dd, J = 8.6, 4.1 Hz, 2H), 7.04 (s, 2H), 3.49 (s, 4H), 3.45 (t,J = 12.4, 4H), 2.67 (t, J = 6.3 Hz, 4H), 2.54 (br, 16H). ^{13}C NMR (101 MHz, Methanol-d_4) δ 164.7, 154.3, 138.2, 134.7, 133.3, 130.7, 129.3, 129.1, 128.5, 124.9, 111.0, 63.9, 57.7, 53.9, 53.8, 42.2. MS-ESI (m/z) Calcd for $C_{44}H_{52}N_8O$ ($[M+H]^+$): 709.4337 Found: 709.4331. Error = 0.8 ppm.

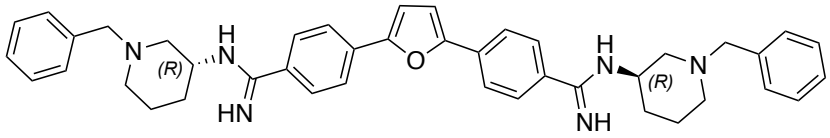

DPFp18

4,4'-(furan-2,5-diyl)bis(*N*-((*R*)-1-benzylpiperidin-3-yl)benzimidamide)

Reaction time: 8 h. ^{1}H NMR (400 MHz, Methanol-d_4) δ 7.86 (d, J = 8.3 Hz, 4H), 7.67 (d, J = 8.2 Hz, 4H), 7.37 – 7.29 (m, 8H), 7.26 (d, J = 9.2 Hz, 2H), 7.03 (s, 2H), 3.77 (s, 2H), 3.58 – 3.49 (m, 4H), 2.90 (d, J = 11.6 Hz, 2H), 2.79 (s, 2H), 2.71 (d, J = 11.6 Hz, 2H), 2.18 (d, J = 9.3 Hz, 4H), 1.95 (d, J = 11.2 Hz, 2H), 1.76 – 1.65 (m, 4H), 1.44 (d, J = 10.3 Hz, 2H). ^{13}C NMR (101 MHz, Methanol-d_4) δ 159.3, 153.0, 137.3, 133.6, 132.8, 129.2,

127.9, 127.5, 127.0, 123.3, 109.1, 62.6, 57.5, 52.9, 45.7, 29.3, 23.0. MS-ESI (m/z) Calcd for $C_{42}H_{46}N_6O$ ($[M+H]^+$): 651.3806. Found: 651.3802 Error = 0.6 ppm.

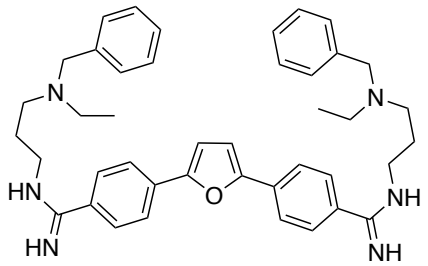

DPFp19

4,4'-(furan-2,5-diyl)bis(*N*-(3-(benzyl(ethyl)amino)propyl)benzimidamide)

Reaction time: 8 h. ^{1}H NMR (400 MHz, Methanol-d_4) δ 7.85 (d, J = 8.4 Hz, 4H), 7.66 (d, J = 8.4 Hz, 4H), 7.36 – 7.25 (m, 8H), 7.24 – 7.19 (m, 2H), 7.03 (s, 2H), 3.59 (s, 4H), 3.37 – 3.32 (m, 4H), 2.59 (dt, J = 14.1, 6.8 Hz, 8H), 1.89 (p, J = 6.6, 4H), 1.09 (t, J = 7.1 Hz, 6H). ^{13}C NMR (101 MHz, Methanol-d_4) δ 163.1, 152.9, 138.5, 133.84, 132.6, 129.1, 127.9, 127.3, 126.7, 123.4, 109.1, 66.6, 57.5, 50.6, 41.4, 25.2, 10.2. MS-ESI (m/z) Calcd for $C_{42}H_{50}N_6O$ ($[M+H]^+$): 655.4119. Found: 655.4118. Error = 0.2 ppm.

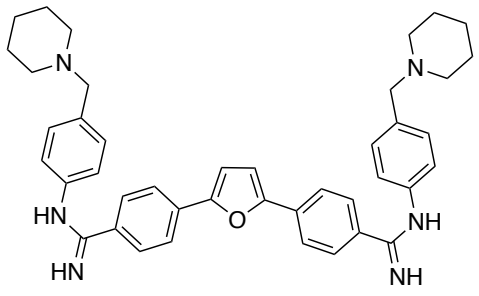

DPFp20

4,4'-(furan-2,5-diyl)bis(*N*-(4-(piperidin-1-ylmethyl)phenyl)benzimidamide)

Reaction time: 8 h. ^{1}H NMR (400 MHz, DMSO-d_6) δ 8.19 – 7.96 (m, 4H), 7.91 (d, J = 7.7 Hz, 4H), 7.40 – 7.03 (m, 6H), 6.84 (d, J = 6.5 Hz, 4H), 3.37 (s, 4H), 2.33 (s, 8H), 1.72 – 1.40 (m, 8H), 1.42 – 1.28 (m, 4H). ^{13}C NMR (101 MHz, DMSO-d_6) δ 153.1, 149.4, 135.1, 132.2, 131.7, 130.1, 128.1, 123.5, 121.7, 120.1, 109.9, 63.2, 54.3, 26.1, 24.6. MS-ESI (m/z) Calcd for $C_{42}H_{46}N_6O$ ($[M+H]^+$): 651.3806. Found: 651.3801. Error = 0.8 ppm.

F. ^{1}H and ^{13}C NMR characterization spectra and HPLC chromatograms

2,5-bis(4-(1-benzyl-1,4,5,6-tetrahydropyrimidin-2-yl)phenyl)furan (DPFp12)

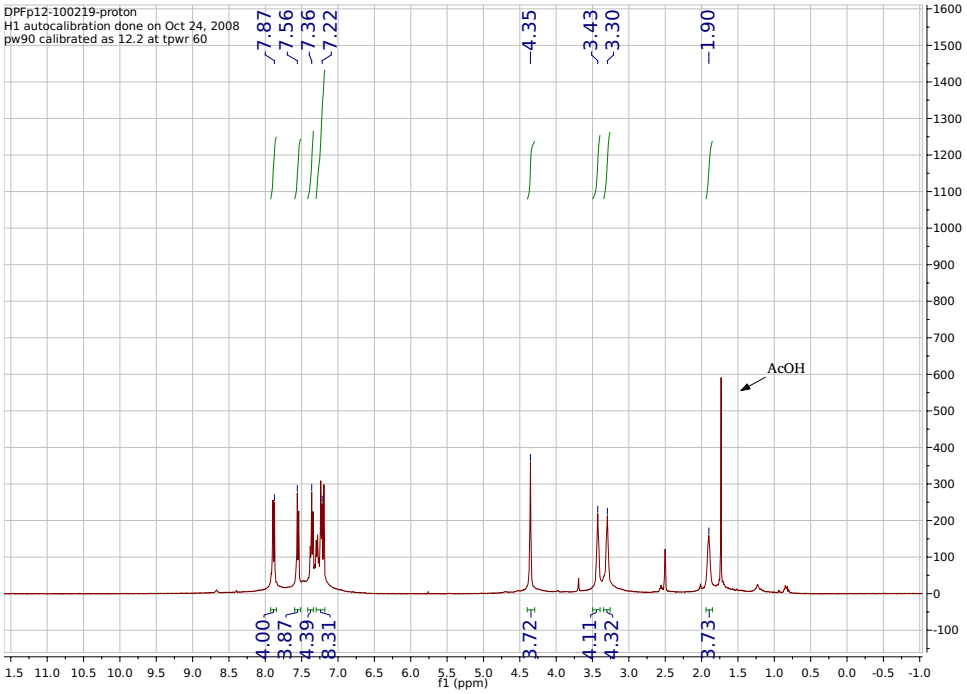

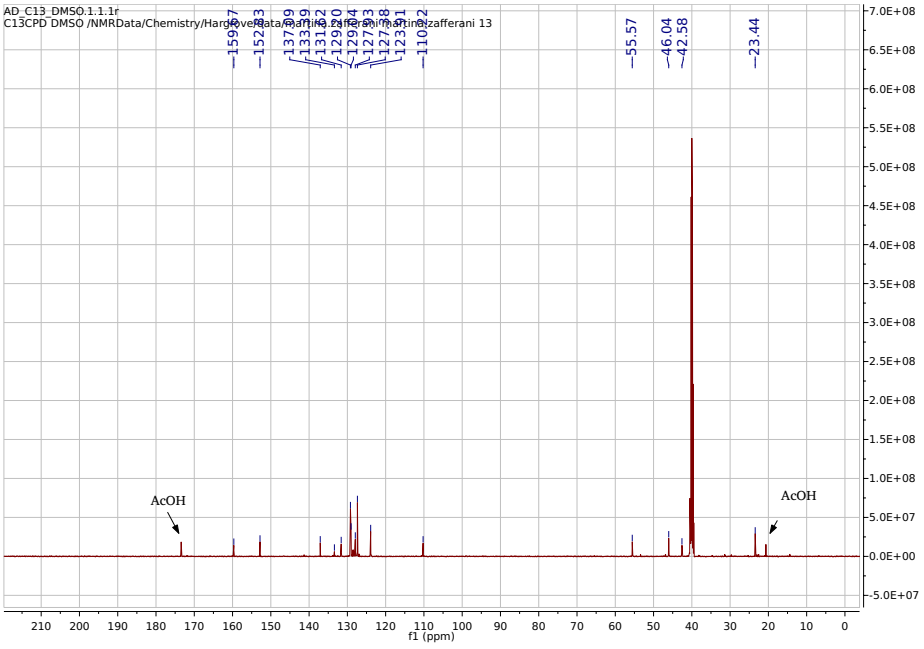

SHIMADZU LabSolutions

Analysis Report

<Sample Information>

Sample Name	: AD-4-111-CLMN2		
Sample ID	: AD-4-111-CLMN2		
Data Filename	: AD-4-111-CLMN2.lcd		
Method Filename	: NNP-Grd10-90_Slow_PDA_D2only.lcm		
Batch Filename	: AD-4-111-2NDCLMN.lcb		
Vial #	: 1-13	Sample Type	: Unknown
Injection Volume	: 10 uL		
Date Acquired	: 10/18/2018 10:24:42 AM	Acquired by	: chemist
Date Processed	: 10/18/2018 10:42:46 AM	Processed by	: chemist

<Chromatogram>

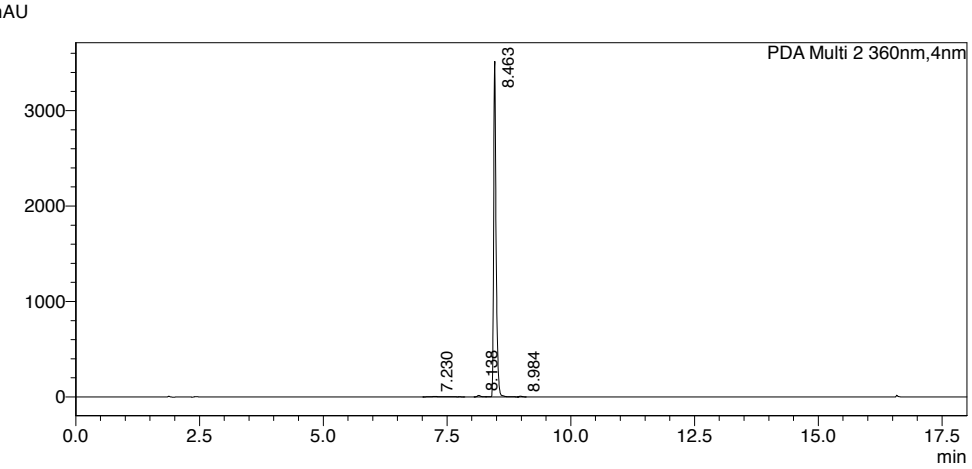

<Peak Table>

RF-20A Ex:350nm,Em:450nm

Peak#	Ret. Time	Area%
Total		

PDA Ch1 254nm

Peak#	Ret. Time	Area%
Total		

PDA Ch2 360nm

Peak#	Ret. Time	Area%
1	7.230	0.460
2	8.138	0.543
3	8.463	98.786
4	8.984	0.210
Total		100.000

4,4'-(furan-2,5-diyl)bis(*N*-(2-(1-benzylpiperidin-4-yl)ethyl)benzimidamide) (DPFp13)

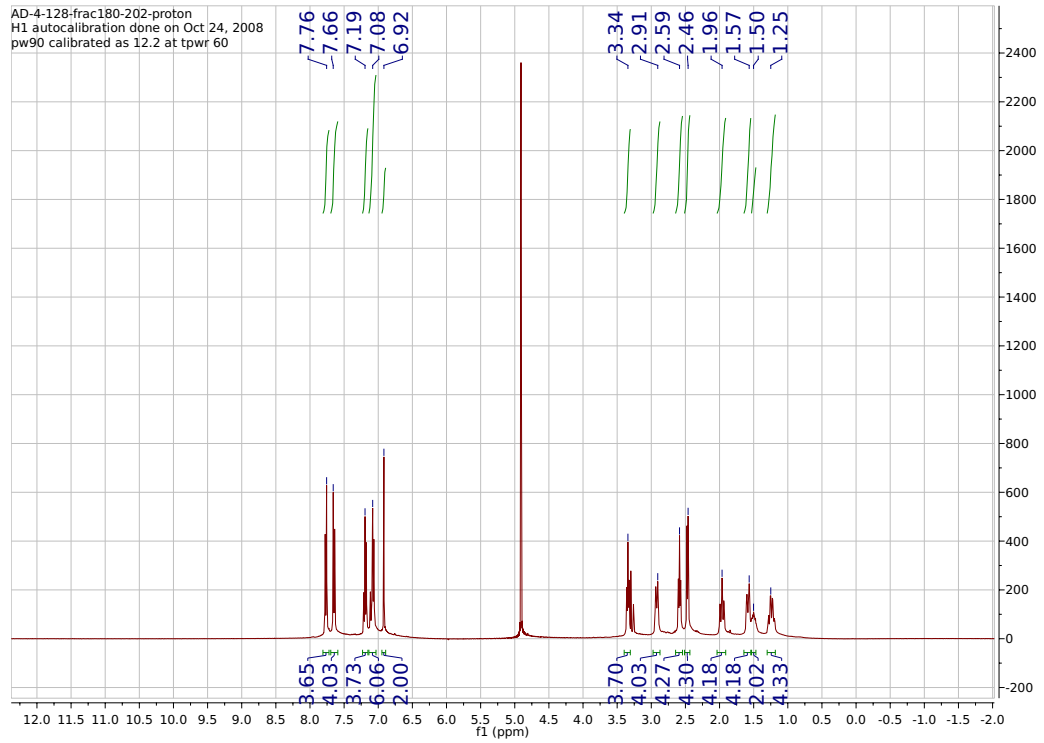

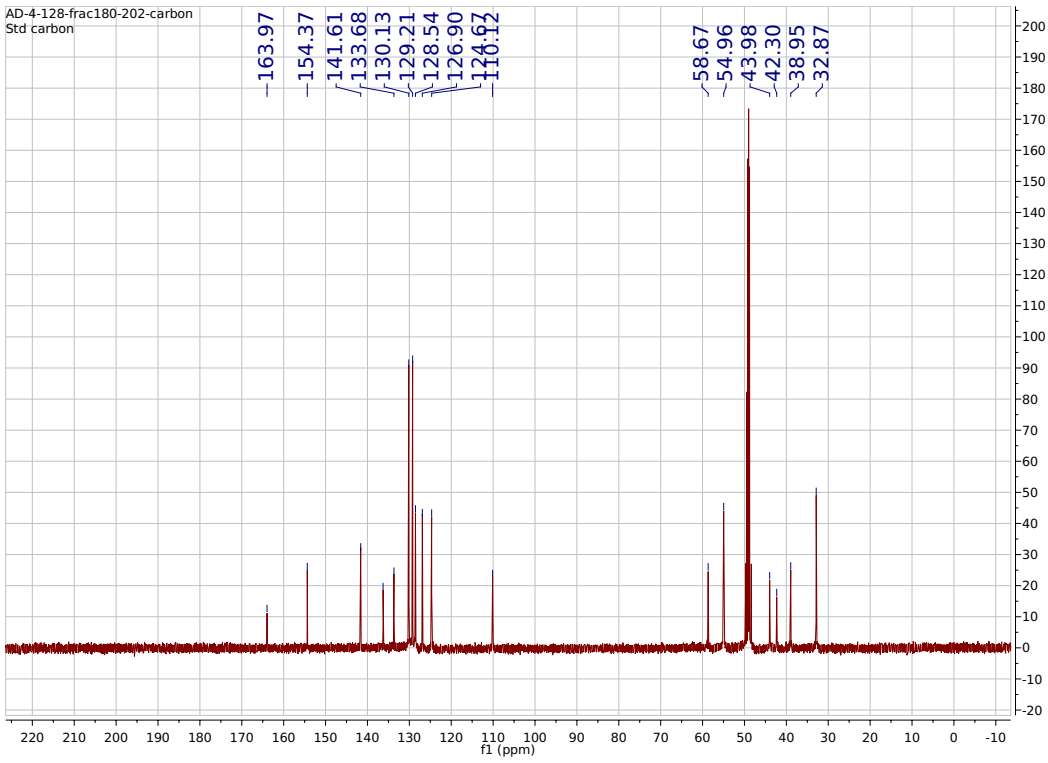

SHIMADZU LabSolutions

Analysis Report

<Sample Information>

Sample Name	: AD-4-128-frac200-conc		
Sample ID	: AD-4-128-frac200-conc		
Data Filename	: AD-4-128-frac200-conc.lcd		
Method Filename	: NNP-Grd10-90_Slow_PDA_D2only.lcm		
Batch Filename	: 101018-lastDPFconc.lcb		
Vial #	: 1-6	Sample Type	: Unknown
Injection Volume	: 10 uL		
Date Acquired	: 10/10/2018 5:36:28 PM	Acquired by	: chemist
Date Processed	: 10/10/2018 5:54:31 PM	Processed by	: chemist

<Chromatogram>

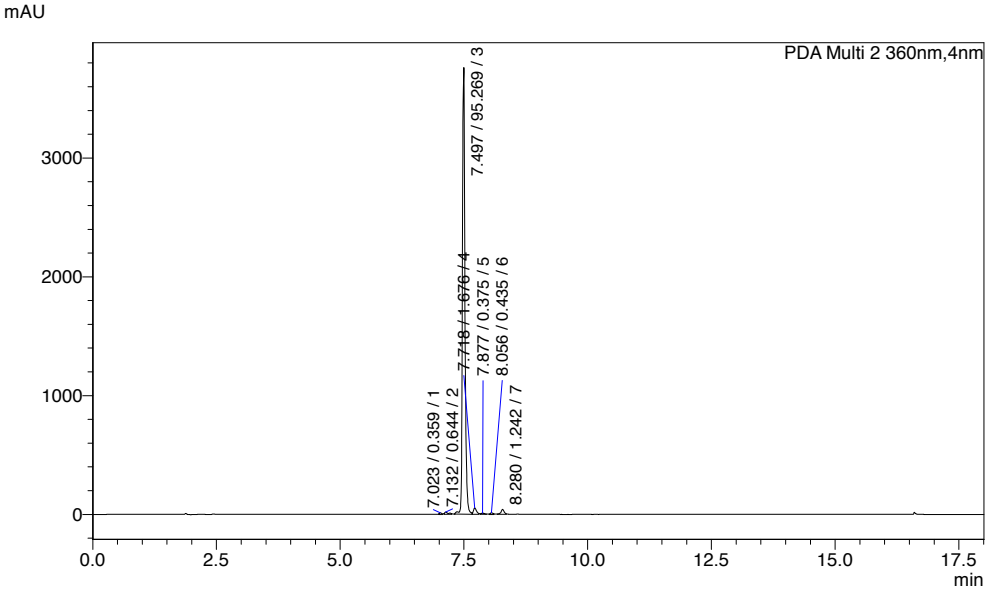

<Peak Table>

RF-20A Ex:350nm,Em:450nm

Peak#	Ret. Time	Area%
Total		

PDA Ch1 254nm

Peak#	Ret. Time	Area%
Total		

PDA Ch2 360nm

Peak#	Ret. Time	Area%
1	7.023	0.359
2	7.132	0.644
3	7.497	95.269
4	7.718	1.676
5	7.877	0.375
6	8.056	0.435

4,4'-(furan-2,5-diyl)bis(*N*-(1-methylpiperidin-4-yl)benzimidamide) (DPFp14)

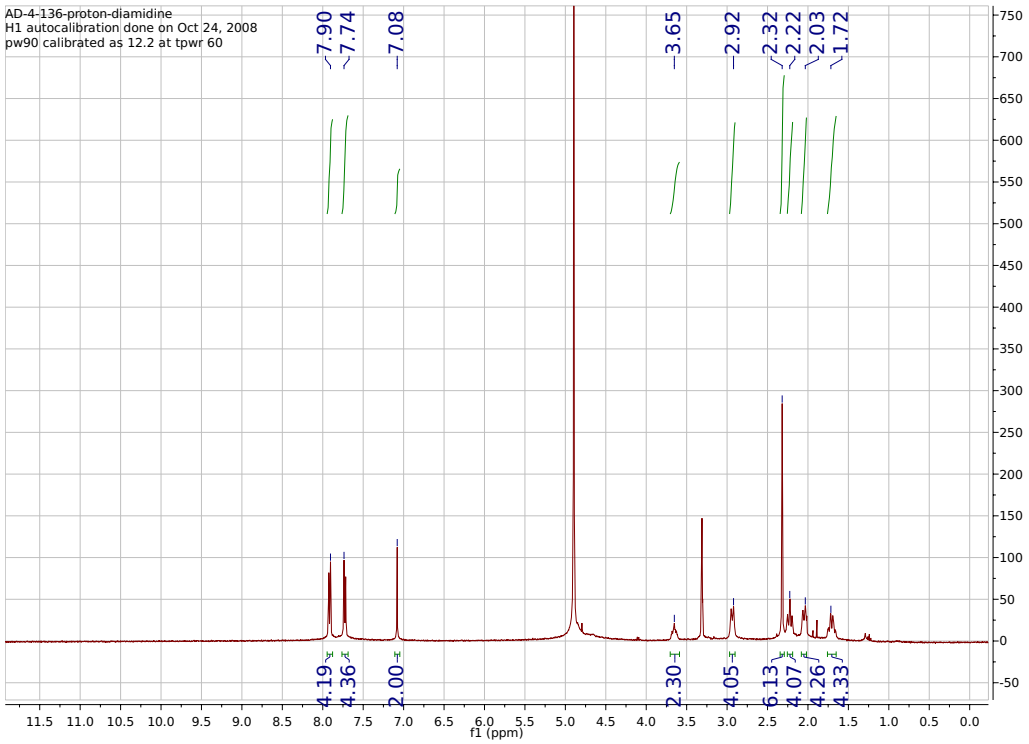

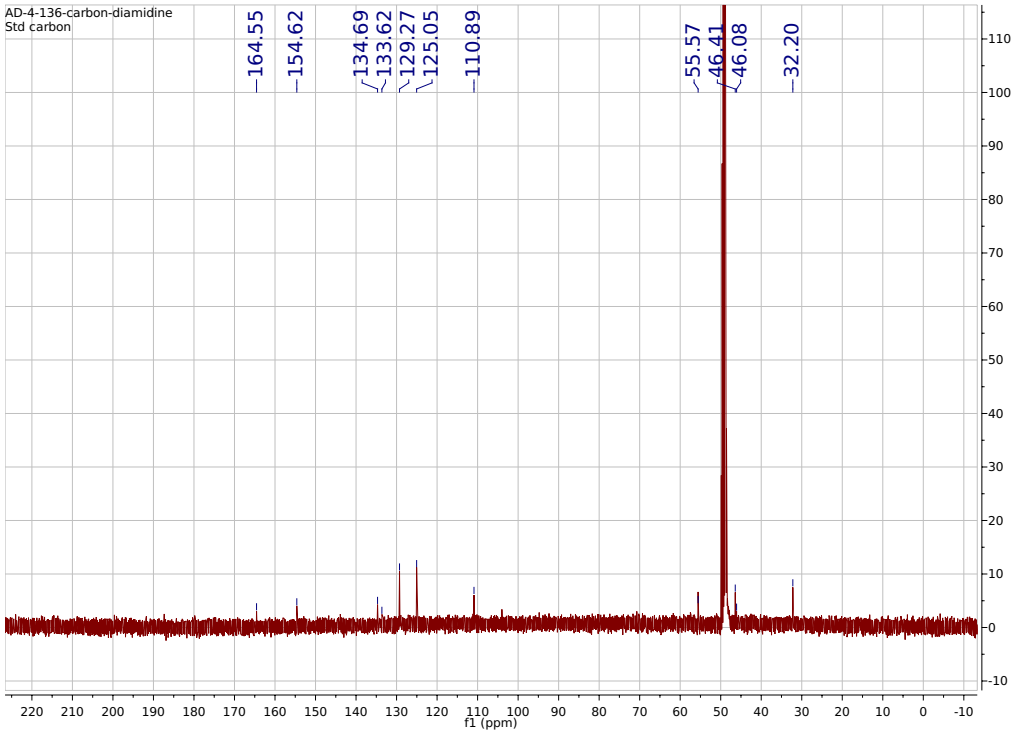

SHIMADZU LabSolutions

Analysis Report

<Sample Information>

Sample Name	: p14_final		
Sample ID	: p14_final		
Data Filename	: p14_final		
Method Filename	: NNP-Grd10-90_Slow_PDA_D2only.lcm		
Batch Filename	: 101018-TFA-newDPFs.lcb		
Vial #	: 1-5	Sample Type	: Unknown
Injection Volume	: 10 uL		
Date Acquired	: 10/10/2018 12:41:50 PM	Acquired by	: chemist
Date Processed	: 10/10/2018 1:39:07 PM	Processed by	: chemist

<Chromatogram>

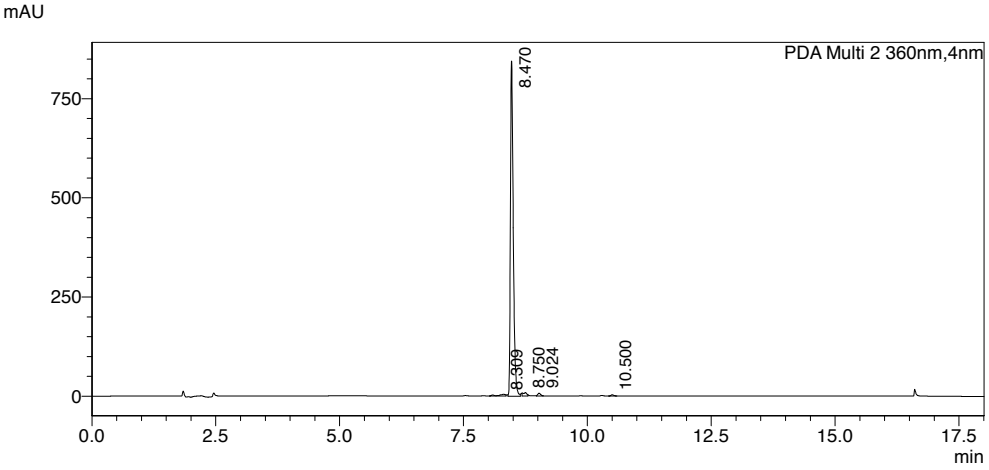

<Peak Table>

RF-20A Ex:350nm,Em:450nm

Peak#	Ret. Time	Area%
Total		

PDA Ch1 254nm

Peak#	Ret. Time	Area%
Total		

PDA Ch2 360nm

Peak#	Ret. Time	Area%
1	8.309	1.389
2	8.470	95.952
3	8.750	1.360
4	9.024	0.897
5	10.500	0.402
Total		100.000

4,4'-(furan-2,5-diyl)bis(*N*-((*S*)-1-benzylpiperidin-3-yl)benzimidamide) (DPFp15)

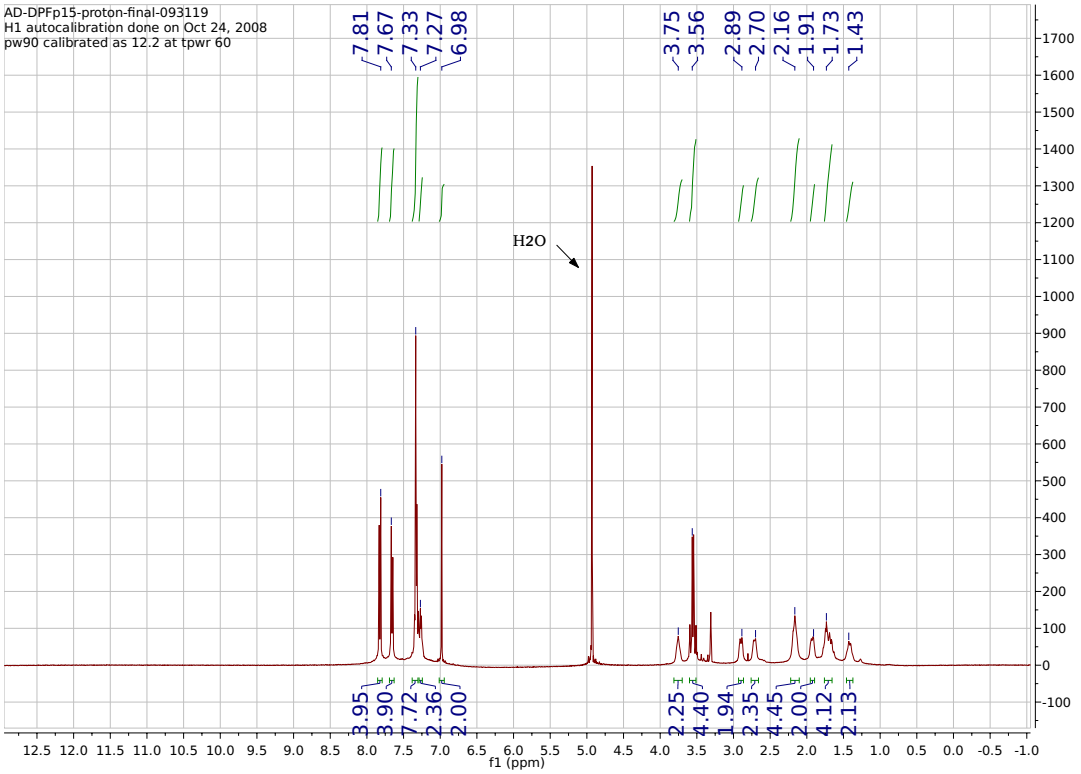

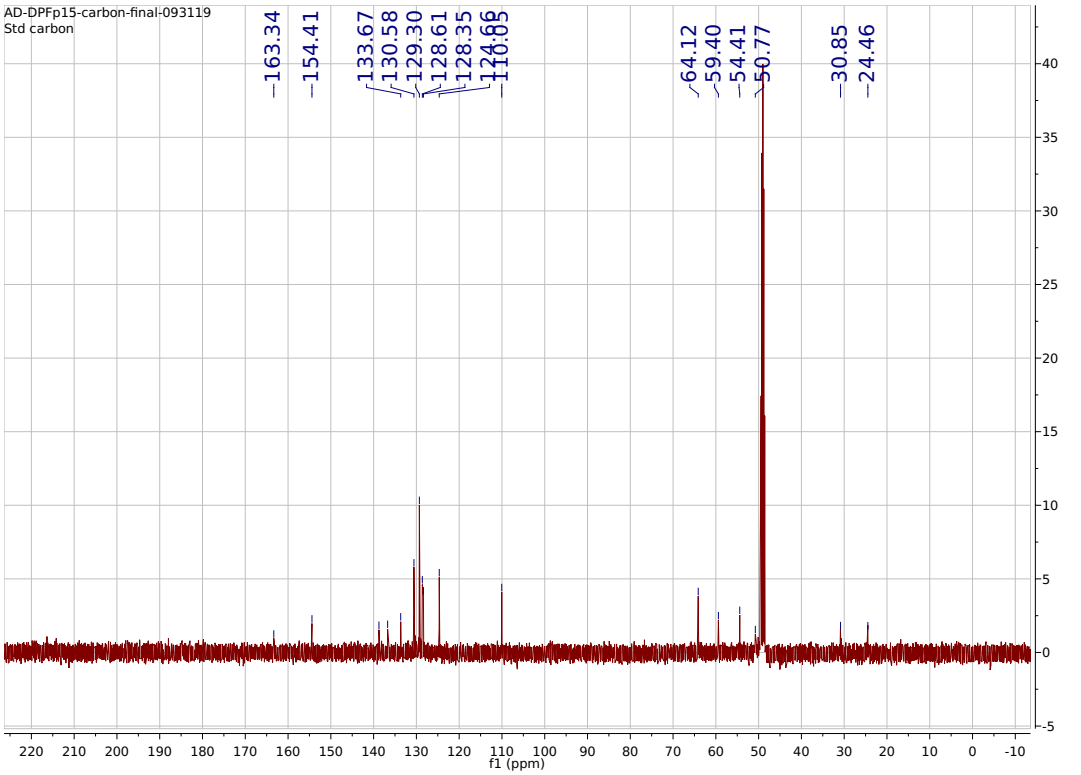

SHIMADZU LabSolutions

Analysis Report

<Sample Information>

Sample Name	: DPFp15		
Sample ID	: DPFp15		
Data Filename	: DPFp15.lcd		
Method Filename	: NNP-Grd10-90_Slow_PDA_D2only.lcm		
Batch Filename	: AD-100219-dpfs.lcb		
Vial #	: 1-19	Sample Type	: Unknown
Injection Volume	: 10 uL		
Date Acquired	: 10/2/2019 11:22:02 AM	Acquired by	: chemist
Date Processed	: 10/2/2019 11:40:05 AM	Processed by	: chemist

<Chromatogram>

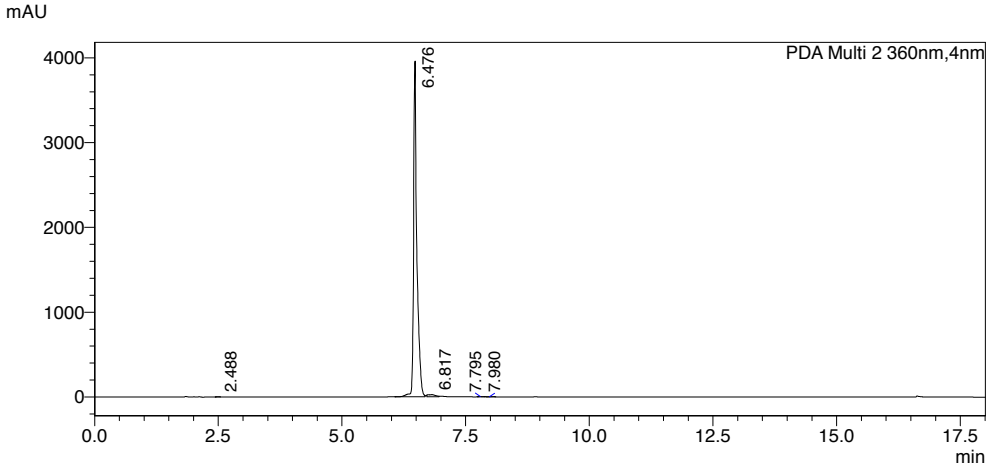

<Peak Table>

PDA Ch2 360nm

Peak#	Ret. Time	Area%
1	2.488	0.068
2	6.476	98.349
3	6.817	1.440
4	7.795	0.085
5	7.980	0.057
Total		100.000

4,4'-(furan-2,5-diyl)bis(*N*-((1-methylpiperidin-4-yl)methyl)benzimidamide) (DPFp16)

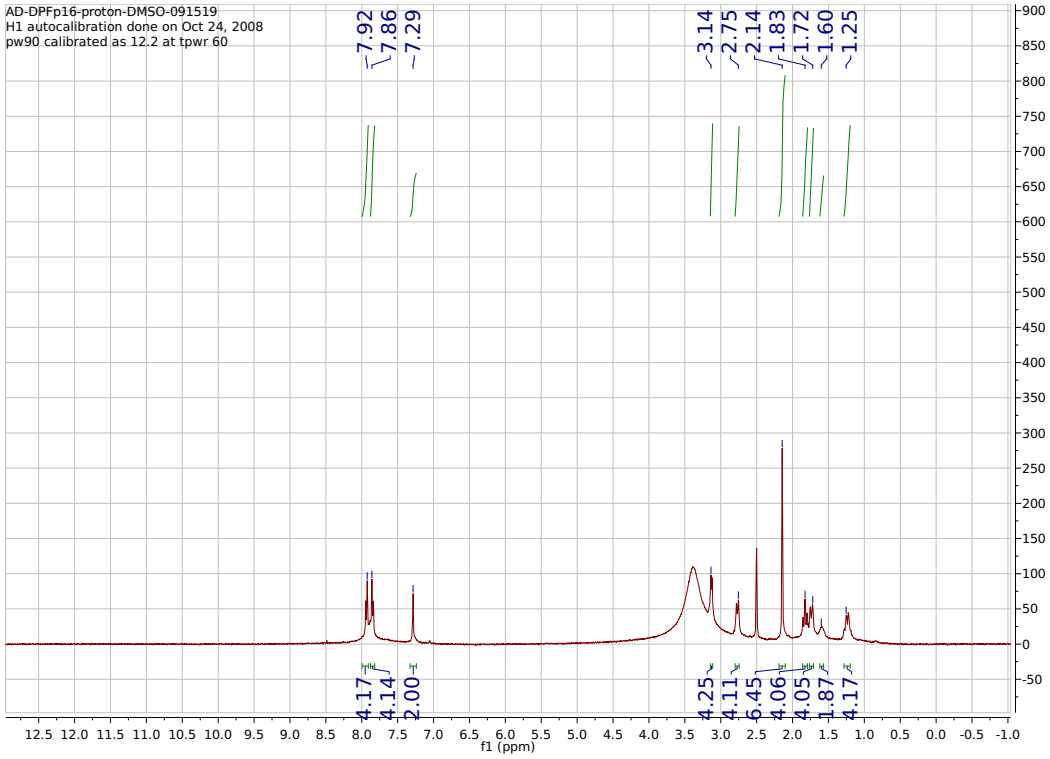

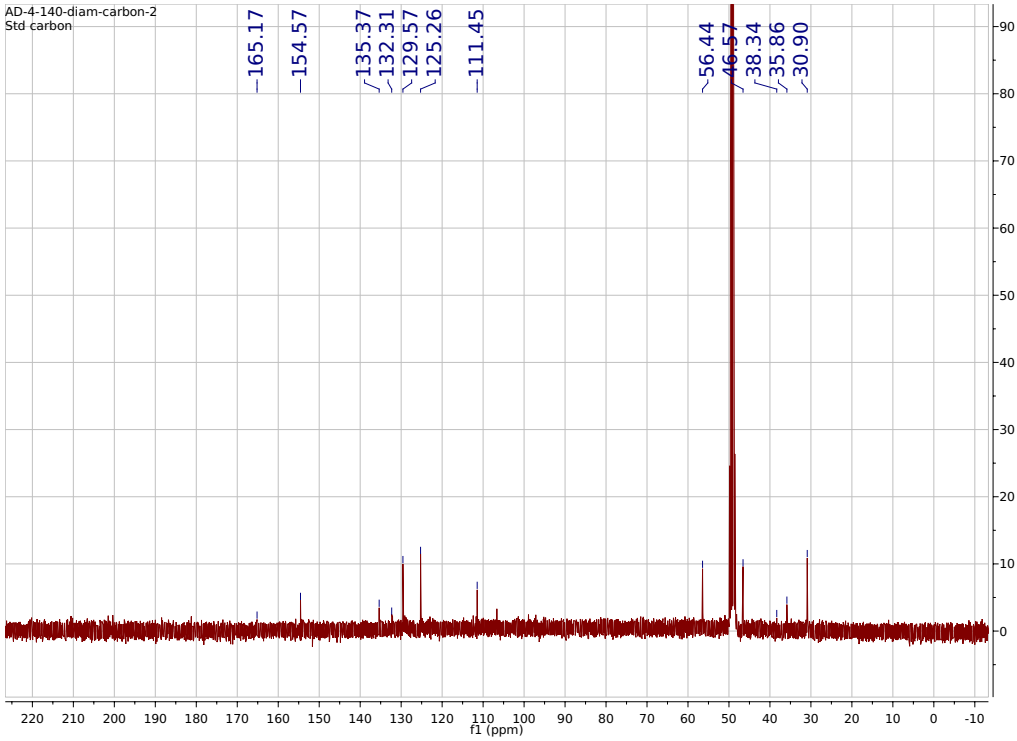

SHIMADZU LabSolutions

Analysis Report

<Sample Information>

Sample Name	: AD-4-140-DIAM		
Sample ID	: AD-4-140-DIAM		
Data Filename	: AD-4-140-DIAM.lcd		
Method Filename	: NNP-Grd10-90_Slow_PDA_D2only.lcm		
Batch Filename	: ad-4-140-CLMN.lcb		
Vial #	: 1-3	Sample Type	: Unknown
Injection Volume	: 10 uL		
Date Acquired	: 11/7/2018 10:04:59 AM	Acquired by	: chemist
Date Processed	: 11/7/2018 10:23:02 AM	Processed by	: chemist

<Chromatogram>

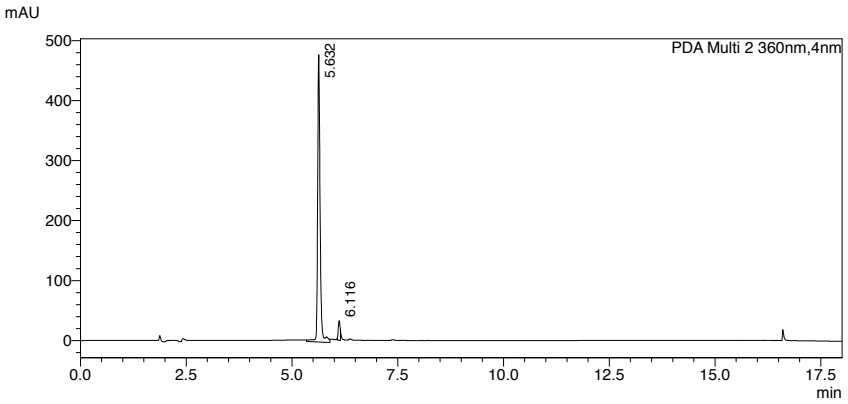

<Peak Table>

RF-20A Ex:350nm,Em:450nm

Peak#	Ret. Time	Area%
Total		

PDA Ch1 254nm

Peak#	Ret. Time	Area%
Total		

PDA Ch2 360nm

Peak#	Ret. Time	Area%
1	5.632	95.265
2	6.116	4.735
Total		100.000

4,4'-(furan-2,5-diyl)bis(*N*-(2-(4-benzylpiperazin-1-yl)ethyl)benzimidamide) (DPFp17)

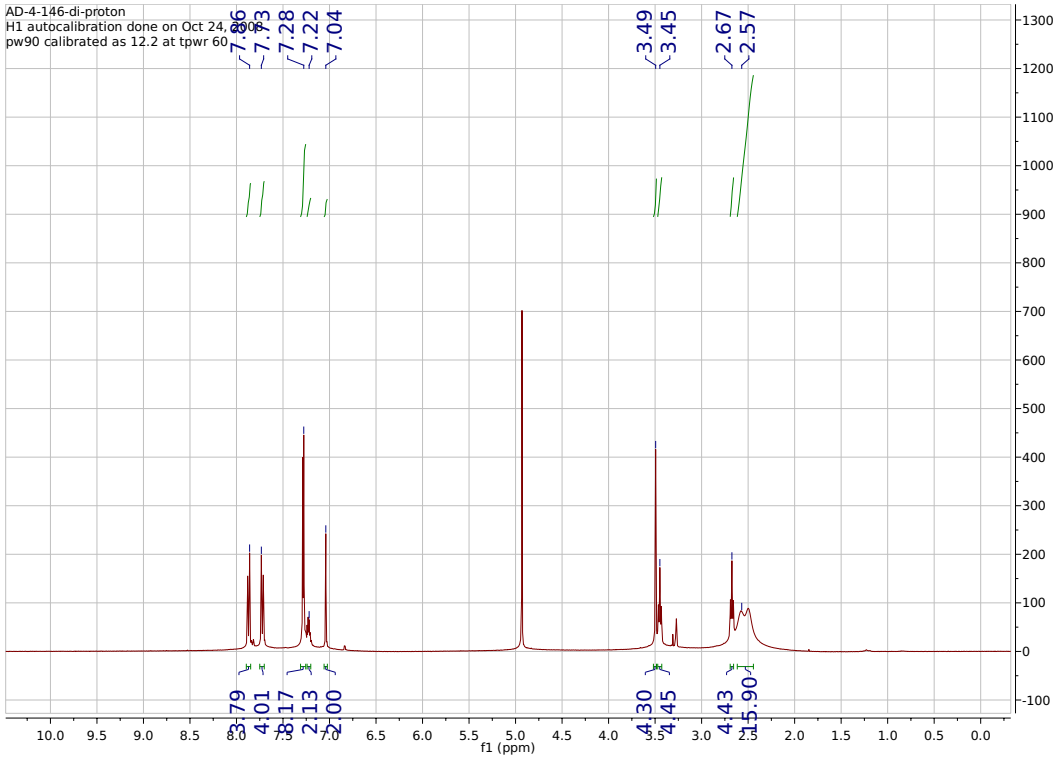

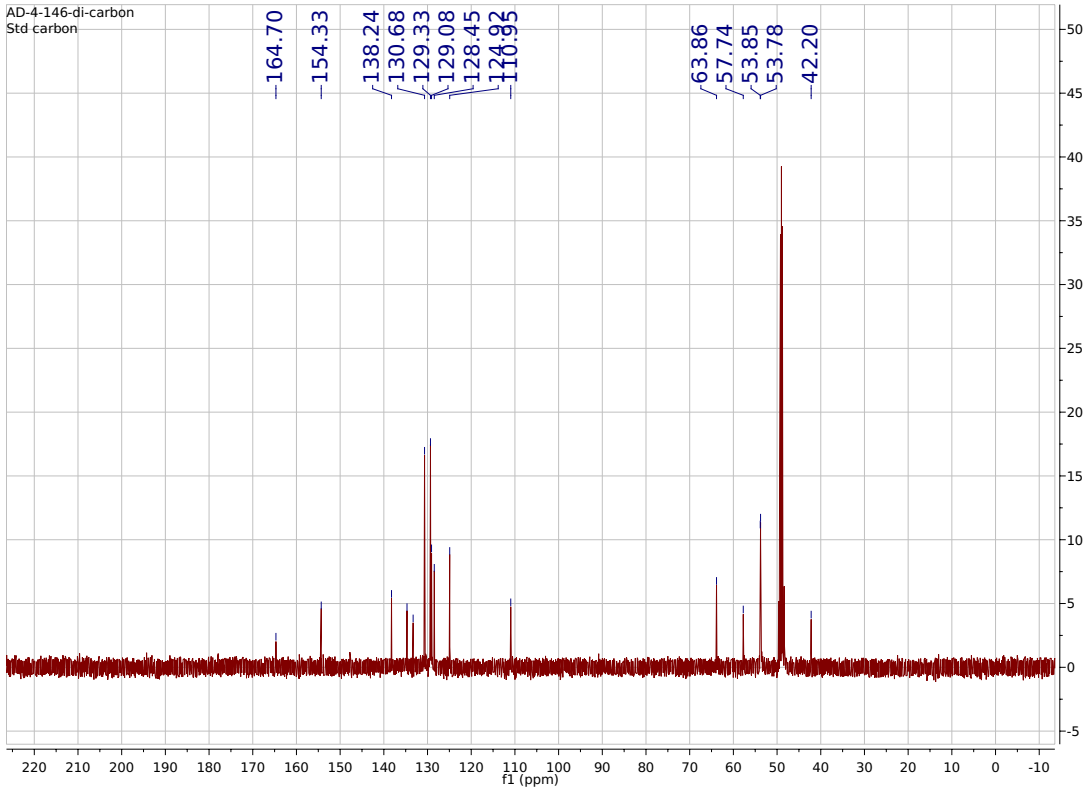

SHIMADZU LabSolutions

Analysis Report

<Sample Information>

Sample Name	: AD-4-146-DI		
Sample ID	: AD-4-146-DI		
Data Filename	: AD-4-146-DI.lcd		
Method Filename	: NNP-Grd10-90_Slow_PDA_D2only.lcm		
Batch Filename	: AD-4-146-CLMN.lcb		
Vial #	: 1-83	Sample Type	: Unknown
Injection Volume	: 10 uL		
Date Acquired	: 11/19/2018 10:56:46 AM	Acquired by	: chemist
Date Processed	: 11/19/2018 11:30:54 AM	Processed by	: chemist

<Chromatogram>

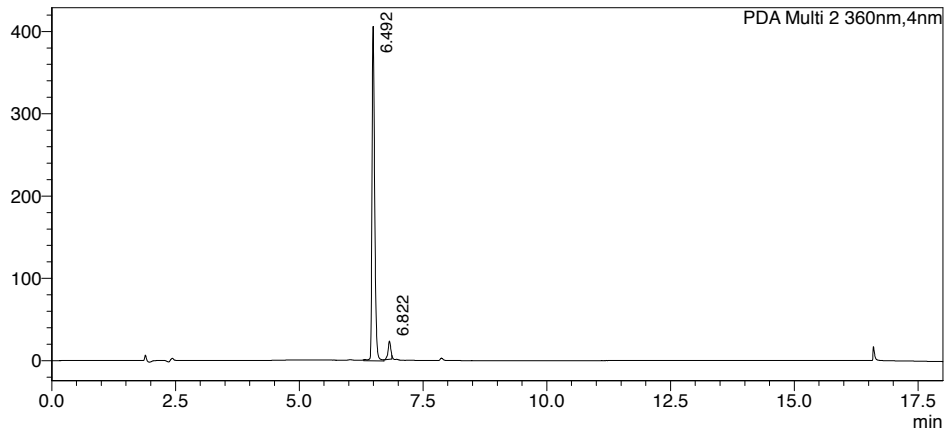

<Peak Table>

RF-20A Ex:350nm,Em:450nm

Peak#	Ret. Time	Area%
Total		

PDA Ch1 254nm

Peak#	Ret. Time	Area%
1	2.049	100.000
Total		100.000

PDA Ch2 360nm

Peak#	Ret. Time	Area%
1	6.492	94.772
2	6.822	5.228
Total		100.000

4,4'-(furan-2,5-diyl)bis(*N*-((*R*)-1-benzylpiperidin-3-yl)benzimidamide) (DPFp18)

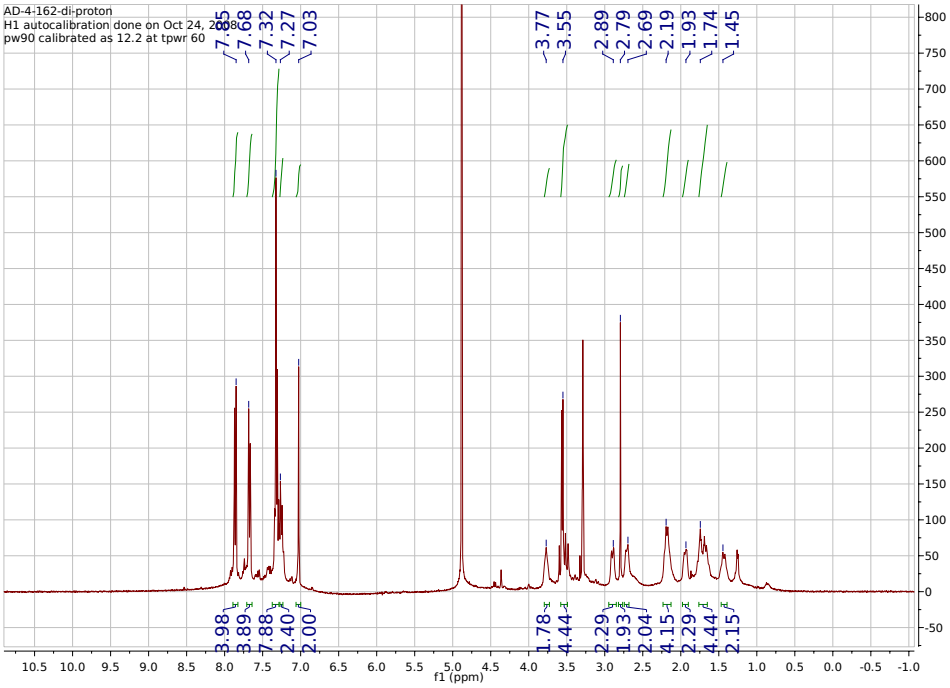

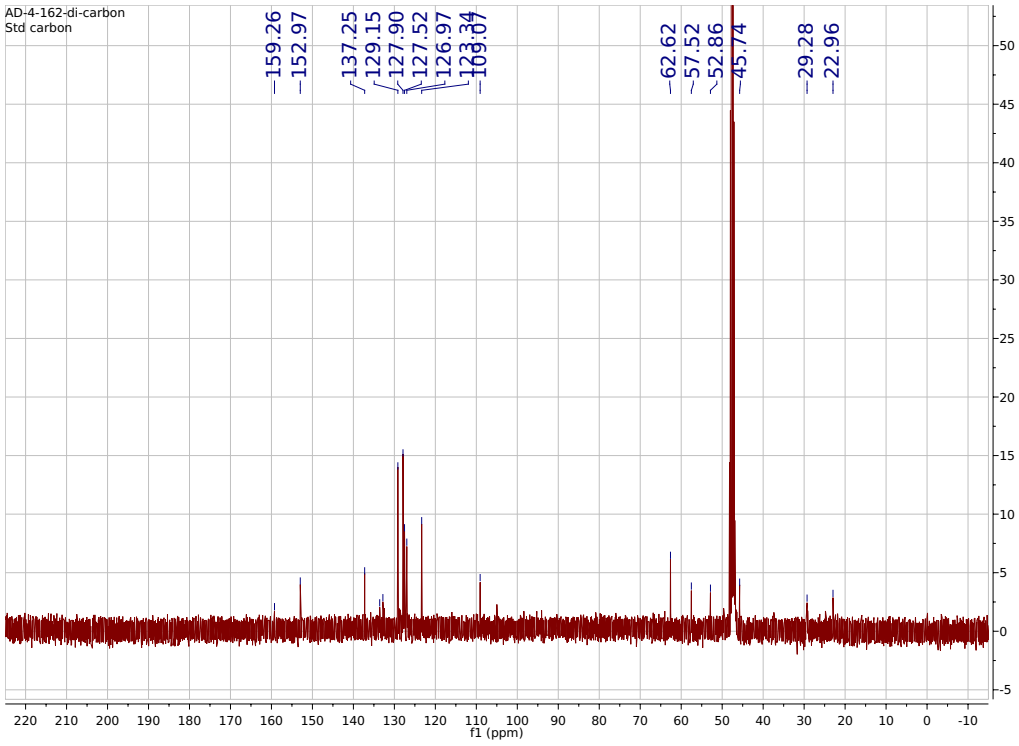

SHIMADZU LabSolutions

Analysis Report

<Sample Information>

Sample Name	: AD-4-162-DI		
Sample ID	: AD-4-162-DI		
Data Filename	: AD-4-162-DI.lcd		
Method Filename	: NNP-Grd10-90_Slow_PDA_D2only.lcm		
Batch Filename	: AD-4-162-CLMN.lcb		
Vial #	: 1-102	Sample Type	: Unknown
Injection Volume	: 10 uL		
Date Acquired	: 11/27/2018 10:09:21 AM	Acquired by	: chemist
Date Processed	: 11/27/2018 10:35:23 AM	Processed by	: chemist

<Chromatogram>

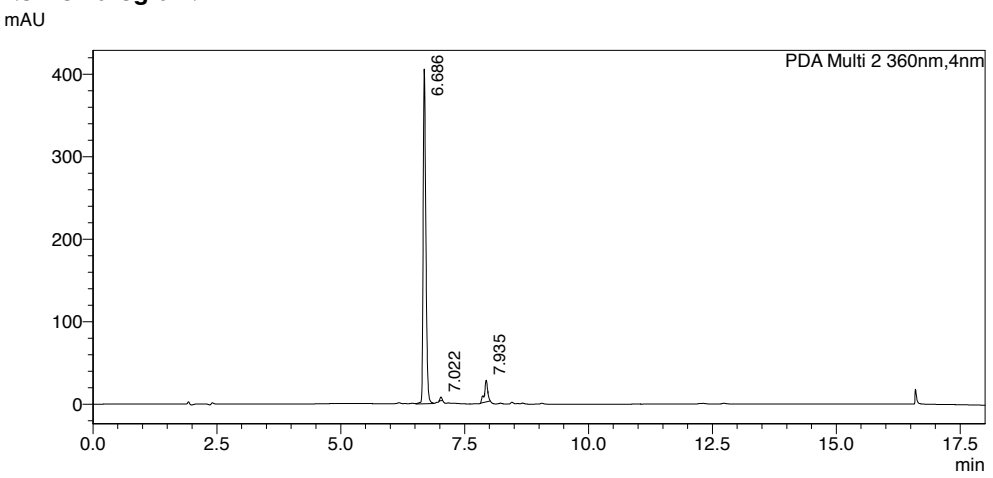

<Peak Table>

PDA Ch2 360nm

Peak#	Ret. Time	Area%
1	6.686	96.539
2	7.022	0.669
3	7.935	2.793
Total		100.000

4,4'-(furan-2,5-diyl)bis(*N*-(3-(benzyl(ethyl)amino)propyl)benzimidamide) (DPFp19)

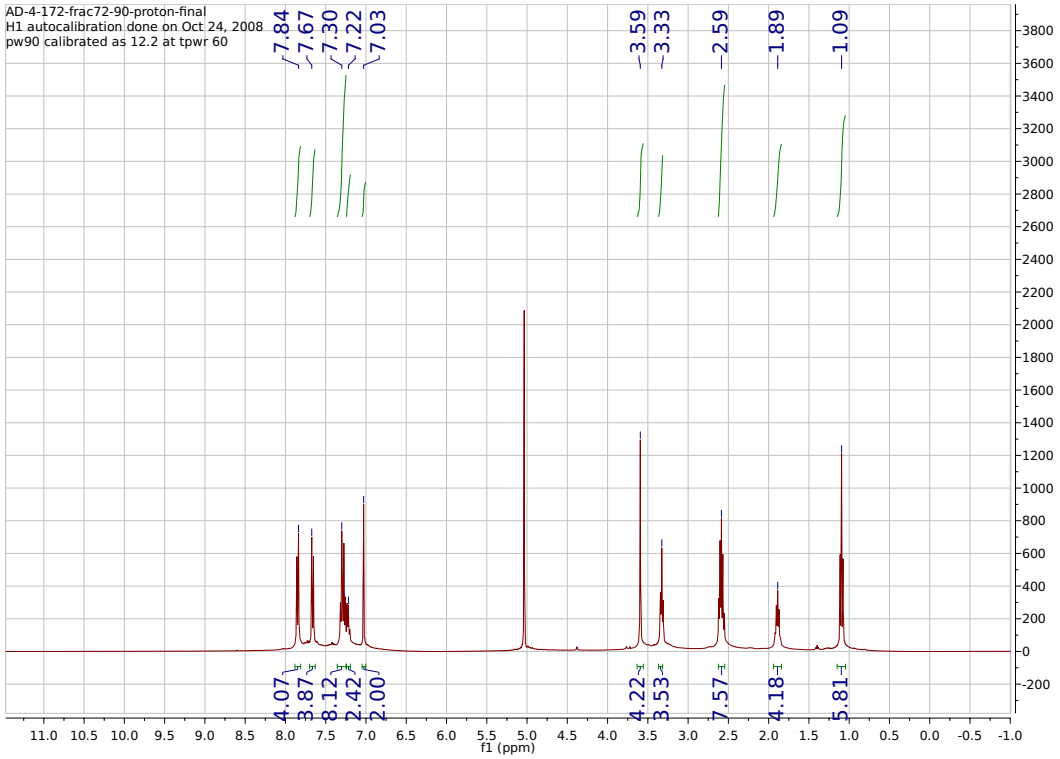

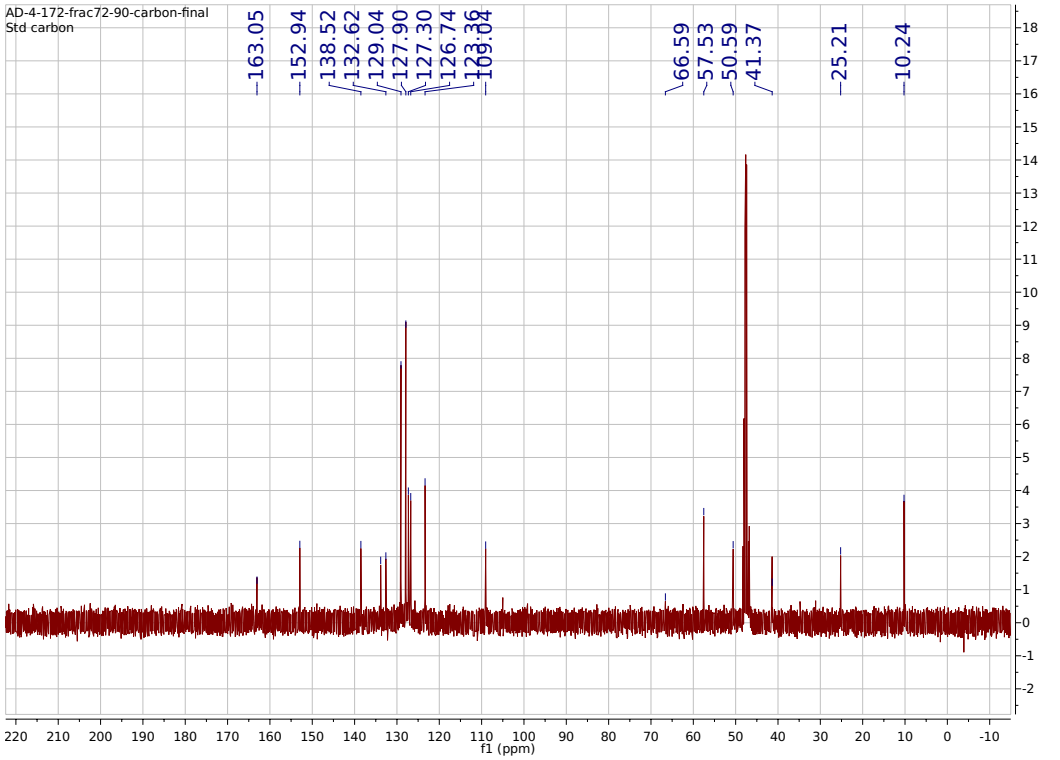

SHIMADZU LabSolutions

Analysis Report

<Sample Information>

Sample Name	: AD-4-172-diam		
Sample ID	: AD-4-172-diam		
Data Filename	: AD-4-172-diam.lcd		
Method Filename	: NNP-Grd10-90_Slow_PDA_D2only.lcm		
Batch Filename	: AD-4-172-clmn.lcb		
Vial #	: 1-3	Sample Type	: Unknown
Injection Volume	: 10 uL		
Date Acquired	: 12/17/2018 12:07:35 PM	Acquired by	: chemist
Date Processed	: 12/18/2018 11:34:57 AM	Processed by	: chemist

<Chromatogram>

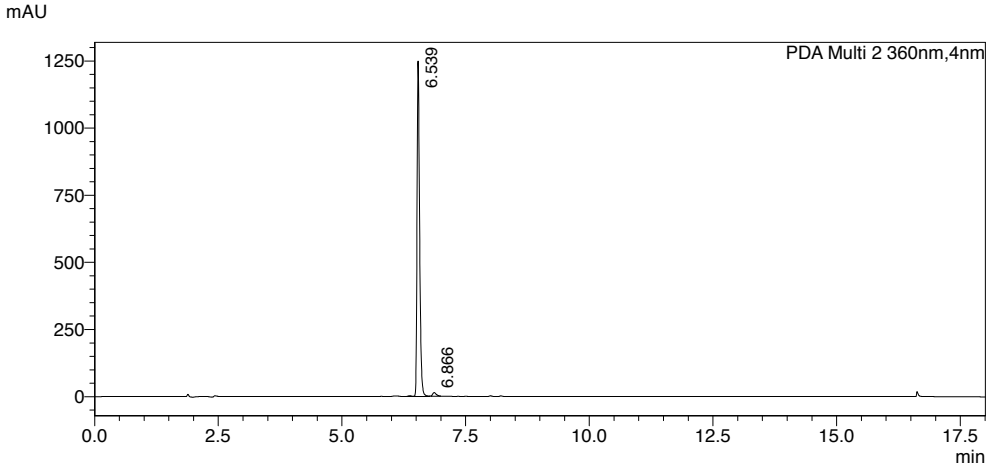

<Peak Table>

RF-20A Ex:350nm,Em:450nm

Peak#	Ret. Time	Area%
Total		

PDA Ch1 254nm

Peak#	Ret. Time	Area%
Total		

PDA Ch2 360nm

Peak#	Ret. Time	Area%
1	6.539	98.460
2	6.866	1.540
Total		100.000

4,4'-(furan-2,5-diyl)bis(*N*-(4-(piperidin-1-ylmethyl)phenyl)benzimidamide) (DPFp20)

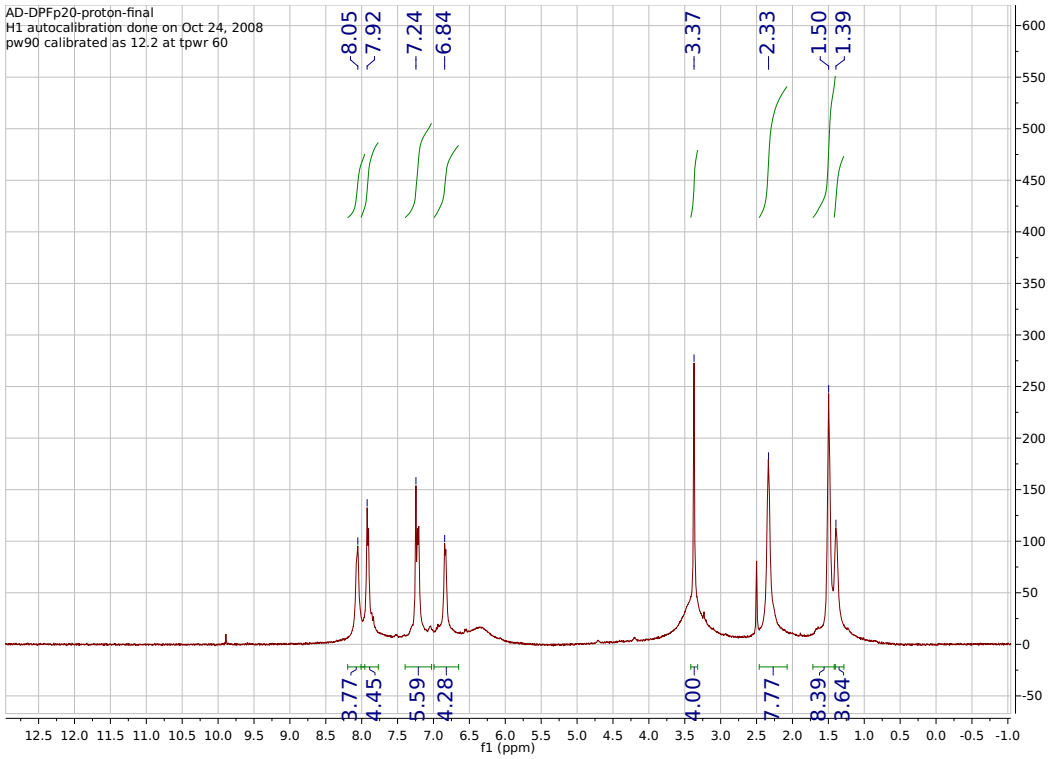

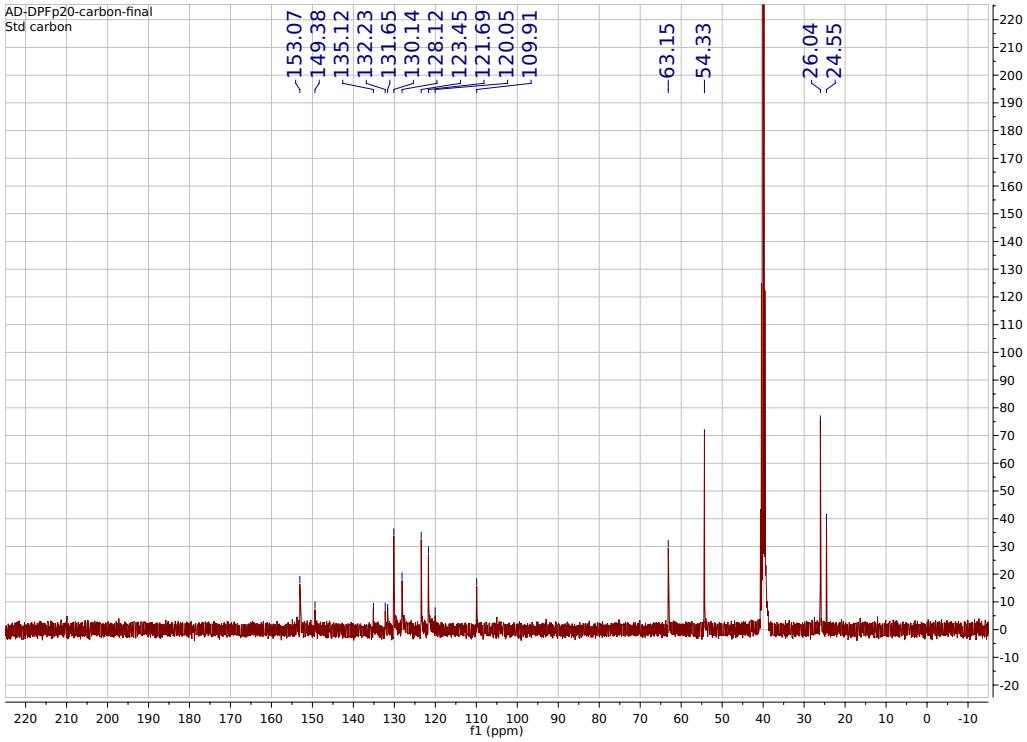

SHIMADZU LabSolutions

Analysis Report

<Sample Information>

Sample Name	: AD-4-176-recrystall		
Sample ID	: AD-4-176-recrystall		
Data Filename	: AD-4-176-recrystall.lcd		
Method Filename	: NNP-Grd10-90_Slow_PDA_D2only.lcm		
Batch Filename	: AD-4-170x-2.lcb		
Vial #	: 1-4	Sample Type	: Unknown
Injection Volume	: 10 uL		
Date Acquired	: 1/11/2019 3:53:46 PM	Acquired by	: chemist
Date Processed	: 8/6/2019 2:23:11 PM	Processed by	: chemist

<Chromatogram>

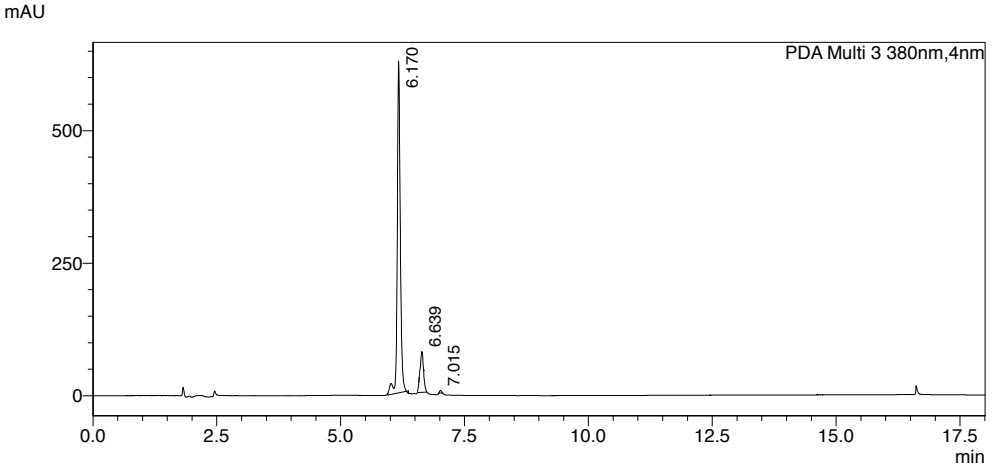

<Peak Table>

PDA Ch3 380nm

Peak#	Ret. Time	Area%
1	6.170	94.520
2	6.639	4.979
3	7.015	0.501
Total		100.000

G. Gel Images from RNase R Exonucleolytic Decay Experiments

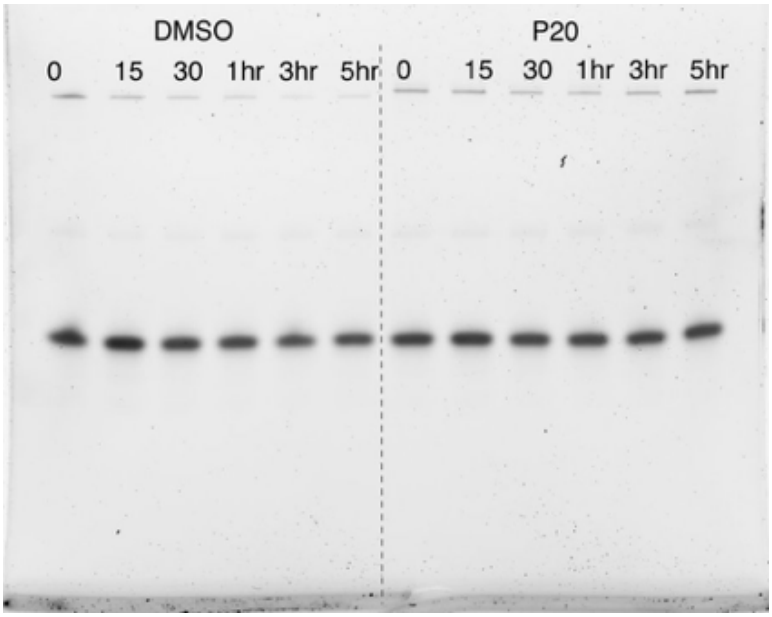

Figure S37. Representative denaturing gel image of an RNase R exonucleolytic degradation experiment with 5 time points to confirm linear decay as described in Materials and Methods section. 0.2 μM RNA and 0.2 μM DPFp20 were incubated with 5U of RNase R in low ionic buffer conditions. Top band represents the triple helix RNA and bottom band represents the DNA loading control.

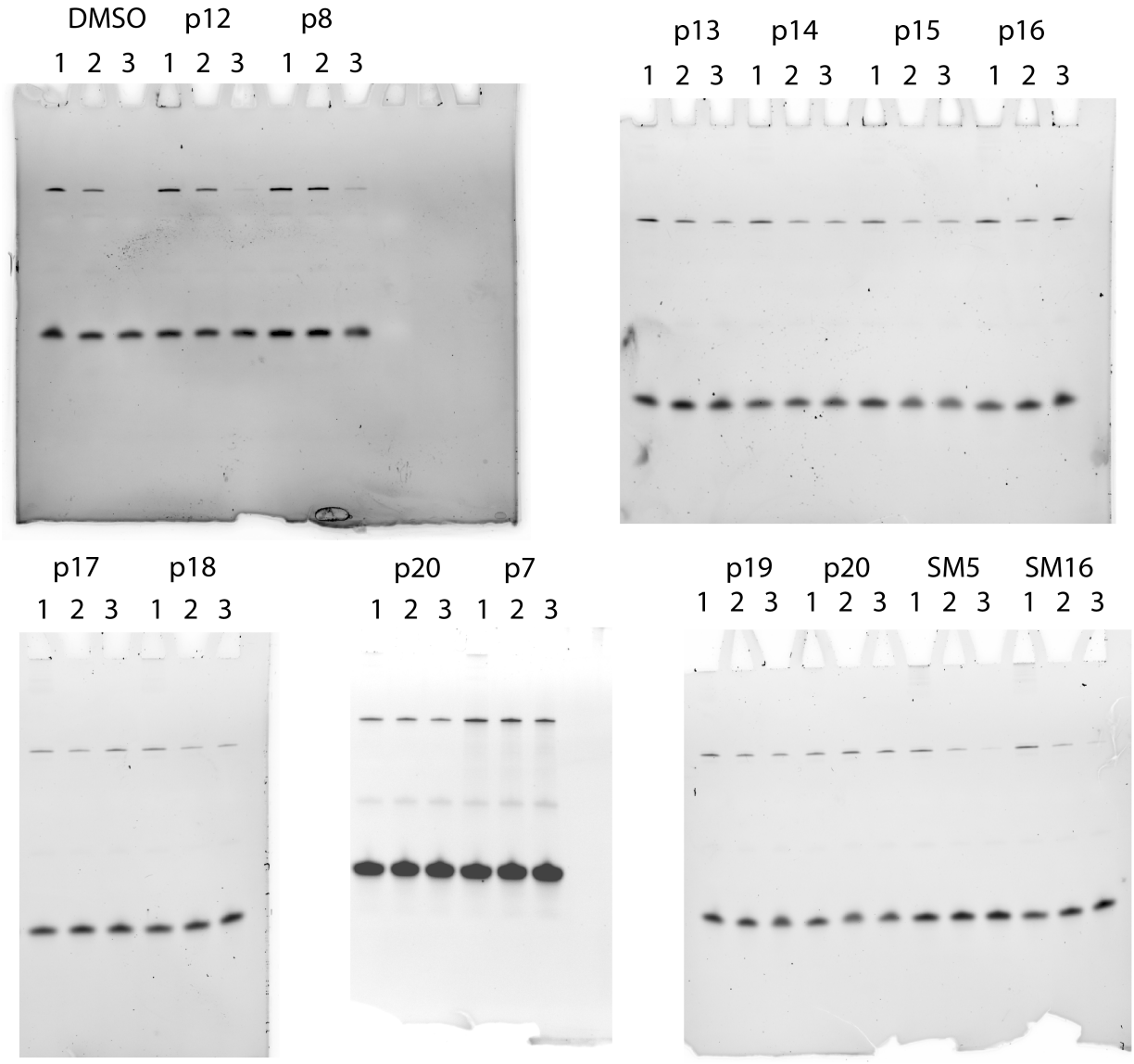

Figure S38. Representative gel images of RNase R exonucleolytic degradation experiments with 3 time as observed by denaturing gel electrophoresis and described in Materials and Methods section. 0.2 μM RNA and 0.2 μM DPFp20 or 1 μM SM5 or SM16 were incubated with 5U of RNase R in low ionic buffer conditions. 1 = 0 min, 2 = 30 min, 3 = 300 min. Top band represents the triple helix RNA and bottom band represents the DNA loading control.

H. References

1. Donlic, A., Morgan, B.S., Xu, J.L., Liu, A., Roble, C., Jr. and Hargrove, A.E. (2018) Discovery of Small Molecule Ligands for MALAT1 by Tuning an RNA-Binding Scaffold. *Angew Chem Int Ed Engl*, **57**, 13242-13247.
2. Brown, J.A., Valenstein, M.L., Yario, T.A., Tycowski, K.T. and Steitz, J.A. (2012) Formation of triple-helical structures by the 3'-end sequences of MALAT1 and MENbeta noncoding RNAs. *Proc Natl Acad Sci U S A*, **109**, 19202-19207.
3. Liu, L., Wang, F., Tong, Y., Li, L.F., Liu, Y. and Gao, W.Q. (2019) Pentamidine inhibits prostate cancer progression via selectively inducing mitochondrial DNA depletion and dysfunction. *Cell Prolif*, e12718.
4. Sun, T. and Zhang, Y. (2008) Pentamidine binds to tRNA through non-specific hydrophobic interactions and inhibits aminoacylation and translation. *Nucleic Acids Res*, **36**, 1654-1664.
5. Warf, M.B., Nakamori, M., Matthys, C.M., Thornton, C.A. and Berglund, J.A. (2009) Pentamidine reverses the splicing defects associated with myotonic dystrophy. *Proc Natl Acad Sci U S A*, **106**, 18551-18556.
6. Zhang, Y., Li, Z., Pilch, D.S. and Leibowitz, M.J. (2002) Pentamidine inhibits catalytic activity of group I intron Ca.LSU by altering RNA folding. *Nucleic Acids Res*, **30**, 2961-2971.
7. Abulwerdi, F.A., Xu, W., Ageeli, A.A., Yonkunas, M.J., Arun, G., Nam, H., Schneekloth, J.S., Dayie, T.K., Spector, D., Baird, N. *et al.* (2019) Selective Small-Molecule Targeting of a Triple Helix Encoded by the Long Noncoding RNA, MALAT1. *Acs Chem Biol*, **14**, 223-235.
8. Schneider, C.A., Rasband, W.S. and Eliceiri, K.W. (2012) NIH Image to ImageJ: 25 years of image analysis. *Nat Methods*, **9**, 671-675.
9. Gilad, Y. and Senderowitz, H. (2014) Docking Studies on DNA Intercalators. *Journal of Chemical Information and Modeling*, **54**, 96-107.